ADVANCED MASTERS IN STRUCTURAL ANALYSIS
OF MONUMENTS AND HISTORICAL CONSTRUCTIONS

Master's Thesis

Francesco Vanin

Analysis of applicability of classic calculus methods on arches with a critically low number of voussoirs

UNIVERSITAT POLITÈCNICA DE CATALUNYA

University of Minho

Education and Culture

Erasmus Mundus

ADVANCED MASTERS IN STRUCTURAL ANALYSIS
OF MONUMENTS AND HISTORICAL CONSTRUCTIONS

Master's Thesis

Francesco Vanin

Analysis of applicability of classic calculus methods on arches with a critically low number of voussoirs

This Masters Course has been funded with support from the European Commission. This publication reflects the views only of the author, and the Commission cannot be held responsible for any use which may be made of the information contained therein.

Spain | 2014

Declaration

Name:	Francesco Vanin
Email:	checco.vanin@hotmail.it

Title of the Msc Dissertation:	Analysis of the applicability of classic calculus methods on arches with a critically low number of voussoirs
Supervisor(s):	Prof. Lluís Gil
	Dr. Ernest Bernat Masó
Year:	2014

I hereby declare that all information in this document has been obtained and presented in accordance with academic rules and ethical conduct. I also declare that, as required by these rules and conduct, I have fully cited and referenced all material and results that are not original to this work.

I hereby declare that the MSc Consortium responsible for the Advanced Masters in Structural Analysis of Monuments and Historical Constructions is allowed to store and make available electronically the present MSc Dissertation.

University:	Technical University of Catalonia, Spain
Date:	13-07-2014
Signature:	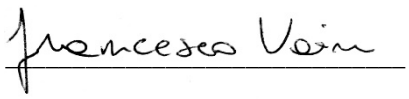

Acknowledgements

On the completion of this work, I would like to express my sincere gratitude to all the people that contributed and helped me along this year of master course.

I would like to thank professor Lluís Gil, my thesis supervisor, for the his kind guidance and support, and for giving me the opportunity to work in a theme that I particularly love, as well as Dr. Ernest Bernat Masó, for the directions he gave me and for the practical contribution, both for the experimental and the theoretical work. I need to express my thanks also to the people that helped me in the laboratory in Terrassa, particularly to Vicenç and to Alex Garrido for their assistance.

I am really grateful to the professors of the Department of Civil Engineering in University of Minho, in particular to prof. Paulo Lourenço, prof. Daniel Oliveira and prof. Luís Ramos for the quality of their teaching and for the passion which they put in their work.

A due mention is for the Erasmus Mundus Scholarship Program, for selecting me and providing the financial support that allowed me to join the SAHC master program.

I also want to thank my colleague and friend Federica, for the countless hours of work and of fun that we spent together, and all the friends of the SAHC group and the PhD students in Guimaraes. It has been a real pleasure and a fortune to share this experience with them. Finally, I would like to thank my family for their support and their presence even if they are far.

Abstract

The structural analyses of masonry structures, and in particularly of arches and vaults, is often based on the application of limit analysis, that represents today a widespread method, which can rely on a basis of studies and researches that validated it and proved its accuracy, despite the apparent simplicity. There are some examples of arches though, on which the application of the limit analysis could be problematic, for their specific nature: it is the case, for example, of arches with a limited number of voussoirs. In these structures, the development of a mechanism is related to the actual position of the joints, as only at a limited number of sections of the arch (the joints) the plastic strains to form a rotational hinge, or, eventually, a sliding plane can take place. The standard hypotheses of limit analysis (material with infinite compressive strength, zero tensile strength and absence of sliding) if extended to the whole structure and not only to the joints are not completely adequate .

The aim of this work is to develop a method for the application of limit analysis to the studied typology of arches, modifying or correcting the approach to take into account the different structural behaviour introduced by the reduced number of joints. To this scope, an experimental campaign has been performed on a model of arch loaded asymmetrically in different load configurations. The experimental results were compared to the analytical results of the application of the limit analysis in two approaches, the first being the limit analysis of the arch modelled as a structure of rigid bodies in contact though interfaces, where all the non-linearity is concentrated, and the second being the numerical solution of the differential equation of the thrust line and the optimisation of the solution, in modified hypotheses.

Specific tools for the limit analysis, in both approaches, were developed, as MATLAB routines allowing to apply all the desired hypotheses to the analysis. A FEM non-linear model of the arch has been developed to compare the results of the different methods. From the comparison of analytical, experimental and numerical results an evaluation is given on the applicability of limit analysis to arches with a low number of voussoirs, concluding that the standard hypotheses should be modified for a more precise study of these arches; the linear analysis of a rigid bodies structure with contact interfaces is considered to be a good option to describe efficiently the failure mechanism and to provide an acceptable estimation of the ultimate load.

Keywords: Limit analysis, arches with low number of voussoirs, thrust line.

Resumen

(Análisis sobre la aplicabilidad de métodos clásicos de cálculo para arcos con un número críticamente bajo de dovelas)

El análisis estructural de estructuras de fábrica y, en particular de arcos y bóvedas, está usualmente basado en la aplicación del análisis límite, método hoy en día muy extendido, asentado sobre una base de estudios e investigaciones que validan y prueban su exactitud, a pesar de su aparente simplicidad.Sin embargo, en algunas situaciones, la aplicación del análisis límite puede ser problemática por su naturaleza: este es el caso, por ejemplo, de arcos con un número limitado de dovelas. En estas estructuras, el desarrollo de un mecanismo está relacionado con la posición actual de las juntas, ya que sólo en un número limitado de las secciones del arco (las juntas) las deformaciones plásticas pueden formar una biela (rotación), o, incluso, pueden dar lugar a un plano de deslizamiento. Las hipótesis estándar del análisis límite (material con infinita resistencia a compresión, nula capacidad a tracción y ausencia de deslizamiento) si se extendiesen a la estructura completa y no solo a las juntas, no serían completamente correctas.

El objetivo de este trabajo es desarrollar un método para la aplicación del análisis límite a la tipología de arcos estudiada, modificando o corrigiendo el proceso, para poder tener en cuenta el distinto comportamiento estructural introducido por este reducido número de dovelas. Para esto, una campaña experimental ha sido llevada a cabo en un modelo de arco, cargado asimétricamente con distintas configuraciones de carga. Los resultados experimentales han sido después comparados con los resultados analíticos, obtenidos de la aplicación del análisis límite llevados a cabo de dos maneras: la primera, basada en el análisis límite del arco modelado como una estructura de cuerpos rígidos en contacto a través de los planos de unión, donde todo el comportamiento no-lineal se concentra; y un segundo acercamiento basado en la solución numérica de la ecuación diferencial de la línea de empujes y de la optimización de la solución, en hipótesis modificadas.

Herramientas específicas para el análisis límite, en ambos acercamientos, han sido desarrolladas, tales como rutinas de MATLAB que permiten la aplicación de todas las hipótesis deseadas al análisis. Un modelo FEM no lineal del arco ha sido también desarrollado para poder comparar los resultados de los diferentes métodos. De la confrontación de resultados analíticos, experimentales y numéricos, se ha realizado una evaluación de la aplicabilidad del análisis límite a arcos con un reducido número de dovelas, concluyendo que las hipótesis estándar deben ser modificadas para obtener un estudio más preciso de este tipo de arcos. El análisis lineal de estructuras compuestas por cuerpos rígidos con superficies de contacto, es considerado una posible buena opción para describir eficientemente el mecanismo de fallo, y proveer una estimación aceptable de la carga última.

Table of Contents

List of Figures

List of Tables

Introduction

The structural typology of arches is widely diffused in historical buildings since antiquity, and characterised for centuries the structural conception of architecture. From the large diffusion of the arches and vaults in all types of historical constructions, from churches, to palaces and bridges, comes the need of adequate methods of assessment of the safety of arched structures. The historical methods of analysis of arches are among the first studies on structural safety, made in the 17th-18th century; their results, and the hypotheses on which they are based, were recovered in the last century and inscribed in the developing context of limit analysis applied to masonry. For the works of many authors, being Heyman and Kooharian two of the most important, the traditional approach to the study of arches, based on the definition of a thrust line, was reformulated and validated by the new theoretical background of limit analysis.

The diffusion of the method, that combines the traditional and intuitive approach of the research of the thrust line, with the sound theoretical structure of the theorems of limit analysis, makes it a world-wide accepted tool of analysis, whose accuracy has been proved throughout the years in many research works. Despite its good applicability to the majority of arches structures, though, it has been observed recently that in some cases the limit analysis method does not reach accurate enough results, for the particular nature of some applications.

One of these cases in which the limit analysis, applied in the standard, common hypotheses, does not provide satisfactory results is when it is used to model the structural behaviour of arches with a limited number of voussoirs. This particular typology of arches, indeed, does not comply with the regular hypotheses that are made, for the absence, or scarcity, of physical joints, and the presence of a certain tensile strength in the voussoirs that modifies the behaviour predicted by standard limit analysis performed in its classic formulation. These arches, moreover, are often constituted of stone blocks with dry joints, or with joints that had some mortar in the past but which, after centuries of service, are turned for the decay of the material, into dry-joints structures. The peculiarities introduced by these characteristics make the application of standard limit analysis problematic.

The diffusion of the structural typology of arches with a low number of voussoirs is large, although it constitutes a minor percentage of arched structures in general. The use of this typology is related to windows, portals, openings, *loggias*, arches of lateral naves in churches, and in general stone arches with little to moderate span The structural behaviour of this typology did not have a proper development in the past, also because, for their characteristics, their dimensions cannot be too large, resulting in arches that are not in general the most structurally challenging.

Although the structural problems on this typology of arches involve generally minor structural elements or non-structural elements, their particular behaviour, anyway, should not be neglected, and adequate

methods to model it should be available. The possible approaches to the structural analysis of these arches are many, from the most traditional techniques to the application of FEM and DEM models. The focus of the work was concentrated on limit analysis because it is considered a powerful tool of analysis, which requires little input parameters, and models in a simple but effective way the characteristic behaviour of materials like masonry. The simplicity of the method and the reasonable hypotheses that are made to formulate the problem, lead to general and intuitive results of the analysis, easy to interpret, that describe efficiently the nature of the structural behaviour of masonry structures, arches in particular.

Objectives and method

The aim of this work is to study the classic calculation methods in order to slightly modify them as they could be confidently applied in the cases of arches with a low number of voussoirs. The main objectives that were pursued are:

- checking the applicability of classic limit analysis on arches with little number of voussoirs, and quantifying the error introduced by its application;
- developing adequate procedures, based on limit analysis, to assess the ultimate load capacity of the studied typology;
- validating the developed methods through experimental data;
- comparing the results different analysis approaches (FEM, limit analysis) and give an evaluation on their applicability.

As there is no extensive investigation on the matter, and a set of experimental results to use and compare, the method followed for this work consisted in:

- The definition, preparation and execution of a series of tests of an arch, representative of the studied typology, statically and asymmetrically loaded
- The application of limit analysis method to the study of the tested configurations, with the introduction of a different approach from the “classical” limit analysis, to take into account the presence of a limited number of joints and voussoirs, i.e. a limited number of possible planes of sliding or rotational hinges.
- The development of adequate tools to perform limit analysis and the definition of all the hypotheses needed to model the problem of the analysis of arches with a little number of voussoirs
- The application of a FEM model of the studied arch to estimate its load carrying capacity

- The comparison between experimental, numerical and analytical results in order to verify the applicability of limit analysis (and FE models) for the structural assessment of existing arches of the typology of interest

The development of suitable methods, based on limit analysis, for the description of the structural behaviour of arches with a little number of voussoirs is the main objective of the work. Specific tools, through a Matlab code, will be developed to implement the procedure of limit analysis with the possibility of applying exactly the desired hypotheses to model correctly the problem. A result that will be considered important is the validation of such hypotheses through the observation of the failure mechanisms.

Thesis outline

The first chapter of the thesis will deal with the state of the art, a literature review on the failure mechanisms of arches, the historical approaches developed for the analysis of arched structures, and the more modern tools, including limit analysis, FEM, DEM. One section will be dedicated to the actual state of the research on the typology of arches with little number of voussoirs, or to the influence of the number of joints in determining the structural behaviour of arches.

The second chapter investigates the typological features of the studied arches, to define a case study and reproduce its geometry in a model to test in the laboratory. The execution and results of the experimental campaign will be presented in this section.

The third chapter describes the theory of limit analysis and the hypotheses on which it is based. The method for the limit analysis of structures made of rigid bodies in contact through interfaces is presented and implemented in a Matlab routine, both in the statical and in the kinematic approach. Another method for the thrust line analysis is proposed and implemented, together with the theory that defines the differential formulation of the problem of the thrust line. The results of all limit analysis computations are presented here.

The fourth chapter presents a numerical simplified micro-model of the studied arch and the results obtained through the FEM analysis for the different load configurations..

The fifth chapter presents a comparison of the results obtained through experimental tests, analytical computations (limit analysis) and numerical results of the FEM model. The applicability of the different analysis techniques is discussed, on the basis of the accordance to the experimental results. This accordance of the analytical and numerical results with the performed tests will be evaluated on the adequacy of the estimation of the failure load and on the capability of the method to describe the failure mechanisms.

Chapter 1.

State of the art

1.1 Structural analysis of arches

1.1.1 Failure mechanisms of arches

The understanding of the structural behaviour of arches and the development of adequate methods of analysis must be based on the observation of the mechanisms through which arches reach collapse. From the study of the failure modes suitable methods of analysis and structural hypotheses can be derived.

The characteristics of the material, brick or stone masonry in this case, influence deeply the structural behaviour and the failure mechanisms that can be observed, and, so, the structural hypotheses that will be used. The most relevant characteristics are the limited strength in tension of both the blocks and the mortar, if present, a fairly good strength in compression, the concentration of deformations and cracking mainly in the joints between voussoirs, and a rather high friction between the voussoirs that usually prevents them from sliding, even at failure. Other important factors are related to the structural typology of arches more than to the material: the stress level inside the arch is generally low, if compared to the compressive strength of masonry, and the self-weight, high if compared to the applied loads, plays a determinant role.

The main mechanisms through which an arch of the typology studied in this work can collapse are:

- Development of a mechanism (through the formation of a minimum number of hinges)
- Sliding of the voussoirs, for shear action, eventually combined to formation of hinges
- Crushing of the material in compression

The most frequent failure mechanism, at least for “regular” arches, is the formation of a mechanism through an adequate number of hinges; for a single span arches the formation of 4 hinges is sufficient to form a mechanism and to lead, consequently, the arch to failure if the applied load is not reduced. The failure configuration corresponds in real cases to the alignment of three of the hinges, condition in which the arch cannot sustain any load. This mechanism of failure is so common that for some methods of analysis it is the only one that is checked, assuming that the others cannot appear for the characteristics of the material (high strength in compression compared to stresses even at failure and close to hinges, high friction). The hinges are usually considered plastic hinges and treated in the context of limit analysis.

The sliding of voussoirs is controlled by the frictional coefficient of the interfaces, and, in presence of mortar, by it cohesion. Generally a Coulomb model is applied to study the frictional behaviour of the joints. The collapse of the arch for pure sliding of blocks requires the formation of a minimum of three planes of sliding, condition rarely verified in real applications. A more common failure mechanism is a mix of sliding in one interface, typically at the supports, and the formation of hinges in other three sections; the sensibility of arches to small movements at the supports is indeed high. The friction coefficient of the interfaces has a large influence in determining the failure mechanisms (Gilbert et al., 2006), and, with it, the ultimate capacity of the arch. For smaller friction coefficient the failure is only for sliding of blocks (Figure 1, mode III), while for higher coefficients the failure is for pure formation of rotational hinges (mode I) with a higher capacity; an intermediate situation can appear for the formation of some sliding surfaces together with some hinges (mode 2). These two latter modes are the most common, while the first is rather rare.

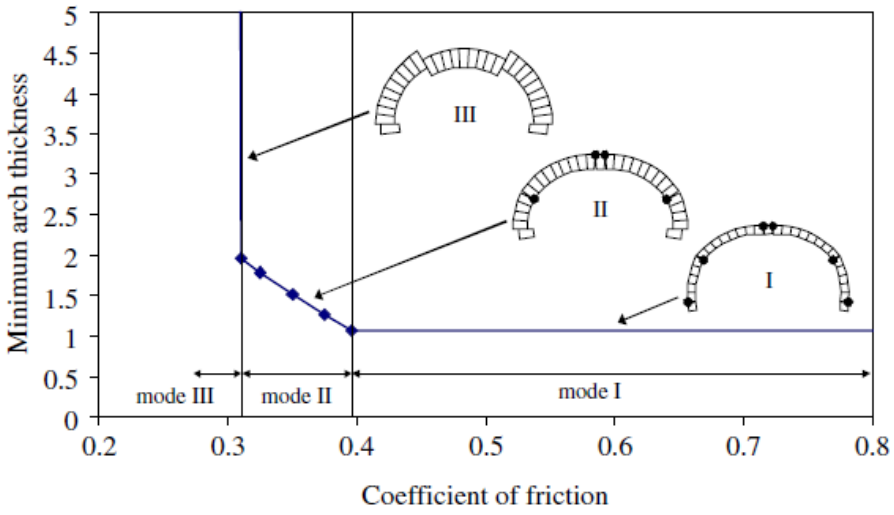

Figure 1. Influence of the coefficient of friction in determining the failure modes and the minimum arch thickness (Gilbert et al., 2006)

The failure for crushing of the material is usually limited to arches with a very small ratio rise/span, for which the formation of a mechanism through hinges requires very high loads or is impossible. For these arches, indeed, if it is possible to connect a point of the supports to the point in which the load is applied with a straight line, then the formation of four hinges (and so the appearance of mechanism) is not possible and the arch will fail for crushing in compression. In other conditions this failure mechanism is rare for the high resistance of the material compared to the common stresses.

Local failure in compression can appear in the hinges, but this does not lead to a collapse for crushing of the material, but rather to the development of the plastic hinge and its collocation in a more internal position. If the material locally fails in compression, indeed, the hinge is not forming in the edge of the section but slightly more internally. For some configurations of geometry and loading the failure in compression of a section can appear combined with a mechanism in the remaining part of the arch.

1.1.2 Historical approaches

The structural analysis of arches and vaults is a branch of engineering that developed since the first studies in the 17th century, although this typology of structures has been widely used since its invention, dated back to 6.000 B.C. (Huerta, 2001), and characterised both the aspect and the structural conception of different architectural styles, such as Roman, Romanesque, Gothic architecture. The construction of arches, in many cases of challenging proportions, has been based, throughout the centuries, on the expertise of the builders and on geometrical rules rather than structural concepts. These criteria, anyway, provided an acceptable level of safety and allowed the construction of impressive monuments, like the Pantheon or the dome of Hagia Sophia, to cite two of the most famous, or infrastructures that lasted until today, like Roman aqueducts and bridges.

A first scientific approach to the structural analysis of arches is due to Hooke (1670) with the famous stating "as hangs the flexible line, so but inverted will stand the rigid arch" (Figure 2a), intending, as was common at the time, for rigid arches the ones built in masonry and for elastic arches the ones in timber, and, centuries later, in steel. His work was followed, and completed, by other engineers and mathematicians, mainly of English school, such as Gregory (1697), Emerson (1754), Hutton (1772). Being based on only equilibrium considerations, without hypotheses on the strength of the material, also because at the time the modern Theory of Structures was not adequately developed, these theories belong to an approach that we can name "equilibration theory" (Huerta, 2002).

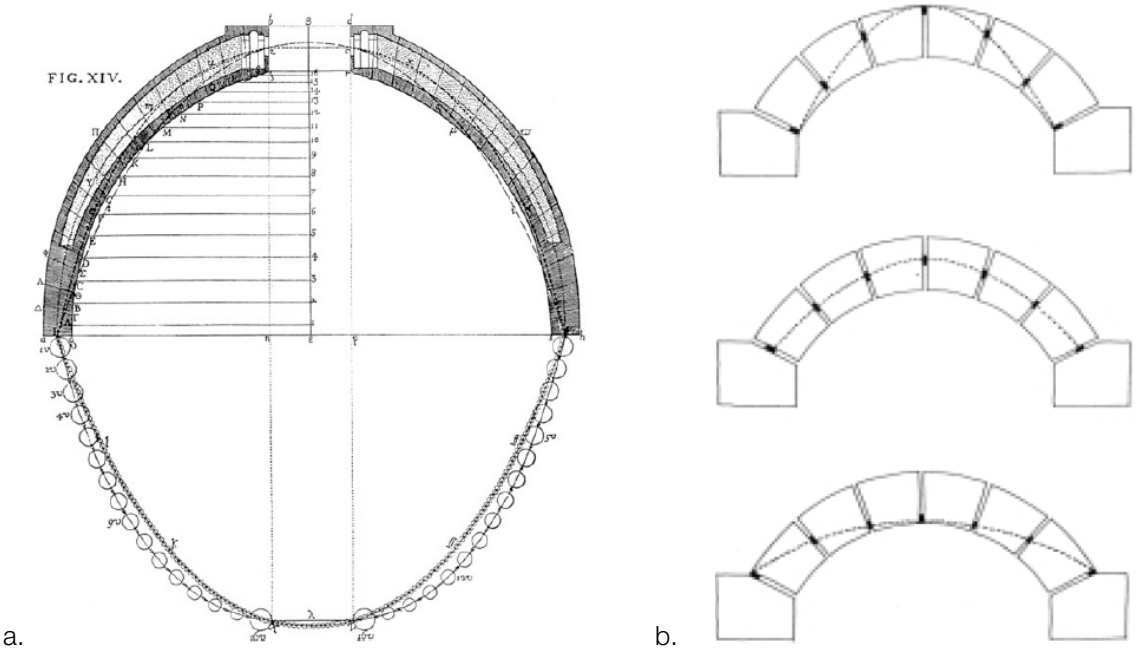

a. b.

Figure 2. a. Poleni's solution of the inverted catenary approach for S. Peter's dome (Roca et al., 2010); b. Barlow's experimental test to demonstrate the existence of different possible thrust lines, from minimum to maximum thrust (Huerta, 2001)

The analysis of the stability of an arch was in this way approached through the determination of the shape of a catenary curve, which needed to fit between the intrados and extrados of the arch. The problem of the determination of a unique thrust line was posed first by Moseley (1833) and solved with different approaches (minimum lateral thrust, imposition of three hinges to make the structure isostatic, coincidence of the thrust line with the middle line of the arch for new arches). With an experimental test performed by Barlow (1846) the existence of a maximum and minimum thrust, and so of multiple possible solutions for the thrust line, was demonstrated (Figure 2b).

The French school developed from the studies of La Hire (1712), with the contributions of Belidor (1729), Couplet (1730) and Coulomb (1773). The main interest of these studies was the determination of the maximum thrust on the abutments to design the buttresses. The approach conceptually consisted in locating the points of rupture (defining a collapse mechanism) and calculating, through equilibrium, the thrust on the buttresses. The main contributions by Coulomb were the introduction of considerations on the friction between blocks, with the conclusion that sliding is rare and only rotational failure can be considered, and the method to calculate the maximum and minimum possible horizontal thrusts with the aim of determining the position of the most unfavourable hinges or sections of rupture (Roca et al., 2010).

The theory of elasticity was developing and was progressively applied also to arches, although in general engineers showed some resistance in applying an elastic theory to a material like masonry. To Bresse (1848) and Poncelet (1852) are due the first applications of elasticity theory to the structural analysis of arches, followed by Castigliano (1879) and Winkler (1879). Castigliano proposed the so-called middle-third rule to avoid any tensile stress in the material, resulting, though in very conservative approach valid mainly for the design of new structures, more that for the assessment of existing arches. Winkler studied in particular the influence of cracking and initial deformations, concluding that the elastic solution was highly sensible to these factors; he suggested to solve the problem the introduction of unnecessary hinges to control the position of the thrust line. The elastic approach was considered the most accurate, and had anyway few alternatives, until at least the middle of the 20th century.

A further development arrived with development of graphic statics(Ungewitter and Mohrmann, 1890), supplying a practical method consistently based on the catenary principle. Graphic statics was used for the assessment of masonry bridges and large buildings up to the beginning of 20th century; an example is given by Rubio's analysis of Mallorca Cathedral (1912,). The appearance of different structural approaches from the theory of elasticity in the first half of the 20th century, then, and in particular the formulations of the basic theorems of limit analysis (Gvodzev 1936, 1960), lead to the development of a new approach, related mainly to the work of Heyman (1966 and successive publications). This approach, that constitutes one of the principal modern methods for the structural analysis of arches, as well as some numerical methods that have been developed more recently, will be briefly presented in the following, after an analysis of the principal mechanisms of failure of arches.

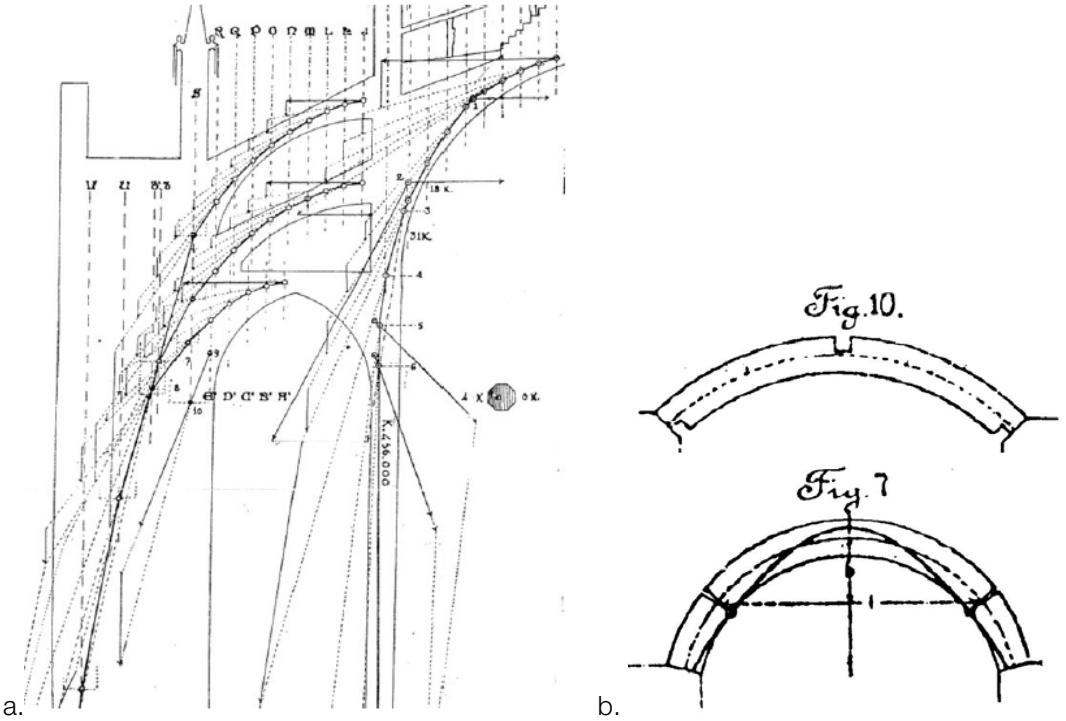

a. b.

Figure 3. Rubio's structural analysis of Mallorca cathedral through graphic statics (Roca et al., 2010); b. solutions proposed by Winkler to control the position of the thrust line (Huerta, 2001)

1.1.3 MEXE method

As described in the beginning of the chapter, the computation of the maximum load that an arch can carry is a problem that was approached in different ways since the first attempts to apply the scientific method to the study of structures. Nowadays this theme is particularly relevant for masonry arched bridges, for which the maximum load corresponds to their serviceability as infrastructures. One method of a certain historical importance for its widespread application for this scope, especially in the UK, is the MEXE method. The name is the acronym of Military Engineering Experimental Establishment.

The method, semi-empirical, is based on the application of the theory of Pippard's elastic method. It consists in the analytical solution of the elastic problem of a parabolic arched beam; the failure criteria is the strength of the material, through the application of Navier's formula. The procedure that commonly was applied consisted in determining the ultimate load according the elastic solution, usually through nomograms, and then introducing some correction factors that turned this approach into a partially empirical method. The factors that were considered are partially geometrical and objective (rise/span ratio, shape of the intrados) and partially subjective or difficult to determine (state of conservation, quality of the material, type of mortar).

This method is no longer applied but some methods, based on this approach, to which some corrections are applied, are still in use.

1.1.4 Limit analysis, lower bound

The formalization of the theory of limit analysis through its fundamental theorems, due to the work of Gvodzev (1936, later published in English 1960), provided a possibility for a different approach on the analysis of masonry arches. The extension of the limit analysis to masonry arches was made by professor Heyman since 1966, with numerous successive contributions.

The limit analysis is based on the concepts of:

- statically admissible configuration: an equilibrated state for which the yield condition is not violated at any point;
- kinematically admissible configuration: any potential failure mechanism for which the external power is positive.

The static theorem (or lower-bound, or safe theorem) states that the load multiplier correspondent to any statically admissible configuration is lower or equal than the collapse load multiplier. On the other hand, the kinematic theorem states that for a kinematically admissible configuration the load multiplier, for which the work of external loads corresponds to the work done by energy dissipation, is bigger or equal to the collapse load. The uniqueness theorem unifies the two approaches, stating that the load multiplier relative to a configuration that is both statically and kinematically admissible is equal to the collapse load multiplier (Heyman, 1966).

The extension of limit analysis to the study of masonry arches started from the works of Kooharian (1952) and Heyman (1966). The hypotheses that were applied to validate this extension were that masonry has an infinite compressive strength, no tensile strength, and that sliding between voussoirs cannot occur; the applicability of these hypotheses is reasonable, with the exception of the last in some cases. Introducing the concept of thrust line, as the locus of eccentricities of the normal force in each section of the arch, the application of the safe theorem is rather immediate. Given these assumptions, indeed, the yielding criteria corresponds to the condition in which the thrust line is tangent to the edge of the section, being it, for the lack of tensile strength, unable to provide a reaction to higher eccentricities. As all the states for which the thrust line is inside the section do not violate any limit criteria, so, a statically compatible state is determined if any thrust line, equilibrated with the external loads, can be found inside the geometrical boundaries of the arch. Heyman introduced also the concept of geometrical safety factor, i.e. the ratio between the minimum thickness that would be required and the real thickness of the arch.

The approach could be extended to the case in which a finite compressive strength is considered, substituting the concept of thrust line with a thrust zone, corresponding to the area needed to not exceed the crushing strength of the material (Figure 4). The friction can be introduced checking the angle of the thrust line in respect to the joints, limiting this angle to $\tan^{-1}\mu$, if we call μ the friction coefficient (Figure 5).

The extension to the case of masonry arches of the theorems of limit analysis, that were originally formulated strictly for perfectly plastic materials, requires some assumptions. It was demonstrated, since the works of Drucker (1953) and Prager (1955), that it is possible to extend the theory of limit analysis to the case of masonry-like materials (Lucchesi et al., 1997, Del Piero, 1998) provided that the plastic domain is convex the flow rule is associative. Experimental observations, though, do not confirm that all these assumptions are completely acceptable. In particular, the associated flow rule can be discussed, as the friction angle is considerably different from the dilatancy angle, considered equal to 0 in the Mohr Coulomb friction model and, even if the surfaces are rough, of low value. Some non-associative models can be applied and extended to limit analysis, losing though the uniqueness of the ultimate load assured by the theorems in case of associated flow rule. These models are in the context of non-standard limit analysis (Lourenço and Orduña, 2005, Gilbert et al., 2006)

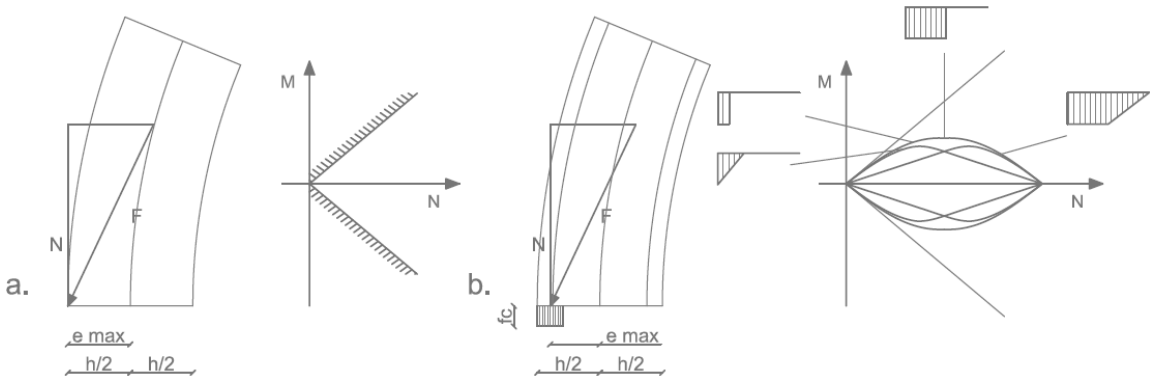

Figure 4. Limit state domains for the sections of the arch, infinite compressive strength (a) and finite compressive strength (b)

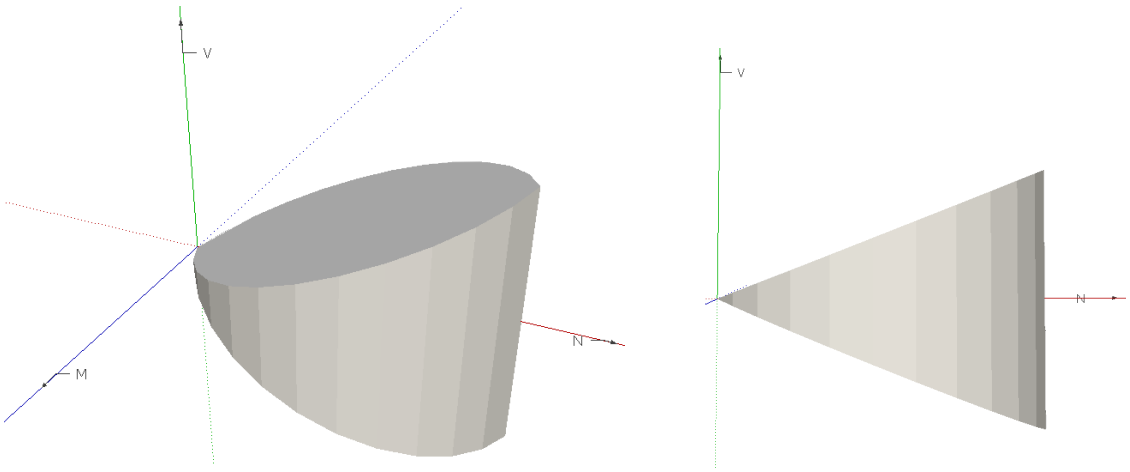

Figure 5. Limit state domains with the introduction of a Mohr Coulomb friction law without cohesion

This method can be easily applied with the use of graphic statics; to simplify the application, though, some computational strategies can be adopted. In Andreu et al. (2007) a cable deformable element is proposed, and used to numerically calculate the shape of an equilibrated funicular system, equivalent

to a thrust line. The deformability of the cable is introduced to avoid numerical problems of convergence; equilibrium is imposed in the deformed configuration. The thrust line corresponding to the failure load is found through a numerical optimization process that maximizes the geometrical safety factor. The failure load, in this approach, is the higher load corresponding to a geometrical safety factor still positive. The method can be applied in 2D or 3D.

Another computational method is presented in Block and Ochsendorf (2007), aimed mainly in extending the approach of limit analysis through the safe theorem to vaulted tri-dimensional systems.

1.1.5 Limit analysis, upper bound

Limit analysis can be applied to the study of masonry arches (and masonry structures in general) also through its reciprocal formulation, the upper bound theorem (kinematic formulation). In this case the upper bound theorem is used, stating that if the work of external loads load is equal to work done in energy dissipation, then the load multiplier is greater than or equal to the ultimate load factor.

The first applications of the method (Pippard and Baker, 1936, Heyman, 1966) are based on the assumptions of infinite strength of the material, no tensile strength and no sliding of voussoirs. Under these hypotheses, the masonry material becomes an assemblage of rigid parts, held up by mutual pressure, and the collapse of the structural elements is characterised by the development of non-dissipative hinges transforming the structure into a mechanism. As the method overestimates the ultimate load (Figure 6a), the application must be based on the evaluation of all kinematic multipliers (De Luca et al., 2004). The procedure, for 2D arches, is not complicated, as, once determined the collapse mode to check (4 hinges or 5 hinges for symmetrical loading) the position of the hinges that minimizes the load multiplier can be determined by numerical methods.

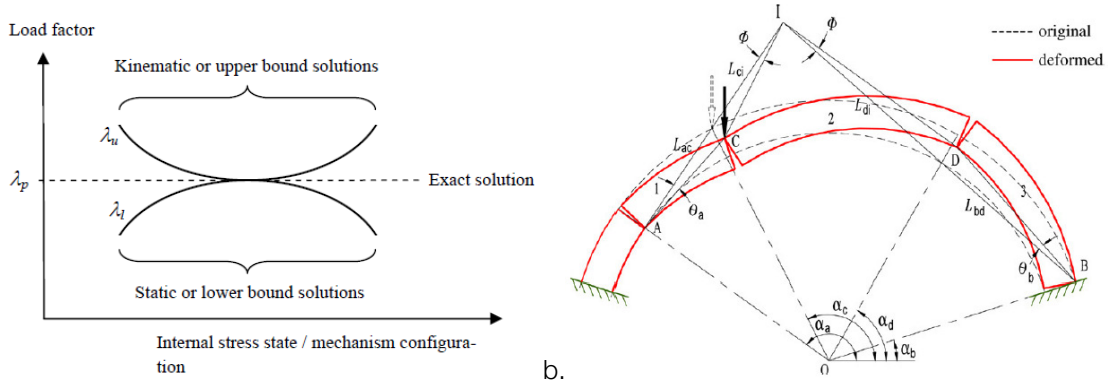

Figure 6. a. Estimation of ultimate load multiplier through upper bound and lower bound solutions (Gilbert, 2007); b. Virtual displacements for a generic four-hinge collapse mechanism (Chen et al., 2007)

The application of different hypotheses is possible (Crisfield and Packham, 1987) taking into account the compressive strength of masonry, the distribution of the applied load through the fill and the lateral earth pressure. Other authors (Boothby, 2001) used a mechanism analysis that accounted for sliding modes of failure involving three sliding surfaces or a combination of sliding surfaces and hinges, as well as the four-hinge mechanism. He concluded that collapse involving a sliding mechanism was more likely to occur in masonry arches with low-rise-to-span ratios and thick arch rings, cathegories to which arches with a low number of voussoirs usually belong.

The application of the kinematic formulation of limit analysis is particularly effective with the implementation of linear programming procedure, to find the mechanism with the lower load multiplier. Chen et al. (2007) proposed a method to estimate the ultimate load through kinematic analysis of a four-hinge arch mechanism, taking into account the compressive strength of the material, the internal dissipation, and the possible presence of steel or FRP reinforcement. The method minimizes the load multiplier through a linear programming procedure that corrects the position of the four hinges.

In Cavicchi and Gambarotta (2006) a method to find upper bounds on the collapse load and the corresponding mechanism was presented. Arches were modelled as beams made up of non-tensile resistant and masonry ductile in compression, while the fill was represented as a cohesive frictional material. A linearization of the limit domains allowed the upper bound on the collapse load and the corresponding mechanism to be obtained as a solution of a linear programming problem.

Some software tools are also available for the limit analysis approached through lower bound theorem (ArchieM) or kinematic formulation (Ring).

1.1.6 Finite Element Methods

Modern methods based on finite element analysis have also been developed for the study of masonry structures and, among them, of arches. Two approaches to the modelling of masonry arches through FEM can be roughly individuated (Drosopoulos et al., 2006):

- Discrete models (micro-models and meso-models)
- Continuum models (macro-models)

In discrete models the structure is divided into discrete parts such as stone arch parts and mortar joints. The possible approaches to this type of models depend of the level of detail with which the joints are modelled. In a deteailed micro-modeling (Lourenço et al., 2006) units and mortar in the joints are represented by continuum elements, while the unit-mortar interface is represented by discontinuum elements. In this approach, Young's modulus, Poisson's ratio and inelastic properties of both unit and mortar are taken into account; the interface represents a potential plane for crack or slip. This allows

to study the combined action of unit, mortar and interface in detail, but requires high computational cost and a considerable number of parameters to estimate to model all materials and interfaces.

In simplified micro-modelling (or meso-models) the units (or the voussoirs) are represented by continuum elements and the behaviour of the joints is lumped in discontinuum elements, aggregating the behaviour of the mortar and the interface between mortar and stone or brick. In these models each joint, consisting of mortar and the two unit-mortar interfaces, is lumped into an average interface, and masonry is thus considered as a set of elastic blocks bonded by potential lines of fracture or slip at the middle plane of the joints.

The behavior of the contact surface between them is described by a unilateral law, possibly with friction, while the discrete elements may be assumed to behave elastically, when, as happens in general in the study of arches, the stress levels inside the voussoirs are low and the study of local states of stress is not the main interest of the model. To simplify the computation, a limit approach can be to consider the voussoirs as rigid bodies and concentrate all deformations and non-linearities in the joints.

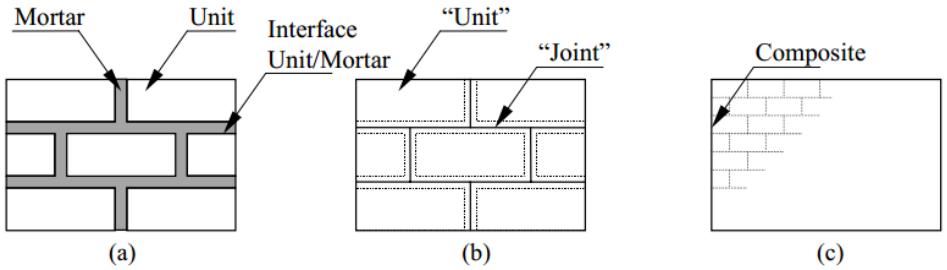

Figure 7. Modelling strategies for masonry structures: a-micromodeling; b-meso-modelling; c-homogenization technique for macro-models (Lourenço et al., 2006)

In continuum models, no distinction between individual blocks and joints is made, and the mechanical behavior is described by a nonlinear constitutive law. The behaviour of this continuum can be deducted from experimental tests on representative volumes of material, containing an adequate number of joints and blocks, whose results can be idealized in the context of an inelastic theory, taking into account, for example, fracture or damage. Another approach can be deriving the mechanical behavior on the basis of a homogenization theory; a review of the possbile approaches is presented in Lourenço et al. (2006).

For the nature of the material and of the collapse mechanisms of arches, the linear elastic analysis is not a reliable method of analysis, as the elastic analytic methods were proven to be not applicable. The non-linearity can be implemented through suitable nonlinear models that take into consideration different ultimate tensile and compressive strength values and different inelastic behaviours. These models are generally related to plasticity theory or to damage theory. As said before, the non-linearity can be smeared in the continuum, in macro-models, or concentrated in the joints, as in simplified micro-models.

A significant number of studies on the structural behaviour of masonry arches has been developed through the use of FEM (Molins and Roca, 1998, Choo et al., 1991, Roca et al., 2010, Pelà et al., 2009). To study the particular behaviour of arches made of few voussoirs the macro model approach is not the most suitable as it does not include information on the position and quantity of joints. A micro-model or a simplified micro-model would be necessary to correctly model the influence of the number of voussoirs on the structural behaviour of arches.

1.1.7 Discrete Elements Method

The Discrete Element Method is a group of methods first defined by Cundall and Hart (1992) as a computing approach for discontinuous bodies. The main features of the approach are that it enables finite displacements and rotations of discrete bodies, including their complete separation, and it automatically recognizes new contacts among these bodies. The method is based on explicit numerical integration of equations of motion of rigid blocks over time. In addition to dynamic calculations, the method offers the possibility of obtaining static solutions using viscous damping.

Initially applied to soil mechanics, this method can be successfully applied to the study of masonry, considered as a group of individual blocks mutually connected, and in particular, for their characteristics, to the study of arches (Bicanic et al., 2003, De Lorenzis et al., 2007, Dimitri et al., 2011, Toth et al., 2009). A variety of applications of this method (Thavalingam et al., 2001) to masonry structures has been developed, differing in:

- the discrete element shape: the shape of the elements can be polygonal (block models) or circular/spherical (grain models); apart from the study of stone masonry with grain models, block models are generally applied, particularly in the case of voussoir arches.
- the calculation of contact forces: contacts can be rigid or soft. Soft contacts allow overlapping between two discrete elements in contact, calculating the contact force on the base of the overlapping (smooth-contact formulation). Rigid contacts exclude the possibility of overlapping of discrete elements (non-smooth contact formulation)
- the method used to identify a contact
- the calculation of equations of motion: generally explicit numerical integration of equations of motions over time.

The discrete-element method is appropriate for modelling masonry structures on the simplified micro level where the blocks are presented like discrete elements with contact elements that simulate the presence of mortar.

In most of the DE methods, blocks are treated as rigid, but this is not the best option if the state of strain and deformations inside a discrete element cannot be ignored; the assumption of rigid blocks,

though, is appropriate for modelling masonry structures which break down mostly because of the loss of stability, due to creation of a mechanism. Some methods overcome the problem considering strains and deformations of the blocks. Among them, a method called Discontinuous Deformation Analysis – DDA (Shi and Goodman, 1992) assumes that the condition for strain and deformation in deformable blocks is homogeneous; non homogenous strain inside a block can be considered though higher-order functions or dividing each block into under-blocks.

The state of strain and deformations inside discrete element can be considered also if discrete elements are discretized with their own finite element mesh. In this approach, the finite-element method is used to calculate the field of strain and deformations within a discrete element, while the discrete element method is used to calculate the contact forces (Owen et al., 1998). Among these typology of analyses, the so-called Combined Finite-Discrete Elements Method (FEM/DEM), developed by Munjiza (2004), takes into consideration a fragmentation process of deformable blocks that can crack so that, as a consequence, several blocks can originate from one block during the analysis. The material nonlinearity is modelled and, on this basis, the initiation and propagation of cracks is described.

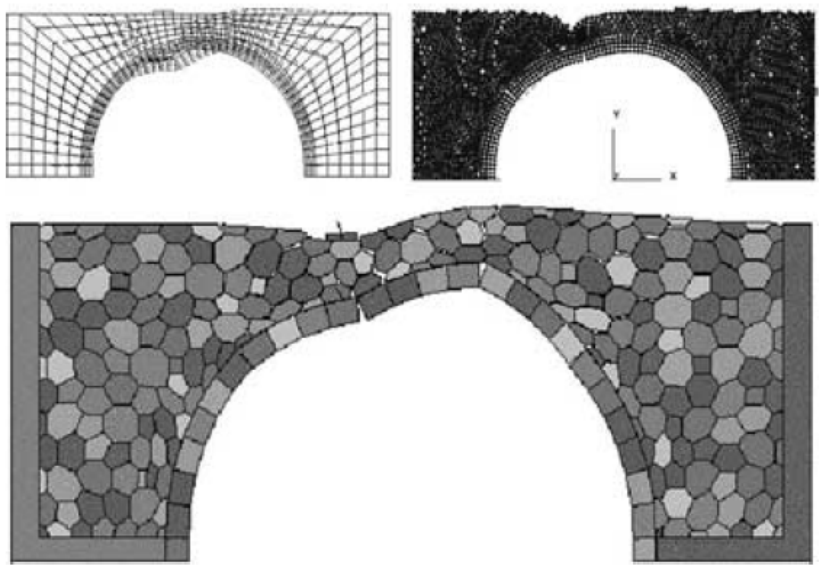

Figure 8. Ultimate load behaviour of a masonry arch, analysed by FEM, particle DEM model and Discrete Deformation Analysis (Bicanic et al., 2003)

1.2 Influence of the number of voussoirs on the structural behaviour of stone arches

The influence of the number of voussoirs on the structural performance of a masonry arch is a theme that was analysed in some papers but that requires a more detailed and organic discussion. In the available literature, the problem was mainly treated in the context of the minimum requirements for the discretization of the arch in a finite number of voussoirs, as a procedure to obtain a numerical approximation of its behaviour. For example, some papers precise the minimum number of subdivisions adopted to obtain a good approximations through block models and kinematic analysis. In these cases, though, in general, the joints are treated as ideal subdivisions and the behaviour that is meant to be simulated is the one of a masonry arch with a larger number of joints, in which the hinges can open in any position.

A specific study, of which this work is a continuation, on arches with a low number of voussoirs and on the methods that can be applied to analyse their performance is presented in Bernat-Maso et al. (2012). Three methods of analysis, funicular limit analysis, kinematic limit analysis and a FE model, were compared and validated through an experimental campaign.

The funicular limit analysis was performed through an equilibrium based numerical method, that calculates the shape under the loads of deformable cable elements to define an equilibrium and optimizes the solution to find the collapse load, minimizing the geometrical safety factor (Andreu et al., 2007). The kinematic analysis was performed according to a procedure presented in Chen et al. (2007), that consists in considering a generic four-hinge mechanism for a quarter-span loading, as the one that was applied in the experimental campaign, and calculating then the position of hinges solving (numerically) an optimization problem to minimize the failure load. The hypotheses of the method were the appearance of purely rotational failure modes and zero tensile stress of the masonry. A FEM micro-model, taking into account the presence and position of joints, was also calibrated and used to compare the theoretical and experimental results.

The experimental campaign consisted in 18 tests on arches with 6 different geometries, with voussoirs built in poor cement mortar and dry joints (Figure 9). The loads were applied at the quarter of the span, step by step, in perfectly vertical direction. The material properties were determined by tests, even if the collapse in these arches is related to geometrical characteristics and not to the strength of the materials, being the stress levels generally low. The failure mechanisms that were observed were in most cases rotational mechanisms with the formation of hinges in the joints; no voussoir broke to for a hinge in between two joints. In some cases the appearance of sliding, or partially sliding mechanisms was observed.

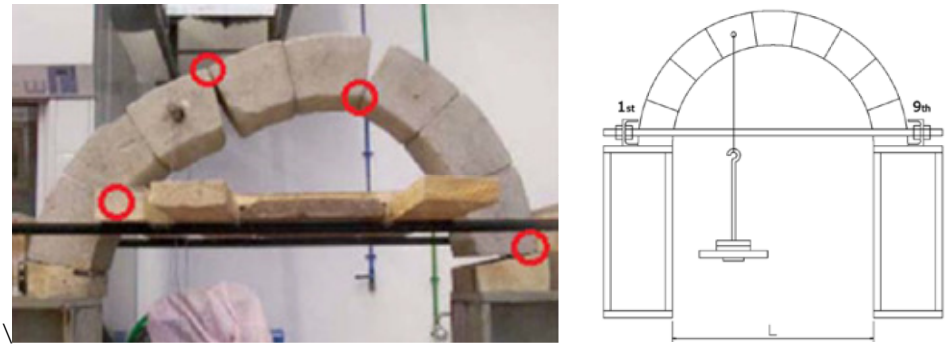

Figure 9. Experimental failure mechanism of one tested arch (Bernat-Maso et al., 2012)

The experimental results were compared to the analytical formulations. The funicular limit analysis was applied considering as safe thrust lines only the ones lying completely inside the arch. The possibility that the thrust line could be out of the arch in the voussoirs, respecting the condition of staying inside the arch (i.e. zero tensile strength) only in the joints, was checked, but produced in some cases non conservative results, and, being this procedure used to calculate a lower limit, was considered not appropriate. The kinematic analysis was applied to the observed mechanisms. To obtain closer results to the experimental values it could have been possible to optimize the solution, moving the position of the 4 hinges, but this would have violated the principle (confirmed by experimental observations) that the hinges could open only in the joints.

The comparison with the experimental results revealed that the funicular analysis did not always produce conservative estimations of the ultimate load, and that the kinematic analysis (considering only rotations) applied to the observed mechanisms gives an upper limit that is in most cases considerably higher (30-150% higher than the correct value. The most reliable method of analysis was the FEM model, which, after calibration and refining of the support conditions, gave results in very good agreement with the experimental values.

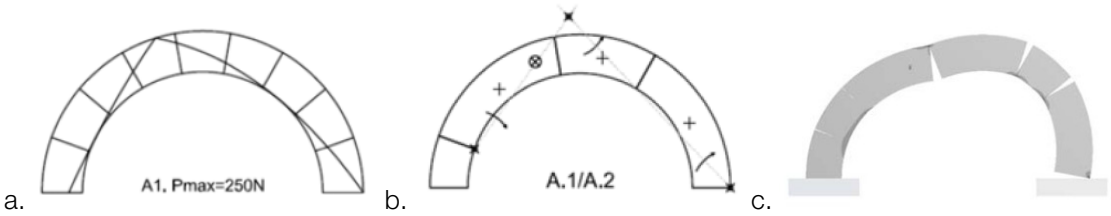

Figure 10. Adopted methods of analysis: a. funicular limit analysis; b. kinematic analysis of the experimentally determined mechanism; c. FEM model (Bernat-Maso et al., 2012)

The different behaviour of arches with a different number of voussoirs, but with the same geometry in terms of span, height and thickness, was studied also in Pèrez-Aparicio et al. (2013), another of the few studies in which both a numerical solution and an experimental test are compared to investigate the behaviour of arches with a low number of voussoirs. Four arches were studied, composed by 9, 17, 27, and 61 voussoirs. by DDA (Discrete Deformation Analysis); the method was implemented in an adapted formulation taking into account the field of deformation inside the single voussoirs, as their dimension in some cases was not negligible. The scope was obtained subdividing each voussoir in sub-elements. The collapse mechanisms that were found are presented in Figure 11.

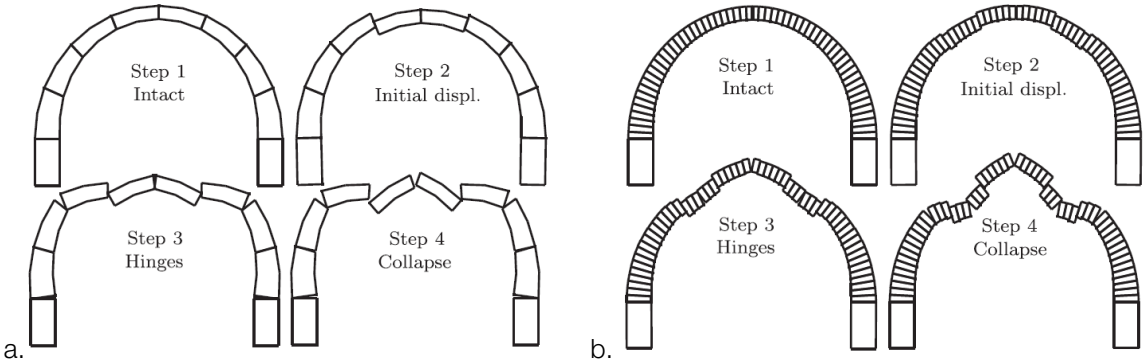

Figure 11. Collapse mechanisms of arches with a different number of voussoirs, numerical simulation: a. 9 voussoirs; b. 61 voussoirs (Pèrez-Aparicio et al., 2013)

The geometry of the arch, to compare and validate the results, was derived by another study (Delbecq, 1982), consisting on experimental tests on real scale masonry arches with the same geometry and a variable number of subdivisions. The arches had a soil filling at the top and an additional growing load applied through jacks. The number of tests that were performed is not sufficient for a statistical validation, as only one or two tests were made for each configuration, but the results could be compared to the numerical solution found through DDA.

The errors between experimental and numerical results were in the range of 0.1-12%, with the larger values for the lower number of subdivisions. The difference in terms of ultimate load between the arch composed of 9 voussoirs and the one with 61 joints, that can be considered as a reference, was in the order of +22% for the experimental test and +36% for the numerical solution. The results of this study confirm a considerable effect of the position and number of internal joints on the behaviour of stone arches, and, at the same time, the sensibility of numerical solutions for the properties given to the interface.

The influence of the number of joints of a stone arch on the its load capacity, through numerical simulations, is treated also in Drosopoulos et al. (2006). In this case the solution were determined through finite element simplified micro-models, in which all interfaces were modelled. A parametric investigation concerning the interaction between their number and the ultimate load was performed.

The interfaces were modelled with a unilateral contact law, with friction according to the static formulation of Coulomb law, admitting in this way the possible occurrence of sliding between voussoirs.

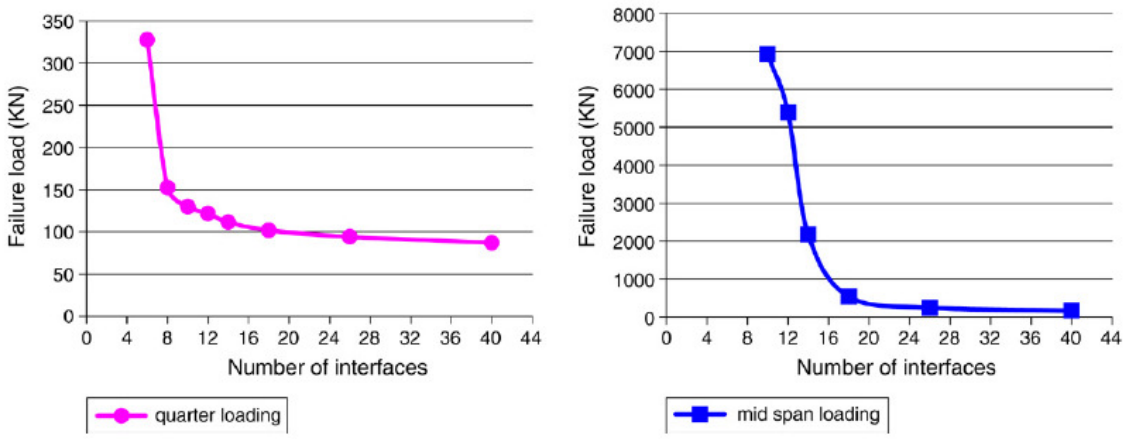

Figure 12. Failure for different number of interfaces considered in the FEM model. Quarter span loading (left) and middle span loading (right) (Drosopoulos et al., 2006)

The validation of the results, in absence of experimental data, was based on the comparison with limit analysis results (kinematic approach, though the software RING), obtaining a satisfactory agreement (3% difference). For the aims of this work: the most meaningful result of that, for the lower number of interfaces, the ultimate load, in all load combinations, is considerably higher than the asymptotical value that is found, as expected, for a high number of joints.(Figure 12).

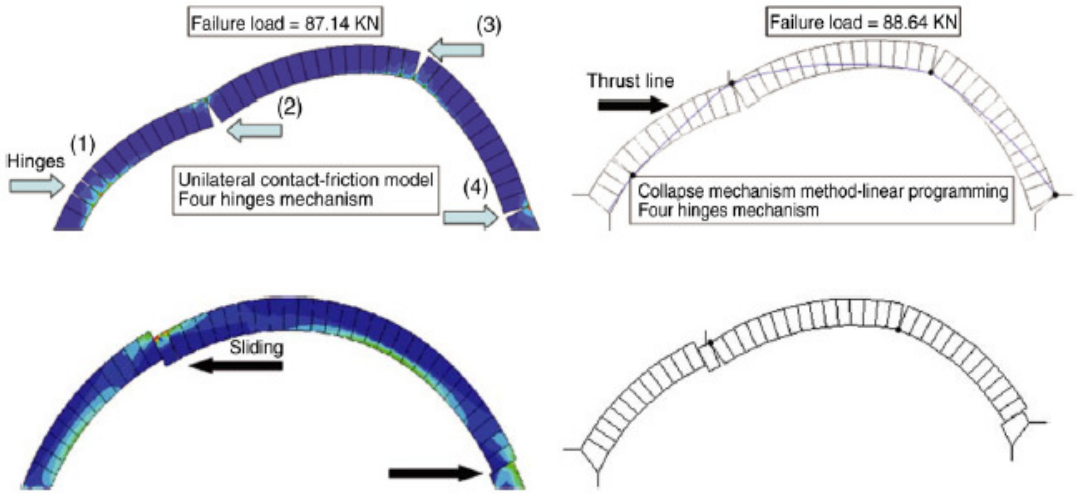

Figure 13. Comparison between FEM (left) and limit analysis (right) failure modes for quarter span loading. a. friction coefficient 0.6; b. friction coefficient 0.3 (Drosopoulos et al., 2006)

The effect for 7-11 interfaces can be quantified in 30-100% for quarter span loading; for middle span loading the effect that was found is much bigger, with an increase in the ultimate load of up to 30 times. The results are obtained with a rather high frictional coefficient (0.6), set to force the mechanism to be rotational and prevent sliding. For more realistic values, the authors noticed that different failure mechanisms take place, involving sliding and rotations around hinges, and smaller ultimate loads are estimated (a reduction of 35% of the ultimate load for an arch with 40 interfaces).

Also Rizzi et al. (2014) studied the influence of some geometrical features of masonry arches, including the number of voussoirs and the position of joints. The authors concentrated on the problem of the minimum thickness of a masonry arch subjected only to its self-weight (the so-called Couplet's problem), deriving the analytical formulation of the position of hinges and of the minimum thickness. The re-derivation of the analytical expressions of the thrust line of a semi-circular arch is due to the fact that slightly different solutions were provided by different authors (in particular, Milankovitch in 1904-1907 and Heyman in 1966), considering different hypotheses on the stereotomy of voussoirs.

The stereotomy, indeed, has an influence on the structural behaviour of arches even if the real number of joints is not considered, but only hypotheses on their orientation are made, for example considering the equilibrium of voussoirs with vertical joints or with joints perpendicular to the intrados. This observation was accepted, years later, by Heyman himself (Heyman, 2009), who wanted re-discuss the topic and correct the mistake present in his first formulation. The theoretical formulations of Couplet's problem, and of the hypotheses that are made on the stereotomy, are presented in Makris and Alexakis, (2013) and will be discussed in more detail in the following.

The analytical solution provided in Rizzi et al. (2014) was compared by the same authors to the numerical results obtained by DDA formulation. It was found, as reported also in other papers (Gilbert et al., 2006), that the friction coefficient is the parameter to which the sensitivity of these analyses is greater, as it modifies the collapse mechanism if sliding of voussoirs is allowed. A comparison with analytical results (Figure 14) constitutes a validation of the model.

The authors, as expected, found a smaller critical thickness for the arches with less voussoirs; what is less expectable is that the numerical solution does not converge to the analytical for the bigger number of voussoirs, and the position of the hinge moves slightly from the analytical formulation. The authors related this result to the fact that, for a great number of joints, the model did not correspond anymore to a continuum material and a frictional deformation could have been relevant in the results, even if a high frictional coefficient was applied.

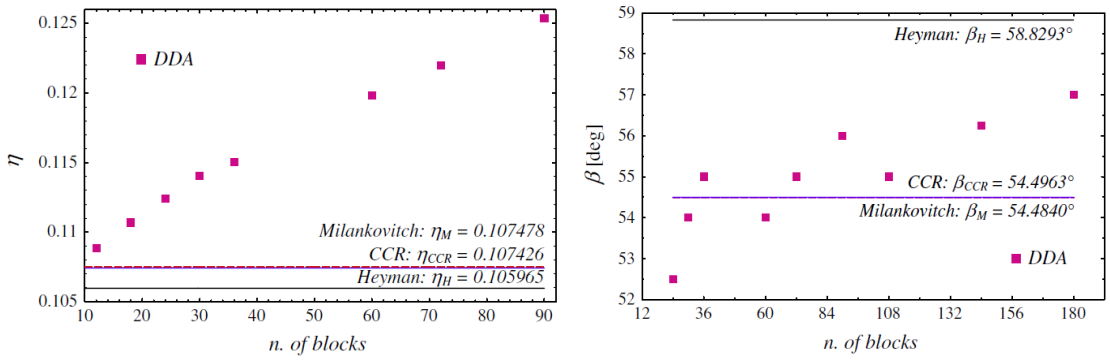

Figure 14. DDA results for different number of voussoirs and comparison to analytical formulations. Left: minimum thickness to radius ratio; left: angular position of the quarter span hinges (Rizzi et al., 2014)

The same authors (Rizzi et al., 2014) studied the influence of the position of the quarter span joint in 4-voussoir arches. The analysis revealed a remarkable effect of the position of the joint, even for little changes of the angle (35°-45°-55°, Figure 15). A complete evaluation of the effect of the position of the quarter span hinge is shown in Figure 16. The numerical results were compared to the limit analysis solution, obtained forcing the thrust line to pass through the imposed hinge, and allowing it to lie outside of the arch thickness in the voussoirs. This method, although not taking into account in any way the internal stoical admissibility of the solution, i.e. the possibility of cracking of a voussoir and consequent formation of a hinge in a different location, is a possible approach to the analysis of arches with a low number of voussoirs that will be taken into account in the following. The correlation with the numerical results appears satisfactory.

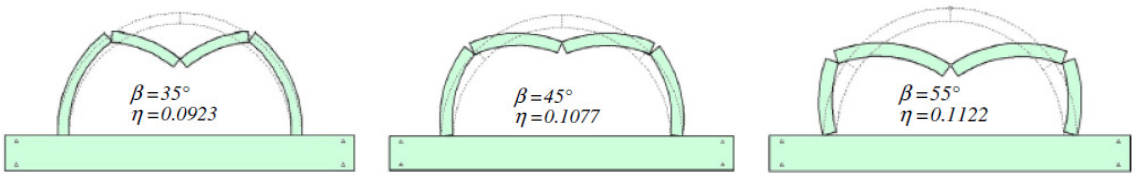

Figure 15. Arches with 4-voussoirs, critical thickness to radius ratio η for different position of the joints (Rizzi et al., 2014)

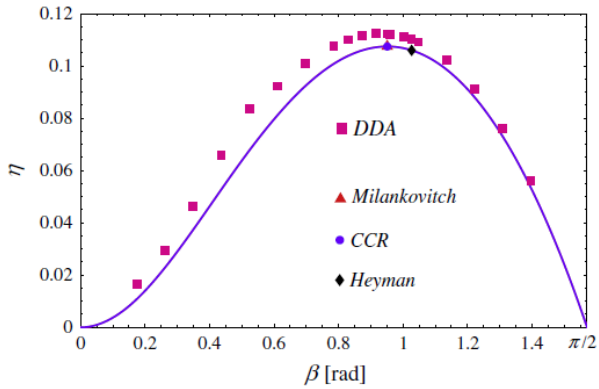

Figure 16. Minimum thickness to radius ratio for different position of the joint in 4-voussoir arches (Rizzi et al., 2014)

A study on the influence of stereotomy, i.e. on the position of the joints and shape of both the voussoirs and the arch itself, is presented in de Arteaga and Morer (2012). The authors compared the load carrying capacity of several arches analysing them both in an idealized shape and in the real configuration. The idealized shape was built approximating the arch with two circumferences (for pointed arches), considering a thickness resulting from three measures taken *in-situ* and uniformly dividing the arch in the real number of joints, regardless, though, of their real position and orientation (considered normal to the intrados). The real geometry, instead, was defined through the integrated use of topographic methods, photogrammetry and laser scanner, approximating the measured point with splines but keeping all the relevant geometrical information.

The structural analysis was performed for the two models of 21 case studies, in the hypotheses of infinite compressive strength, null tensile strength, and high frictional coefficient to prevent sliding. The results of the analysis showed a consistent influence of the geometry in determining the ultimate load. In the 19% of cases the difference was acceptable; in one third of the cases, the difference between the results of an idealized geometry and the real geometry were between 10% and 40%, while in the 14% of cases this difference was higher than 40%. The higher sensitivity was found for the more slender arches and, as expected, for those whose geometrical error was higher. The simplified approach, followed in the common practice, lead to non-conservative results in some cases, evidencing the role of stereotomy and geometry in the structural behaviour of arches.

Another approach to the analysis of arches with few voussoirs is presented in Sánchez-Beitia (2013). The method consisted in considering the limit condition of the arch considered as an assembly of several blocks, just before collapse, when movement is imminent. In this situation it is possible, indeed, as the structure becomes isostatic, to determine a unique solution for the magnitude and direction of the internal forces applying only equilibrium conditions. Among all the possibilities of movement of all the combinations of blocks that it is possible to define in the arch, the imminent movement is the one that requires the minimum friction (Sánchez-Beitia, 2013). The stability conditions of a group of voussoirs can be determined in isostatic conditions considering 4 possibilities of movement (2 rotations and 2 translations, one per each direction), and deriving the relative analytical expressions.

The method was validated by an experimental campaign: an arch, with a 2 m span, was built with 17 timber voussoirs without mortar joints. From the analysis of the all possible mechanisms (144 cases) a solution was determined for the incipient movement of the group that required the minimum friction. The comparison with the experimental test did not confirm exactly the prediction, but a similar collapse mode was reproduced. The authors explain the differences with possible slight differences in the geometry of the voussoirs between the real arch and the idealized geometry, due to the cutting process. As a conclusion the authors underline that the stereotomy of arches has a primary role in the stability of the arch itself. The test setup and the approach that was followed can constitute a useful element for the experimental campaign that will be carried out in the context of this work.

Figure 17. Experimental campaign on timber arches, collapse mechanism (Sánchez-Beitia, 2013)

A procedure to extend, and adapt, the approaches for the analysis for unreinforced arches, based on limit analysis, to arches with different configurations, for which the hypotheses of the limit analysis are not completely applicable, is given in Roca et al. (2007). In the specific case, the study focused on reinforced brick masonry arches or cylindrical shells, extending the conventional plastic analysis to this typology of arches. Similarly to what is expectable for arches with a low number of voussoirs, indeed, in reinforced masonry arches, or concrete arches, the tensile strength of the material (due to the presence of steel reinforcement) allows to consider different boundaries for the limit position of the thrust line.

As the material provides a consistent tensile strength, the possible eccentricity of the normal force can be higher than half of the height of the section, resulting in a position of the thrust line out of the geometrical boundaries of the arch. The possible eccentricity of the thrust line depends on the tensile strength (on the reinforcement in this case) and on the normal force that is applied in each section. For this reason, different boundaries, named strength boundaries in this study, can be defined. These boundaries do not have a constant distance from the intrados and extrados of the arch, as this distance depends on the applied normal load, and is subjected to abrupt changes when concentrated loads are applied (Figure 18). Different graphical approaches are proposed in the study to represent the results of the analysis: the real thrust line can be drawn considering the change in thickness of the strength boundaries, or the distance between the strength boundaries can be normalized, or, lastly, the ratio between the maximum moment and the calculated moment can be represented. In these two last approaches, though, the physical meaning of the thrust line would be lost.

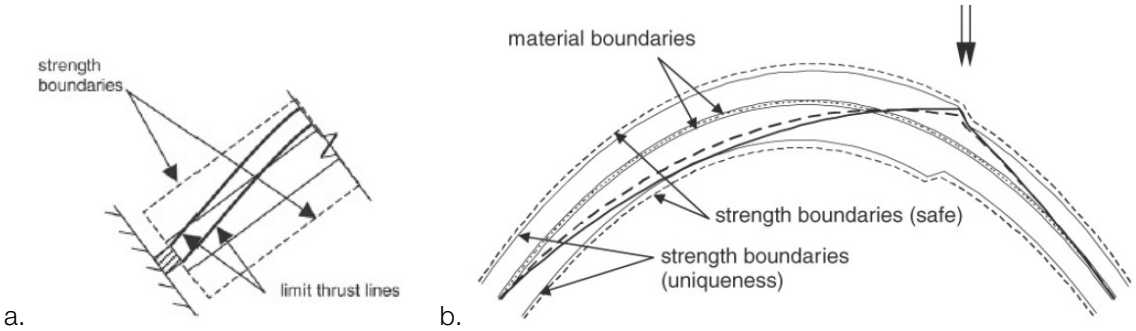

Figure 18. Definition of strength boundaries for the position of the thrust line in reinforced masonry arches. a. limit thrust lines at the supports; b. changes on strength boundaries due to concentrated loads (Roca et al., 2007)

The results of this analysis were compared to FEM analysis and to experimental results on real scale arches and vaults built in reinforced masonry, confirming the applicability of the methodology with results in good agreement with both the numerical analysis and the experimental campaign. The approach of this study can be useful in the scope of this work, in order to adapt the limit analysis methods to the study of arches with low number of voussoirs, in which, similarly to this case, the position of the thrust line can be defined not only by the geometry, but also by the tensile strength of the material and by the position and number of the joints.

Another field of research on arches related to the theme of this work is the behaviour of partially reinforced masonry arches. In these arches, the presence of reinforcement (typically FRP) in a part of the intrados or extrados of the arch provides a (local) tensile strength of the material and moves the hinges of the collapse mechanisms, improving the ultimate load. In the areas where reinforcement is present, the common assumption that is made is that, for the introduction of tensile strength, hinges cannot develop (at the opposite side of the reinforcement). A study on the effectiveness of this typology of strengthening intervention on arches is provided in Buffarini et al. (2006).

The typical applications of this intervention, though, require the introduction of FRP reinforcement for a significant portion of the intrados of extrados, much bigger than a single voussoir even for arches with a very low number of joints; nevertheless, the approach and the estimation of the effect of this intervention can be useful for the present work. The study, as shown in Figure 19, considered the application of reinforcement for different ratios of reinforced and unreinforced length of the arch, and for different loading conditions. The most relevant portions of the graphs are the one relative to a very small reinforced length (not more than 0.3-0.4, to reproduce the condition of an arch with few voussoirs).

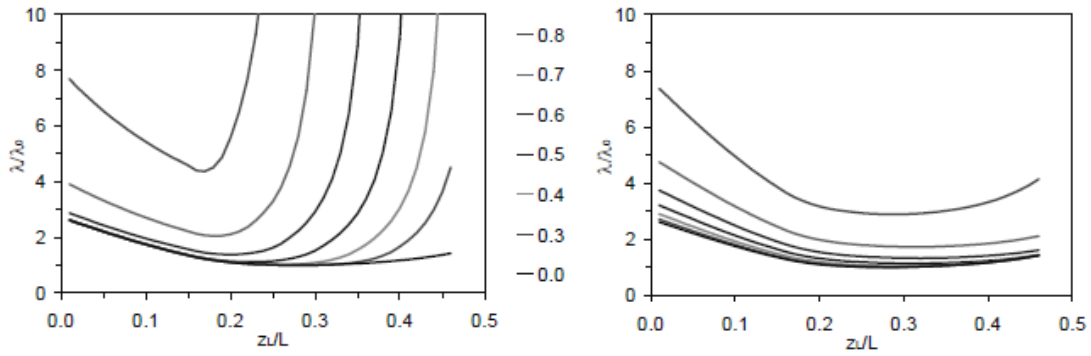

Figure 19. Effectiveness of the partial introduction of FRP reinforcement, for different ratios between reinforced and unreinforced area, in the ultimate load of a masonry arch; a- reinforcement at the extrados; b- reinforcement at the intrados. In x axis the position of the load (Buffarini et al., 2006)

Chapter 2.

Case study: experimental tests on the arch of the Palladian *Basilica* in Vicenza

2.1 Typologies of arches with a limited number of voussoirs

Arches with a limited number of voussoirs, that are studied in this work, can be characterized by some common typological features, that identify this type of arches in the general context of masonry arches. The main typological characteristics that can be identified for voussoir arches, meaningful in the scope of structural analysis, are:

- geometrical dimensions (span, rise, thickness)
- material
- shape of the intrados (round arch, pointed arch, etc.)
- shape of the extrados
- stereotomy and number of voussoirs

One first assumption to characterize the typology can be made on the material. Voussoir arches, indeed, are made in stone (regular) masonry. Not all stone masonry arches can be included in this typology, as there exist also irregular stone masonry arches that are not of interest in this context. There are some examples with the use of more than one type of stone, typically one of dark colour and one light, to evidence the geometry of the voussoirs. The type of stone depends on the location of the building, but, from a structural point of view, the it has little influence in the behaviour of the arch. For stone materials, indeed, with the exception of very weak stones like tuff (rather rare in stone arches), we can make the hypothesis of a high compressive strength, compared to the common stresses in arches, and of a certain, lower, tensile strength that might be considered. As a result, the assumptions that will be done on the mechanical properties, are acceptable in most of the cases for the whole typology of interest.

The geometrical proportions of arches are an important typological feature and are parameters that more often were prescribed in the historical literature on arches. For centuries, when the structural analysis of arches was not developed, the main design criteria were the prescriptions, available in many treatises of different historical periods, on the geometrical proportions to adopt. Generally the treatises recognised ratio between the thickness and the span (or the radius) of the arch the main parameter to control the structural safety, even before any structural theory on arches. Some of the prescriptions of historical treatises, and some rules deriving from the first theories on arches developed in the 18th and 19th centuries, are collected in Huerta (2004) and Oliveira et al. (2010) and presented in Table 1.

Table 1. Prescriptions on the geometry of arches according to historical treatises (Oliveira et al., 2010, Huerta, 2004)

Date	Author	Deep arch	Shallow arch	Limitations
15th cent.	Alberti	$t = s/10$	-	
16th cent.	Martìnez de Aranda	$t = s/6$		$s < 3\ m$
16th cent.	Martìnez de Aranda	$t = s/8$		$3\ m < s < 6\ m$
16th cent.	Martìnez de Aranda	$t = s/10$		$s > 6\ m$
1550	Gìl de Hontanon	$t = s/5 \sim s/6$		
1714	Gautier	$t = 0.32 + s/15$		$s > 10\ m$
1777	Perronet	$t = 0.325 + 0.035s$	$t = 0.325 + 0.0694\rho$	
1809	Gauthey	$t = 0.325 + s/48$		$s < 16\ m$
1809	Gauthey	$t = s/24$		$16 < s < 32\ m$
1809	Gauthey	$t = 0.67 + s/48$		$s > 32\ m$
1845	Déjardin	$t = 0.30 + 0.045s$	$t = 0.30 + 0.025s$	
1854	L'Eveillé	$t = 0.33 + 0.033s$	$t = 0.33 + 0.033\sqrt{s}$	
1862	Rankine	$t = 0.19\sqrt{R}$		
1870	Dupuit	$t = 0.20\sqrt{R}$	$t = 0.15 + \sqrt{R}$	
1885	Croizette	$t = 0.15 + 0.20\sqrt{\rho}$		
1914	Séjourné	$t = 0.15 + 0.15\sqrt{s}$		

Before the Renaissance, the historical treatises are few and do not fix explicit proportions for arches. A famous rule, that influenced by many authors until the development of the first structural theories, is due to the Italian architect Leon Battista Alberti (1404-1472), who expressed in his *De re aedificatoria* the principle that the thickness should be 1/10 of the span. The source of Renaissance treatises was the experience of author, based on the building tradition, and the observation of the remains of the classical antiquity, particularly of the Roman buildings. For this reason we can consider this rule as the proportion of the classical arch, to which architects in the Renaissance were aiming as a “perfect” arch (to the point of considering the round arch as the best option, also structurally). Roman arches nevertheless, although being approximately around the range stated by Alberti, do not present constant proportions.

The simpler rules of the Renaissance produce an design of the thickness of the arch slightly too conservative for the bigger spans (Figure 20), but are in the same range for the spans that are more common for the typology of arches, with low number of voussoirs, object of this study. For the smaller spans, the thickness of the arch is typically bigger, with deeper arches as a result.

These different proportions, as will be described in the following, can have an influence in the collapsing mechanism of the arch, increasing the probability of a sliding failure instead of a rotational mechanism. As a conclusion, considering the practical origin of many of these rules, we can state that the thickness/span ratio for arches of small span, the ones of major interest for this work, is typically in the range of 1/6-1/10 (Figure 21).

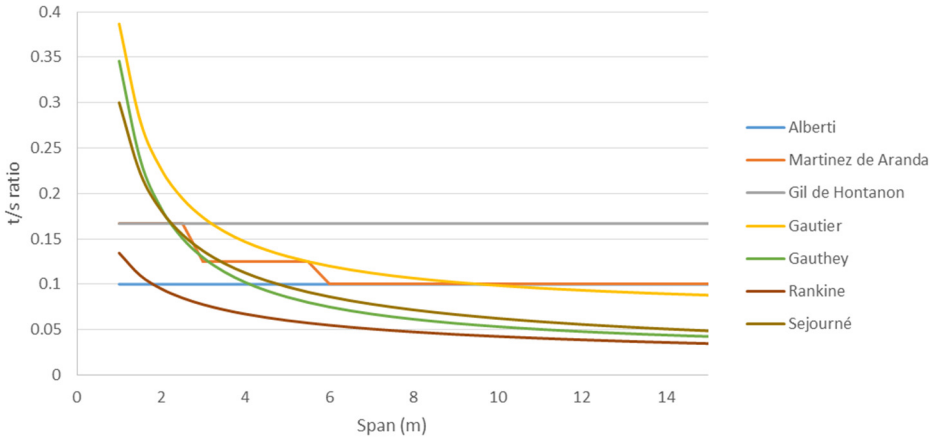

Figure 20. Historical rules for the thickness of arches (Oliveira et al., 2010, Huerta, 2004)

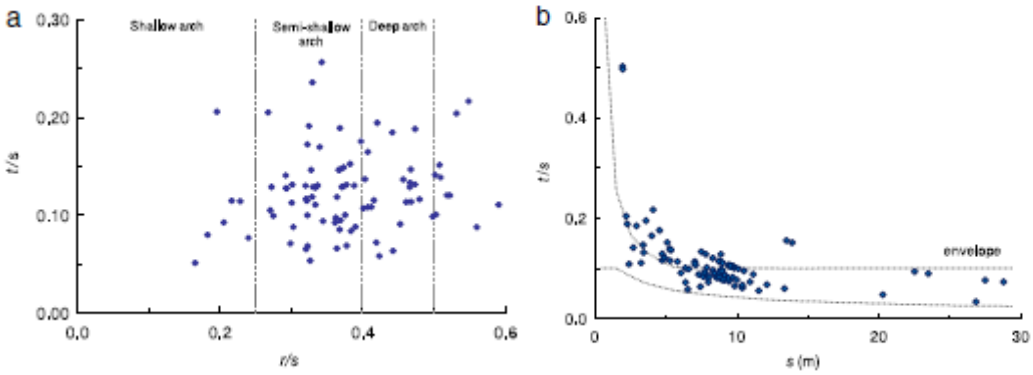

Figure 21 Typological study on 54 bridge arches in Northwest Iberian peninsula: a. thickness to span ratio in function of the depth (rise to span ratio) of the arch; b. thickness to span ratio in function of the span (Oliveira et al., 2010)

As said, among the other geometrical features that typologically define the class of arches which is analysed in this work, the span has a major role, closely linked to the number of voussoirs and their maximum dimension. As the definition of a critical number of voussoirs is among the objectives of this work, this theme will be discussed in the following. Nevertheless, if we include in this typology arches with up to 13-15 voussoirs, and we consider the common dimensions of stone voussoirs, we can conclude that spans of these arches are typically lower than 6-8 m. More frequently, they are in the order of 2-4 m, the range of dimensions of portals, windows, arches of façades and lateral naves of churches.

Another parameter that strongly characterizes both typically and structurally an arch is the shape of intrados. A variety of arch shapes were built in the past, and this type of arches with few voussoirs, being commonly used for windows or small openings, or in general in not structurally challenging contexts, can present the whole complex of typologies of arch shapes. Although a complete catalogue of the possible typologies is not within the aims of this work, a brief list and nomenclature are presented in Figure 21 and Figure 22.

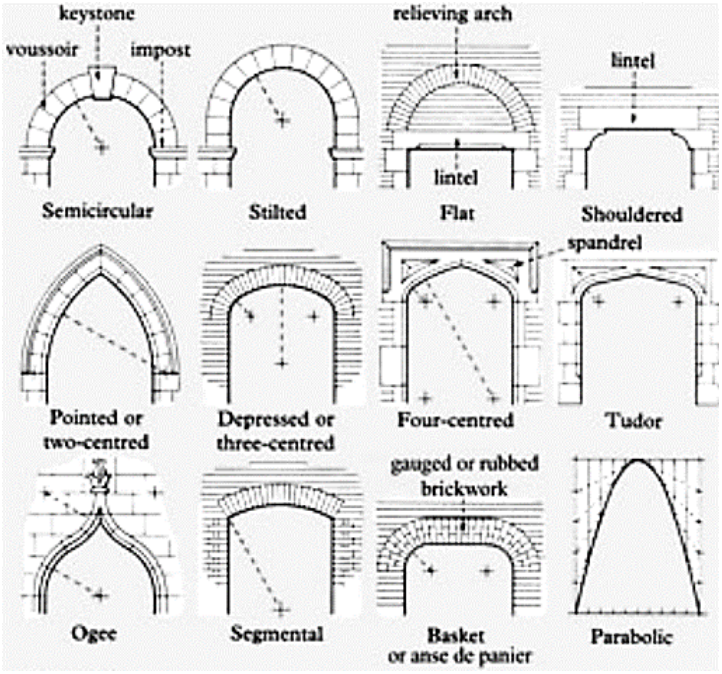

Figure 22. Nomenclature of arch parts and shapes (from www.lookingatbuildings.org.uk/glossary)

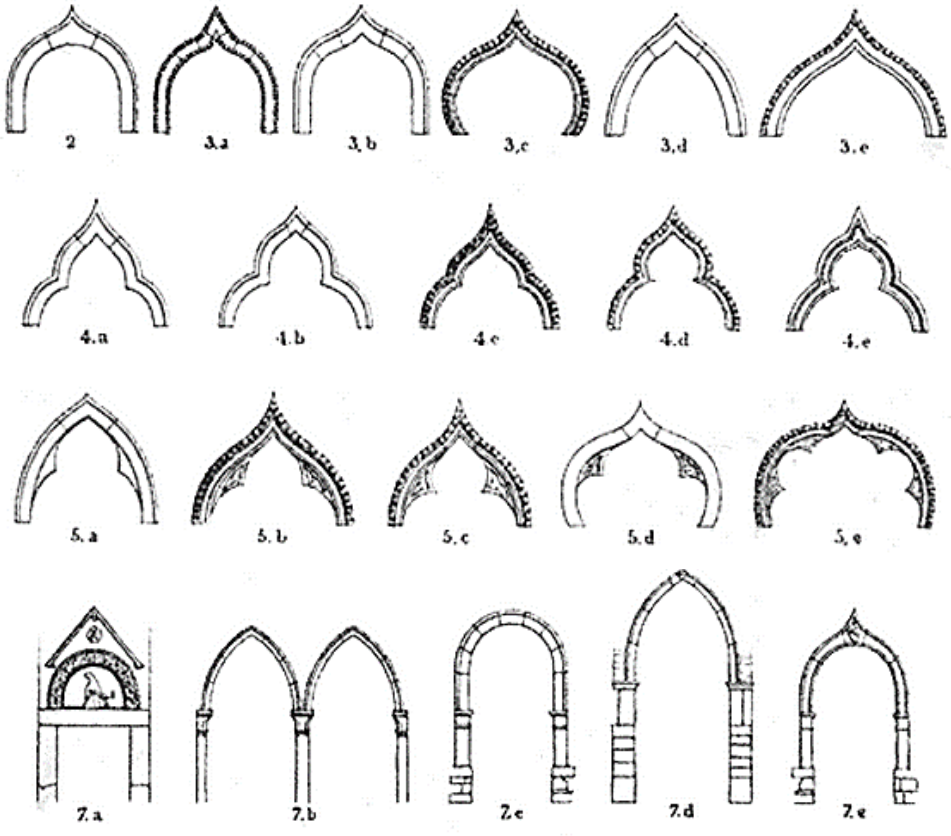

Figure 23 The orders of Venetian arches as classified by John Ruskin (Ruskin, 1851)

The shape of the extrados in these voussoir arches does not correspond necessarily to the shape of the intratrados, and in some cases an extrados cannot properly be defined. The cut of the stones, indeed, can result in a variety of voussoirs combinations, especially when the neighbouring masonry is made in stone blocks that have to fit with the voussoirs of the arch. In this case the arch is called stepped arch, or shouldered arch. The voussoirs can have a pentagonal shape, in the simplest case, or more complex shapes that allow also the interlocking with the blocks of the wall. This typology is common in the architecture of the Renaissance and later, but was not much used, although it was known, in the Roman, Romanesque and Gothic architecture.

The typology that was far the most common before the Renaissance was the one with an extrados, in the majority of the cases with the same shape of the intrados. Some variations can be applied to this model, with the use of a different shape for the extrados. For instance, in some cases, particularly in Italy, we can find an extrados with the shape of a pointed arch combined with a perfectly semi-circular intrados. A slight variation of the shape of the extrados, resulting in a bigger thickness at the keystone, was in some cases adopted for technical reasons, to limit the use of acute angles in the voussoirs, whose execution was problematic.

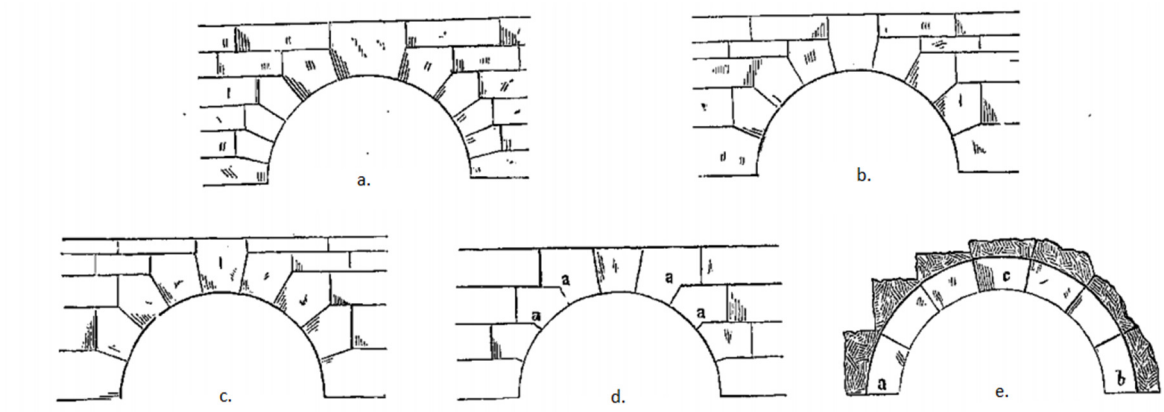

Figure 24. Shapes of voussoirs: a.-c. stepped arch with pentagonal voussoirs; d. stepped arch with interlocking of voussoirs; e. semi-circular extrados

The combination of similarly shaped voussoirs require a proper design of each shape, and a precise process of carving, especially if no mortar, as often happens for this typology, is applied. The complex of technical procedures and geometrical constructions to define the real shape of each voussoir in the three dimensions takes the name of stereotomy. Literally the term indicates the three-dimensional spatial cut of the stones, and by extension it used to indicate the rules and the construction on which it is based. After the first written source in stereotomy, dating back to the 13th century (Villard de Honnecourt's illustrations) the most important treatises were written in the 17th and 18th century, mainly with French contributions; the technique, though, even without written sources, was passed through the generations of masons throughout history even before.

As the problem of structural safety was approached, in the past, mainly from a geometrical point of view, stereotomy was recognised to have a primary role, not only for aesthetical issues but also, and mostly, to ensure the safety of the building, the so-called *firmitas* (Sakarovitch, 2003). From a structural point of view, the stereotomy has an importance for the interlocking of blocks, and consequently for the higher influence of the lateral walls on the behaviour of the arch, and for the direction and number of the joints, the main focus of this work.

The problem of the optimal direction of the joints was treated with two different approaches in the building tradition. A first approach consisted in placing the joints in the direction of a unique centre, whatever the shape of the intrados should be. This configuration of joints is called “radial” or “Vitruvian” (Heyman, 2009). Maybe for difficulties in the realisation, this approach was largely substituted by a second, consisting in designing the joints perpendicular to the intrados. This latter approach originates from the belief that identified in the perpendicular joints the best configuration for the structural safety, and from the major technical feasibility (Aita, 2003). For semi-circular arches the two approaches are the same, but a difference appears for pointed arches and other shapes. Other solutions, mainly with multiple centres for the direction of voussoirs, were developed for specific types (the Tudor arch, for example).

After the first structural theories on arches, and in particular after the concept of friction was progressively developed, the problem of the best orientation of joints was faced with a technical approach and the “intuitive” orientation of joints started to be discussed. A solution was proposed by Gerstner (1789), with the aim of requiring zero friction between voussoirs, being the joints perpendicular to the calculated line of pressure (Sakarovitch, 2003). Typologically, though, the most common orientation of joints remained the Vitruvian, and, for poli-centrical arches, the perpendicular.

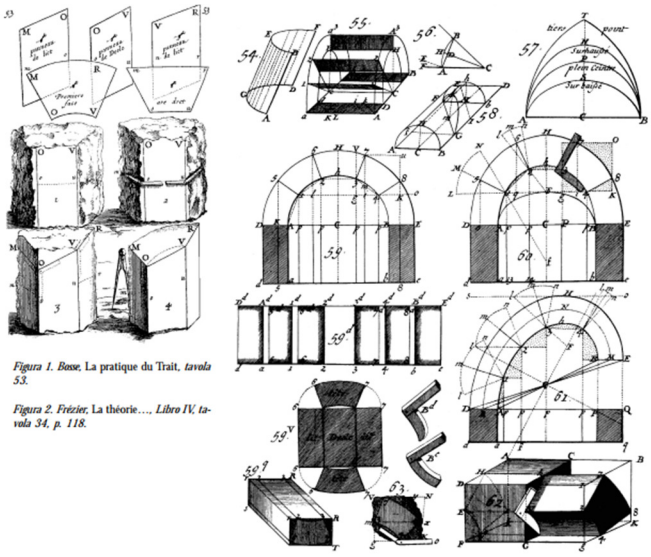

Figura 1. Bosse, La pratique du Trait, *tavola 53.*

Figura 2. Frézier, La théorie…, *Libro IV, tavola 34, p. 118.*

Figure 25. Stereotomical design of the voussoirs of arches (from the historical treatises La pratique du trait by Abraham Bosse, 1643, and La théorie et la pratique de la coupe de pierre by Amédée François Frézier, 1737)

The stereotomy of voussoirs has an influence on the structural behaviour of arches, even if no assumption is made on the number of voussoirs (or on the tensile strength of the material of the voussoirs), as discussed in Heyman (2009) and in Makris and Alexakis (2013); for this reason it is included here among the features that characterise structurally the typology of arches with a limited number of voussoirs. An analytical proof of the influence of stereotomy and a discussion on the different possibilities to define a thrust line depending on it (including the difference between statically compatible thrust lines and Hooke's catenary curve) will be presented in the chapter on limit analysis.

A last characteristic, but most relevant, that characterizes the typology of arches studied in this work is, obviously, the number of voussoirs. Numerical limitations to the number of voussoirs for the arch to be included in this typology will be discussed in the following. The subdivision in a certain number of voussoirs depended mostly on the dimensions of the available material, and on the possibility of lifting and placing blocks of big size.

Architectural principles have a secondary role in defining the number of voussoirs of an arch and their shape, as can be noticed in the works also of the architects that were most concerned in building a "model" architecture, inspired by the classical antiquity and rigorously generated by geometry. Among them, for example, Leon Battista Alberti, appreciated theorist of architecture, in the Malatestian Temple built a series of arches of the same dimensions with a different subdivision in voussoirs for each arch, and using voussoirs of different size in the same arch. In some cases, though, it is possible to recognise a typical subdivision in a certain number of blocks, with a characteristic pattern, in different works of one architect or inside one specific cultural context, as will be discussed for the works of Andrea Palladio.

As a typological feature, it is worth noting that, most commonly, these arches present an odd number of voussoirs, to have a key stone in the middle. This is not a structural necessity, as it is possible to realise an arch with a joint in the middle of the span, or in any case without any key stone, and some examples of this type were realised. For the building tradition, anyway, and for constructive and aesthetical reasons, the typology with a key stone remained largely the most used.

2.2 The Palladian *Basilica* in Vicenza

As the approach of this study is to compare analytical results with the tests on one specific arch, a case study was selected to be reproduced in a model for the experimental campaign. The case study was selected to be representative of the typology of arches with a low number of voussoirs, and to provide results comparable to the ones obtained through the analysis and meaningful from the structural point of view. The case study that was selected is the arched *loggia* of the Palladian *Basilica* in Vicenza, for the reasons that will be discussed.

The Palladian Basilica is a building in Vicenza (Italy) which dominates the view of the central square of the city (Figure 27). The building, originally designed by Tommaso Formenton, was built in 1481-1494, in gothic style, close to the old civic tower (11th century). The original name, that is sometimes used also today, was *Palazzo della Ragione*, name given in Italy to the central palaces, seat of the government of the city, particularly during the Middle Ages and the Renaissance. The element, though, for which this palace is famous, is the addition made 60 years later, the *loggia* that renovated its façades after a partial collapse, designed by a young Andrea Palladio. His project won a competition among the most influent architects of the Venetian Renaissance, including Sansovino, Serlio, Sanmicheli, Giulio Romano among the others. The project was selected in 1546 and the construction started in 1549, lasting until 1614. After this intervention the building was named *Basilica*, as a reference to the Roman architecture that inspired the design. The project is presented by the author himself in his "Four Books of Architecture" The Books contain drawings (plans and prospects, in a very modern conception for the time, as reproduced in Figure 26) with dimensions expressed in feet of Vicenza, the unit used at time in his city, equal to 0.356 m and reproduced in the beginning of the treatise as a reference.

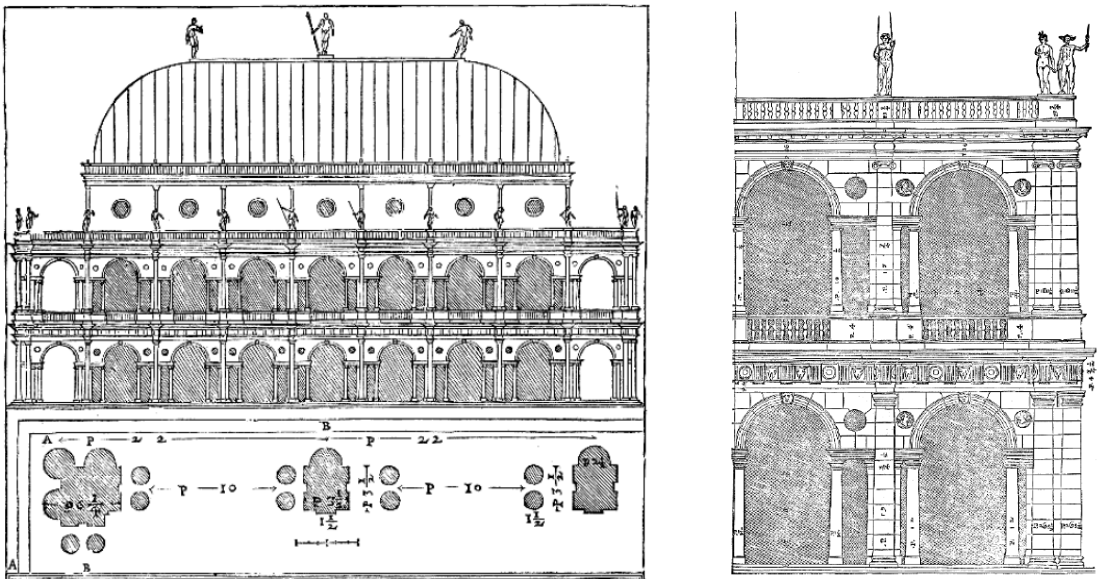

Figure 26. Original drawings by Andrea Palladio of the project for the intervention in the *Basilica* in Vicenza (Palladio, 1570)

a.  b. 

Figure 27. a. Actual prospect of the Palladian *Basilica* in Vicenza from the central square of the city; b. the repeated typological element that characterizes the façade, the *Serliana* window

The Palladian intervention consisted in a two-storey *loggia* (arcade) with Doric and Ionic columns. The dominant element of the design is the repeated unit of three openings, with two lateral rectangular, and the central one arched, supported on pairs of small columns, set off with a larger half column at each bay. This typological element, very diffused in Italian Renaissance architecture, is called "*serliana*", from the name of Sebastiano Serlio, a theorist and architect who wrote about this type of opening in his treatise, and applied it in the *Biblioteca Marciana* in Venice, to cite one of the most famous applications of the *Serliana* window.

This element is not used only in Renaissance architecture, as there are many examples also in later buildings, nor was invented by Serlio, as the first examples date back to the Roman times, with the Diocletian's Palace in Split (actual Croatia), and had been already used in the first Renaissance, for example, by Raffaello for the façade of San Lorenzo in Florence. The *Serliana* window is one of the typological elements that characterise Italian Renaissance, and in particular Palladian architecture, as was soon recognised also in the context of the "palladianist" architecture, that developed in the 17th and 18th century, mostly in England.

The arch of the *Serliana* windows of the Palladian Basilica was selected as a case study not only for the fame and the diffusion of this typological element in the architecture of the Renaissance and of all the architects that referred to that, but mostly because it constitutes a typical example of arch with a low number of voussoirs. This type of arch, indeed, has commonly a limited span, correlated to its use (in most of the cases a window or a portal) and is usually realised in stone voussoirs, for the aesthetical taste of the Renaissance (apart of some examples in which the stone is used only as a cover layer). The arches of the Palladian Basilica in Vicenza, in particular, having a span of 3.56 m and 9 voussoirs, can be collocated in the middle of the range of the arches of interest, as described in paragraph 2.1. The number of voussoirs (9) is limited, but not too low, and the span is enough for the arch to be structurally relevant. Besides, the proportions of the arch are typical for the studied typology, having a

thickness to span ratio of 1/10, as prescribed by Renaissance treatises, that generally referred to Leon Battista Alberti, proportions that were generally followed in all the works of Palladio. This thickness can be considered limited, if compared to the whole studied typology, commonly constituted of thick arches, compared to their span. Romanesque arches of low span, in particular, have usually a thickness to span ratio around 1/6. The selected arch was considered more meaningful, though, to compare experimental results with limit analysis, because, being the thickness close to the standard, the influence of the friction should remain limited. Thick arches, indeed, fail more often for sliding of the voussoirs, and the analysis if this behaviour, although possible (for example, through upper limit theorem), includes more complications.

As in all the architecture of Andrea Palladio, the genesis of the plans and prospects is strictly geometrical. In particular, the prospect of his *Serliana* can be generated by a geometrical construction combining only squares and rectangles in golden section. The division in voussoirs derives from a geometrical construction too, resulting in 9 voussoirs of different dimension (Figure 28). The assumption of voussoirs of the same size, indeed, is rather academic, but it is not always applied in practice, as already discussed in paragraph 2.1. The chord of the arch is slightly lifted from the supports, as was a common practice in Renaissance architecture to correct an optical effect of lowering of the arch; the problem had already been faced by Brunelleschi and Alberti, who introduced a small voussoir (*concio morto*) at the supports.

The material that was used for the voussoirs was a white stone coming from a quarry close to Vicenza, in Piovene Rocchette, exhausted for the construction of this building. As reported also in Palladio's treatise, the stone, not polished and very hard" ("viva et durissima"), was "carved in single blocks, put together with great diligence" (Palladio, 1570). The use of stone as the only structural material, and the remarkable quality of the dressing of the blocks, resulted in a considerably high cost of the works, not comparable to most of the examples of the Venetian Renaissance.

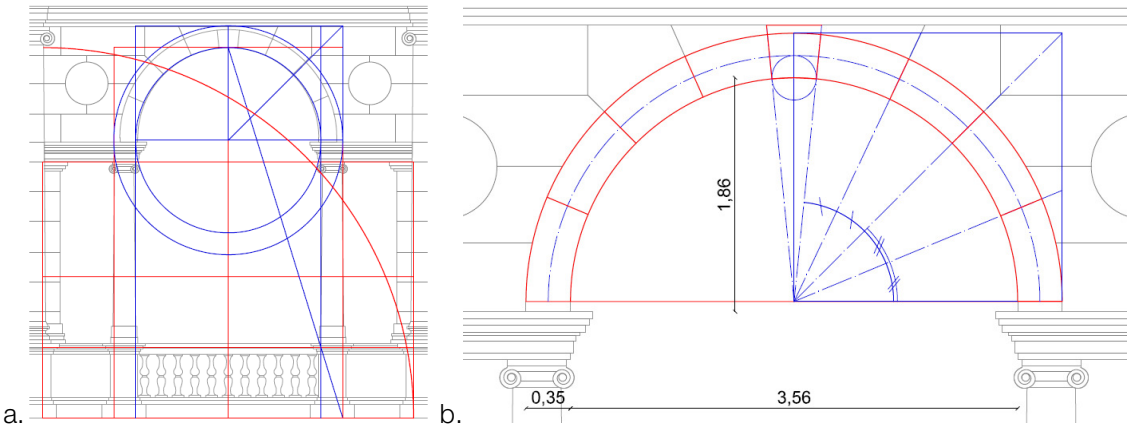

Figure 28 Geometrical genesis of the palladian Serliana of the Basilica (a. dimensions of openings and columns; b. voussoirs of the arch)

2.3 Model of the arch: experimental approach

The arch of the Palladian Basilica was adopted as a reference example of arch with a low number of voussoirs, to build a model, representative of the typology, and test it in the laboratory. The aim of the experimental campaign is to validate the analysis approaches that will be developed for this typology of arches to take into account their peculiarity, the limited number of joints. The experimental campaign, so, will be focused on the study of the failure mechanism and the determination of an ultimate load for the studied arch, to be compared to the analytical and numerical formulations.

The approach followed in the experimental tests is related to the interest of the campaign and the predictable structural behaviour that is studied. As said, the interest is concentrated on the determination of an ultimate load carrying capacity, more than the deformations of the arch, coherently to the approach of limit analysis, to which the results will be compared. The failure of these arches, moreover, like other typologies of arches, should be related to their geometry more than to the strength and elastic properties, resulting in a failure mechanism rather than a crushing of the material. For these reasons, it was considered acceptable to study a model of the arch built in scale and in a different material from the original, knowing, though, the issues that this implies.

The choice of building a scaled model is related to the dimensions of the original arch, 3.56 m, quite demanding to reproduce in the laboratory. The scale that was selected was 1:2, as presented in Figure 29, with a thickness of 10 cm. For the sake of simplicity in building the model, the voussoirs were realised in a straight geometry, not following the original curved shape. This does not result in significant differences in the position of the centre of mass of each voussoir, as will be discussed, nor it should influence the failure mode, as the voussoirs should not break and the deformations should remain localised at the joints, whose position is equivalent to the original.

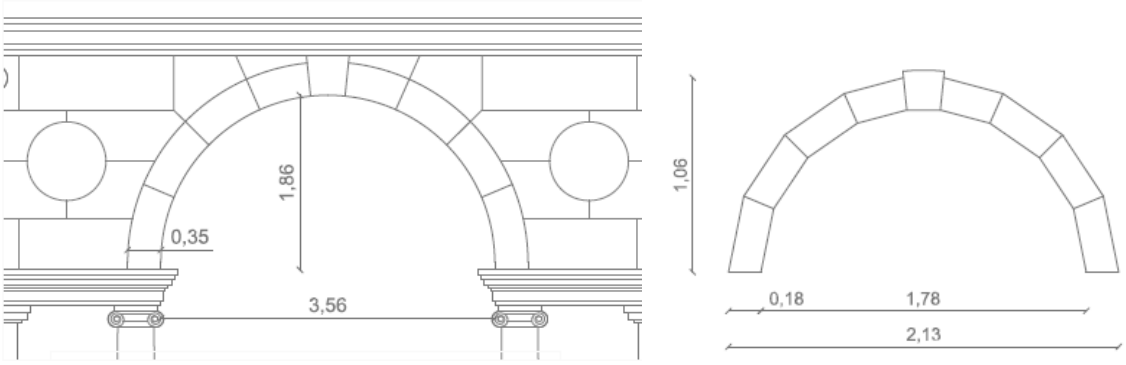

Figure 29. Geometry of the real arch (left) and of the tested timber arch (right)

The material that was selected to build the arch is timber, whose mechanical properties are summarised in Table 3. Voussoirs have been built in full timber. The choice of the material is related to the experience of the work presented in Bernat-Maso et al. (2012), in which a scaled model of an arch was built in

concrete mortar blocks. These blocks can be used only once, as they generally break when the arch fails: for this reason the study of different load combinations, or the repetition of the test results difficult of more expensive. Another problem that was faced is that the geometry of these blocks, typically at the edges, is not clean, clearly definite, but rather rounded, resulting in a difficult determination of the actual thickness of the arch at the joints (situation that is commonly found also in real examples), which has a relevant influence on accuracy of the results.

The timber voussoirs are a choice aimed to solving these problems, as they do not break at failure and their geometry is cleaner. For the adoption of a different material and a different scale, though, some problems arise, such as scale effects. The problem was studied in other cases in which scale models were adopted, and a number of dimensionless relations were developed and verified to correlate the results on a scaled model to the ones of the studied construction. These relations are presented in some specific papers (Royles and Hendry, 1991, Hogg and Choo, 2000), and summarised in Table 2. Nevertheless, in the cited studies, the comparison of experimental results on scaled models and real scale tests, reveals that the estimation of displacement capacity through scaled models is problematic, while good results were found for the ultimate loads.

Table 2 Dimensionless groups for the analysis of scale effects

Variable	Symbol	Dimension	Dimensionless Relations	
Length	l	L	$S_W = S_\sigma \cdot S_l^2$	(1)
Loads	W	MLT^{-2}	$S_W = S_\gamma \cdot S_l^3$	(2)
Stress	σ	$ML^{-1}T^{-2}$	$S_\gamma = S_E / S_l$	(3)
Young's modulus	E	$ML^{-1}T^{-2}$	$S_\mu = 1$	(4)
Compressive strength	fc	$ML^{-1}T^{-2}$		
Specific weight	γ	$ML^{-2}T^{-2}$		
Friction coefficient	μ	1		

These dimensionless groups impose to apply the same scale factor to a group of properties with the same dimension, such as stresses, Young's modulus and compressive strength. The main structural property of interest in this case is the Young's modulus, as it controls the deformations of the blocks, while the crushing of the material in compression should not appear, or, in any case, should have limited influence on the results. For this reason, a scale factor for the properties with the dimension of a MPa should be calibrated on the Young's modulus, obtaining, though, a fictitious value for the compressive strength (higher in this case).

To respect with these relations, the model should have a correction on some properties (the elastic modulus or the density) even if the material is the same as the real one. Once the material is chosen, the scale factor of the elastic modulus is set. There would be the possibility to correct only the density of the material, for instance applying some weights to each block, as, generally, the density of scaled

models has to be increased. In this study, though, for practical reasons, the density was not corrected. The model, in this way, represents an arch with an increased stiffness of the material (5-6 times higher than the expected). As already discussed, though, the main interest being the ultimate load and the applicability of limit analysis procedures, the stiffness of the model was not among the main interests of the study. Hence, the approach will be the observation of experimental results and the validation of analytical results, and the derivation of conclusions on the load capacity of the real arch in an indirect way, correcting the properties of the analytical models.

The values of the mechanical properties and the scale factors to apply, consistent with the presented dimensionless groups, are summarised in Table 3. The value of each property, for the original arch, is derived from reference values taken from the documentation of a quarry of the same type of stone. The properties of the timber, are the characteristic values, from EN 338, assuming a class C24. The value of the density of the timber, was measured on the voussoirs.

Table 3. Mechanical properties of the arch and the scaled model, and scale factors

	Real arch	**Scaled model**	**Scale factor**
Span	3.56 m	1.735 m	0.49
Elastic Modulus	25 GPa	10 GPa	0.40
Compressive Strength	53 MPa	21 MPa	0.40
Density	2400 kg/m^3	385 kg/m^3	0.17
Forces	-	-	0.10
Friction coefficient	0.4-0.6	0.3-0.5	-

The arch was realised with dry joints, reproducing a condition that in some cases is verified in this typology also in reality. For this reason, the mounting of the arch is particularly sensible to slight imperfections, and requires a good precision, in particular, in the determination of the correct span of the arch, and in the (out of plane) planarity of the structure. A little variation of these parameters, in the order of, for example, 5 mm for the span, as will be discussed, causes the opening of some joints before the application of the load, changing partly the structural behaviour. Other characteristics that have a certain relevance in determining the “correct” state of the structure before the application of any load are the planarity of the contact interfaces and the correct shape of the voussoirs, in particular the orientation of the joints. The structure was mounted carefully for all the tests that were performed, but a perfect mounting is very difficult to achieve, at least with dry joints.

To prevent the sliding of the supports and give an effective constraint to the lateral displacements, two steel plates of the weight of around 40 kg were placed at the extrados at the supports, and did not present any movement after all the tests. The arch, for the rest, had no other constraint: the constraint provided by the filling or the interaction with the rest of structure are not among the interests of this work, aimed, mainly, at reproducing the structural behaviour that is modelled through limit analysis.

For the same reason, the load configurations that were tested are rather academic, and did not aim to represent in detail real loading conditions that could be problematic for the studied typology in general or for this arch in particular. The load configurations consisted in a punctual concentrated load, applied at different positions along the span, asymmetrically (Figure 30). The choice of this type of loading is due to the intention to test experimentally those load configurations that are generally studied analytically, and to replicate the expected mechanisms of failure. The loading at one quarter of the span, for a monolithic arch with no tensile strength, the case that most often is assumed, represents the weakest configuration.

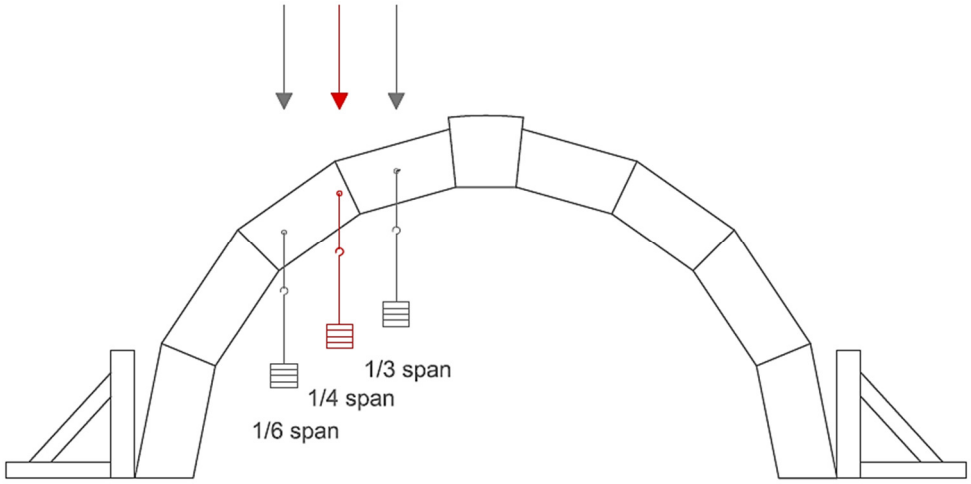

Figure 30. Tested load configurations: 1/3, 1/4 and 1/6 of the span, asymmetrical loading

The test was performed applying manually growing loads until failure. The range of ultimate loads was, as expected, of 5-10 kg. The applied loads were hung to the point of application of the load through a passing bar installed in the voussoir and a hook, as shown in Figure 30. The load was applied in this way (and not, for example, through a jack) to be able to follow the horizontal displacements maintaining perfectly vertical the direction of application of the load. The minimum load step allowed by the instrumentation was 100 g, reduced up to 5 g (the weight of a small bolt) in proximity of the failure load, when possible.

The displacements of the structure were measured in one representative point, coinciding with the point of application of the load. The measures were taken through an analogical extensometer, with a scale of 0.01 mm and a working range of 10 mm. Being the tests performed in load control, it was not possible to measure the softening part of load-displacement curve (nor it was needed for the scope of this work). The failure mechanism was recorded with the use of a camera with an acquisition frequency of 50 Hz, enough to fully describe the development of the mechanism.

For each load configuration, three repetitions of the test were performed, to average the (strong) effect of initial imperfections and all the factors that cause scattering in the results.

a.  b. 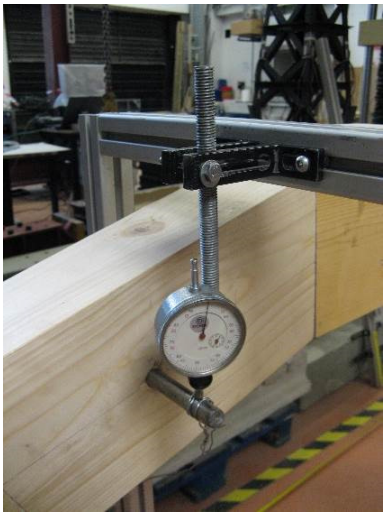

c.  d. 

Figure 31. a. test setup; b. extensometer for the measurement of the displacements; c; application of the loads; d. entity of possible initial imperfections.

2.4 Results of the experimental campaign

2.4.1 Third span loading (test T3 a,b,c,d)

The results of the tests will be presented divided by the 3 load configurations. The data that are available are the load-displacement curve, relative to the point of application of the load, and the recordings of the failure mechanism of one test for each load configuration. The tests are named T3 plus an increasing letter indicating the order in which they were performed. Four tests were repeated for this configuration.

Table 4. Tests T3 a,b,c,d: ultimate loads, displacements before failure, order of opening of the joints

	Ultimate load (N)	Ultimate displ. (mm)	opening joints	Span f the arch (cm)
Test T3a	63.73	1.52	5, 6, 10 (2)	174.0
Test T3b	61.77	1.83	5, 8, 10	173.5
Test T3c	55.79	1.46	5, 8, 10	173
Test T3d	58.73	0.93	5, 8, 10	173.4
Average	60.00	1.44		
Standard deviation	3.48	0.37		
COV	5.8%	26.0%		

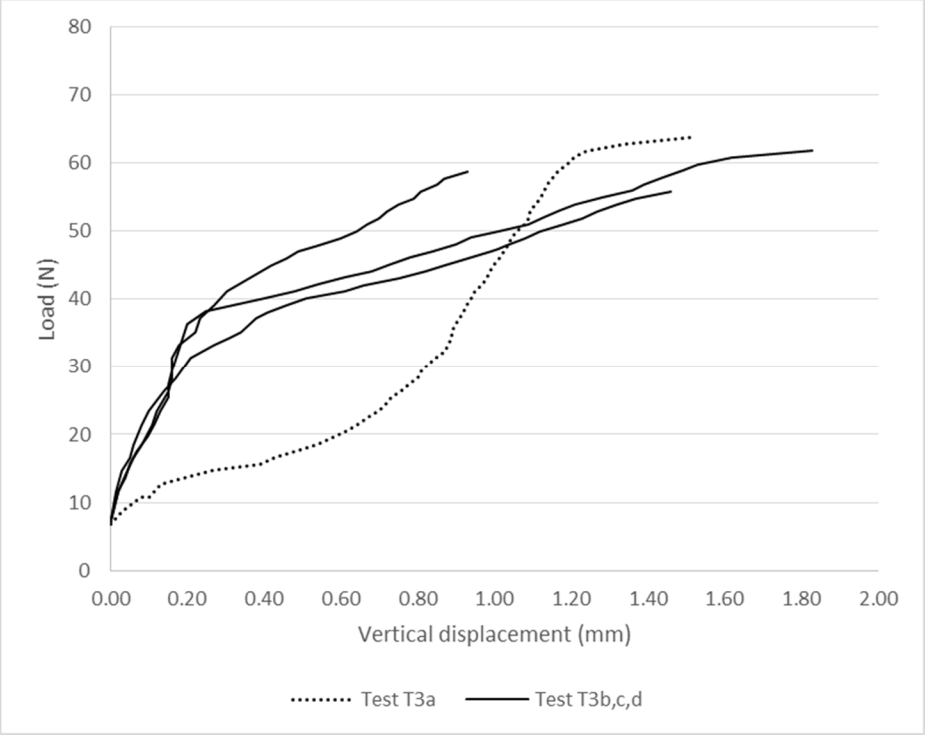

Figure 32. Load displacement curves for tests T3 a,b,c,d (dotted line – test T3a)

The 4 tests can be divided into two groups with provide different ultimate load and a difference in the structural behaviour that is clearly seen in Figure 32. One of these tests (T3a) presents important displacements for low loads, accommodating the initial imperfections and finding a stiffer configuration after this initial deformation. The ultimate load that it reaches is the highest. The other 3 tests (T3b-c-d) present a very similar behaviour within them, with an initial linear part in the load-displacement curve and a second part, still linear but less stiff, until failure. The changes in stiffness of the arches correspond in all cases to the opening of a new joint, being the opening of the third, in order of appearance, the most relevant change in the stiffness.

The cause of this difference in the displacement curve and in the ultimate capacity can be due to differences in the initial configuration (the two groups of tests were performed in different days). For tests T3b-c-d it appears that the initial configuration, although stiffer, and so apparently more precise, did not allow the arch to reach completely its maximum capacity. On the other hand, test T3a, once achieved the initial accommodation of the imperfections, reaches what is expectable to be the full capacity of the arch (if compared also to the analytical and numerical results, chapter 3).

The evolution of the failure mechanism measured in test T3a is presented in Figure 33. Before the displacements start increasing to failure, 3 hinges already appear and the opening of those joints, before the ultimate condition, is in the order of 2-4 mm (in this case joint 5, at the keystone, opens the most). When a fourth hinge appears (joints 2-3 in this case) the structure is turned into a mechanism and collapses. The formation of the fourth hinge in this case takes place almost at the same time at joints 2 and 3. After the mechanism begins to develop, the joints that opened in origin might close and other types of mechanism can form, but this has no relevance in the structural assessment of the arch as the ultimate condition has already been reached and the structure is collapsing.

The mechanism correspond to the expectations, with the formation of four rotational hinges (Figure 34), absence of sliding and collapse for the rotations of three portions of the arch. No damage in the voussoirs for crushing in compression around the hinges was seen after collapse, even after many tests.

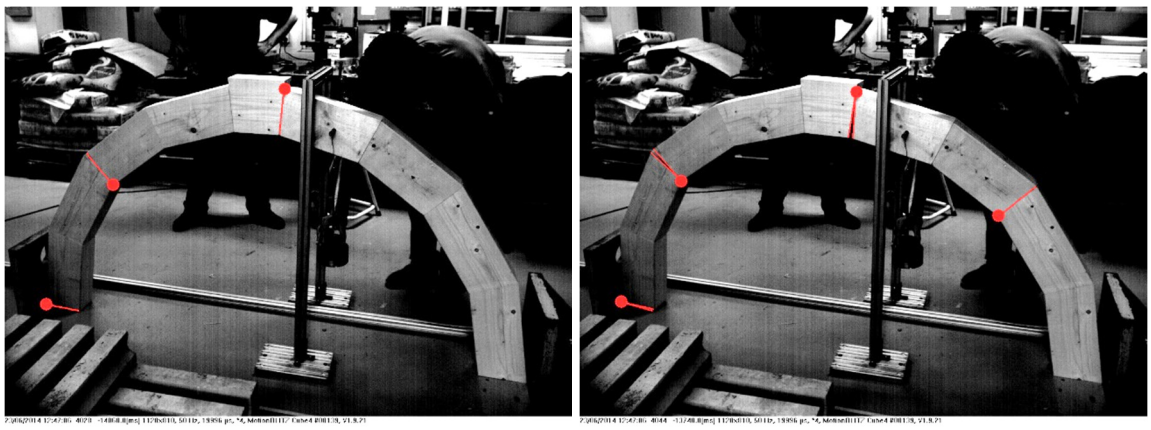

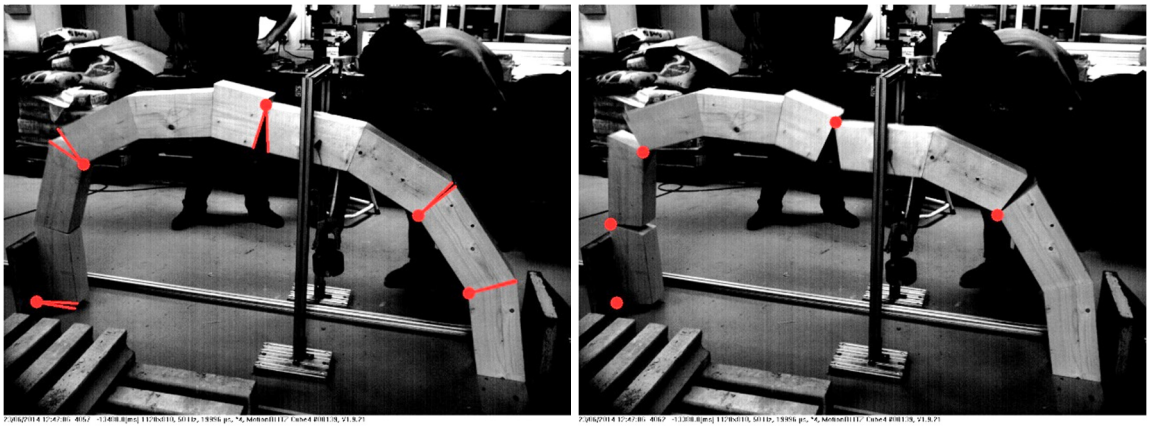

Figure 33. Failure mechanism, test T3a. Evolution of the mechanism until collapse

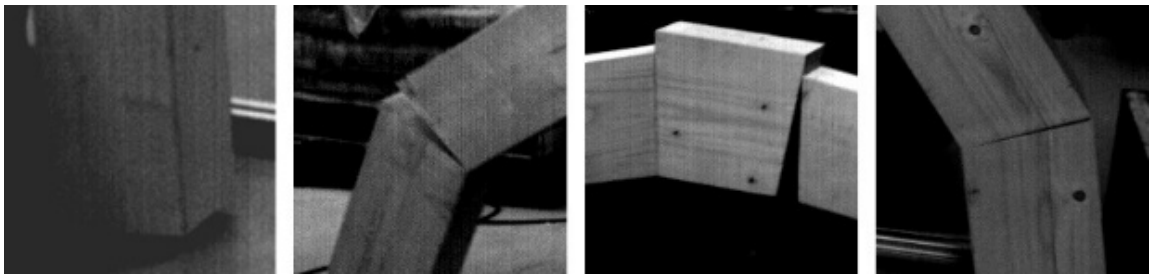

Figure 34.Opening of joints at failure, test T3a

2.4.2 Quarter span loading (test T4 a,b,c,d)

Tests T4 a,b,c,d correspond to a concentrated load at the quarter of the span. This configuration, if the problem of the position and number of joints is ignored, is the one which presents the lower ultimate load. For this reason is this configuration is the most common when an example of asymmetrical loading on an arch is calculated. Four tests were repeated for this configuration.

Table 5. Tests T4 a,b,c,d: ultimate loads, displacements before failure, order of opening of the joints

	Ultimate load (N)	Ultimate displ. (mm)	opening joints	Span of the arch (cm)
Test T4a	62.8	2.530	4 8 6 2	174.0 cm
Test T4b	58.8	3.780	4 8 2	173.5
Test T4c	59.7	3.460	4 8 2	173.3
Test T4d	60.7	3.21	4 8 2	173.2
Average	60.5	3.2		
Standard deviation	1.74	0.53		
COV	3%	16%		

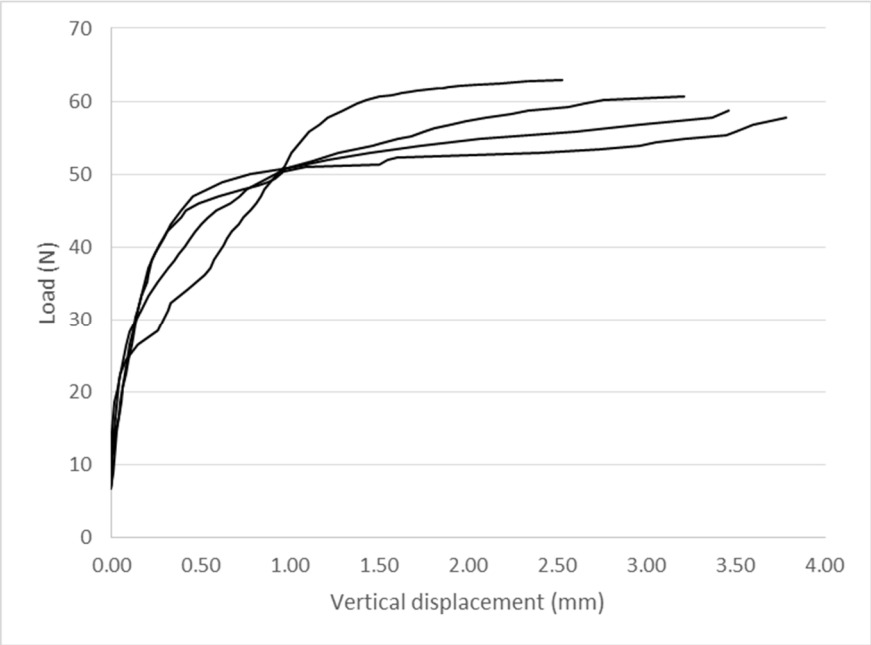

Figure 35. . Load displacement curves for tests T4 a,b,c,d

The test under this load configuration showed a similar behaviour, with a load-displacement curve approximately linear in the first part, and a strong decrease in stiffness once the load gets closer to the ultimate load and the third hinge opens. The initial inevitable differences in the configuration produce a behaviour that in some cases changes the order of opening of some joints. In Test T4a joint 8 opened for a low load, increasing the displacements for moderate loads but reaching a slightly higher ultimate load. The differences in the ultimate capacity are moderate in this case, and the ultimate displacements are the higher of the three load configurations tested. The particularity of this loading is that it was very close to joint 4, resulting in an early opening of the joint close to the load and in a bigger ultimate displacements.

The evolution of the failure mechanism, relative to test T4d, is presented in Figure 36. The order of opening of the joint is 4, 8, 10. Before the formation of the last hinge the openings of the joints were in the order of 6 mm for joint 4 and 4 mm for joint 8. The last joint to open is joint 2, transforming the structure in the expected mechanism. A slight movement out of plane was found in this case in the last part of the evolution of the mechanism, due probably to a not perfect alignment in the out of plane direction of the supports. Anyway, the effect of this is visible only when the structure has almost completely collapsed, much beyond the ultimate condition. The thickness of the arch, 10 cm, was enough to contain the effect of a defective alignment out of plane of the supports even for initial defects evident to the eye (that in any case were corrected and not tested, to avoid torsional and out of plane effects). The opening of joints at failure is shown in Figure 36. Also in this case, the relative moment is a pure rocking of the voussoirs, without sliding and without local crushing of the material. These results will be used to justify the assumptions that will be made for the limit and numerical analysis.

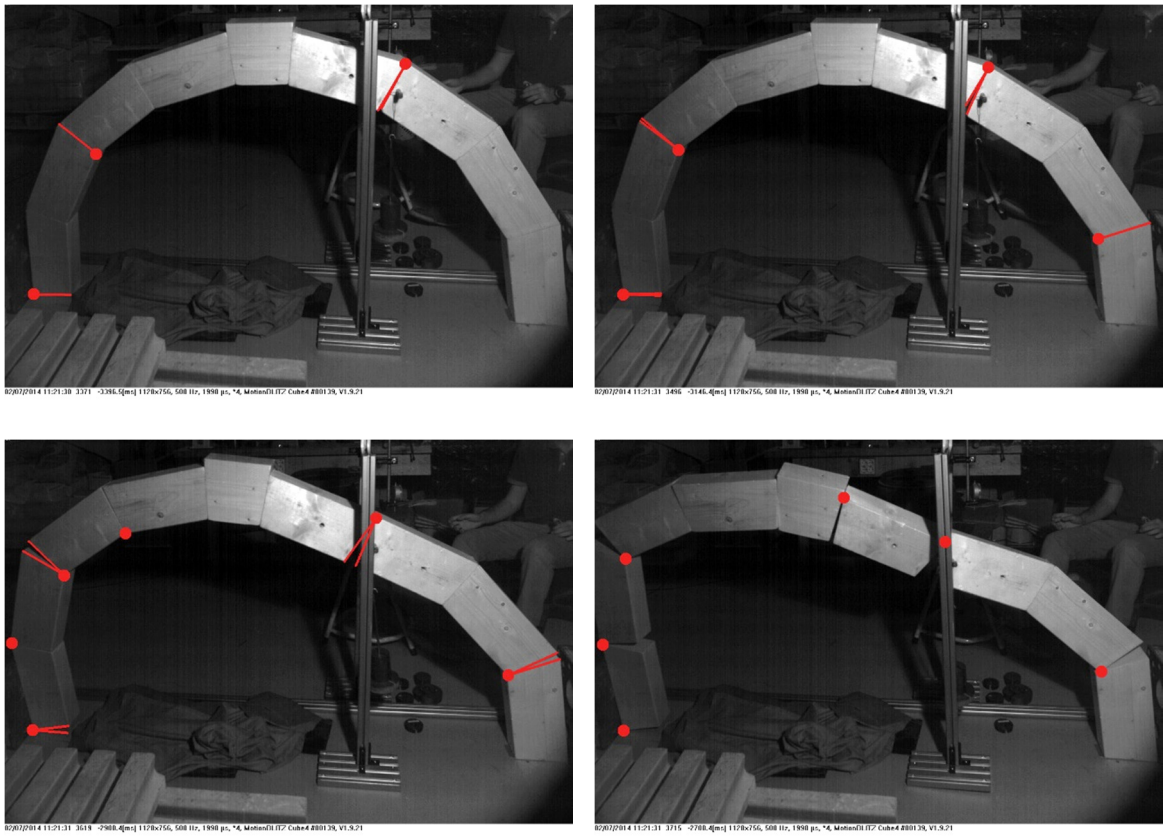

Figure 36. Failure mechanism, test T4d. Evolution of the mechanism until collapse

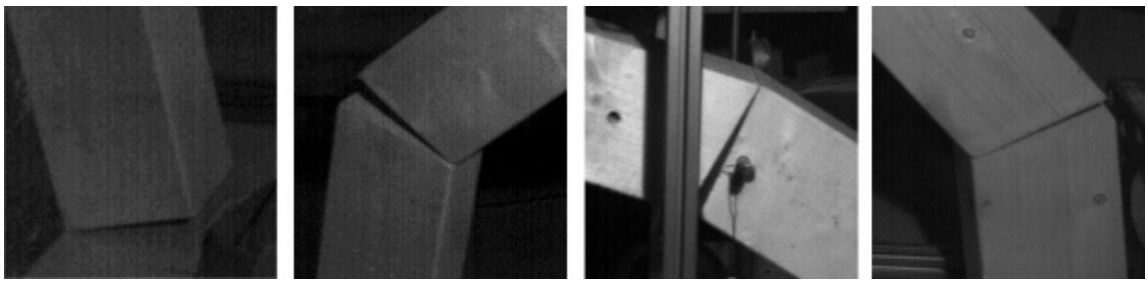

Figure 37 Opening of joints at failure, test T4d

2.4.3 Sixth span loading (test T6 a,b,c)

Test T6 a,b,c was performed, in 3 repetitions, at the sixth of the span. For this position of the loading the capacity of the structure is much larger, as it is quite close to one of the supports. The displacements at the point of application of the load, for the same reason are, smaller.

Table 6 Tests T6 a,b,c: ultimate loads, displacements before failure, order of opening of the joints

	Ultimate load (N)	Ultimate displ. (mm)	opening joints	Span of the arch (cm)
Test T6a	95.03	1.89	6 8 4	173.4
Test T6b	99.93	2.20	6 8 4 10	173.0
Test T6c	96.99	1.45	6 8 4	173.8
Average	97.32	1.84		
Standard deviation	2.47	0.38		
COV	2.5%	20.4%		

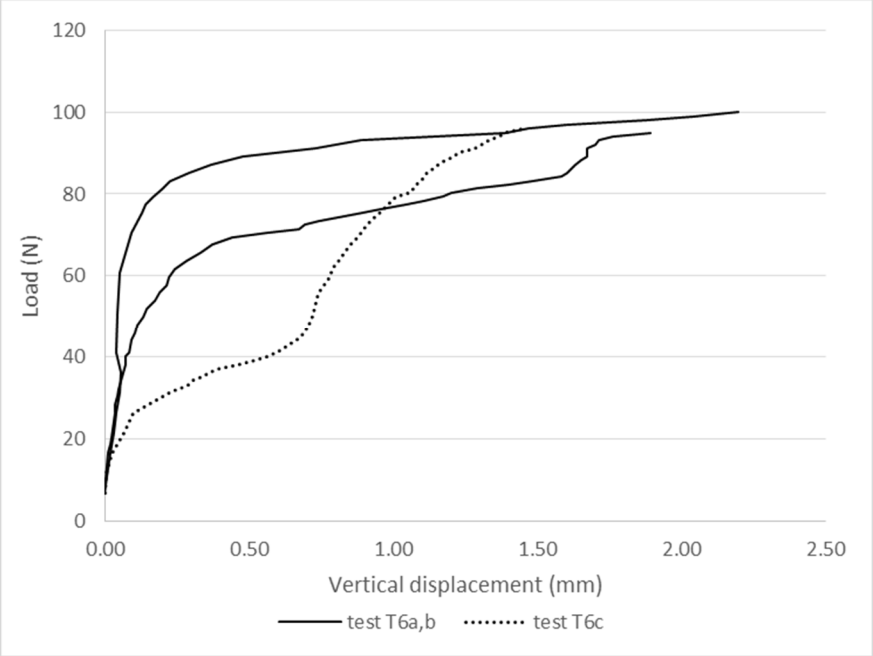

Figure 38. Load displacement curves for tests T6 a,b,c

The three tests that were performed give a similar ultimate load, but show a behaviour which in one case is significantly different. In test T6c, indeed, the displacements for moderate loads increased consistently until a stiffer configuration was reached. One joint, probably, was not perfectly closed and the structure presented a lower stiffness in the initial part of the curve; after finding a more stable configuration, the stiffness increases again and the ultimate load that was reached was close to the one of the other tests.

The evolution of the mechanism is analogous to the one obtained in test T4, with the opening of the same joints, in the same order. Also in this case, no sliding was found, nor crushing, even if this configuration should be the most critical for this type of failures. The mechanism that developed is a pure rocking of the three parts in which the arch is divided (Figure 39, Figure 40).

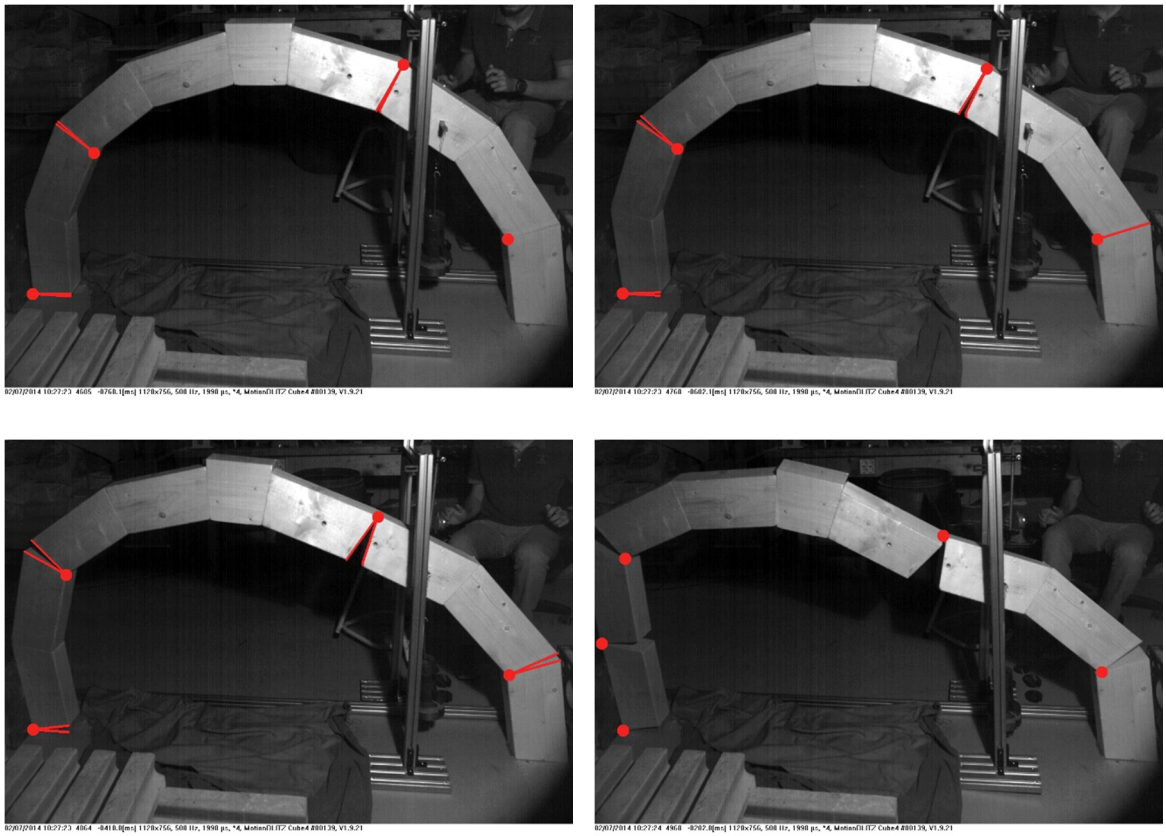

Figure 39. Failure mechanism, test T6c. Evolution of the mechanism until collapse

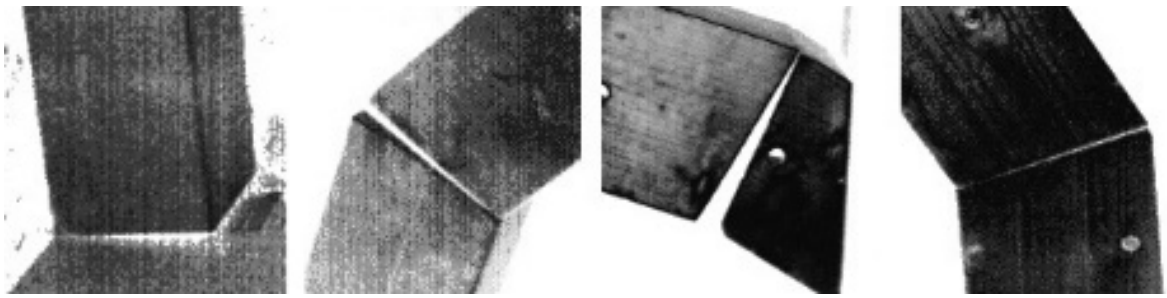

Figure 40. Opening of joints at failure, test T6c

It is worth noting, after presenting all the experimental results, that both ultimate loads and displacement capacity depend much on the initial configuration, and in particular to the presence of little imperfections in the length of the span and in the joints. If one (or more) joints are not closed in the initial configuration a difference is found not only in the load-displacement curve but also, and with a relevant effect, in the ultimate load that the structure can support. Some trials of the tests (not presented here) were performed varying on purpose the initial conditions of the arch, changing, for example, the span of ±0.5 cm. The effect, measured only in terms of ultimate load, of the initial imperfections (due to the imposed displacements at one support) is a reduction in the order of 25% of the capacity.

The effect of these initial variations from a perfect configuration is probably bigger in arches with dry joints, as there is no possibility for the structure to accommodate these imperfections without deforming significantly. The presence of imperfections, such as partially opened joints, imperfect contact surfaces, movements of the supports, is a factor to take into account, as will be discussed in the last chapter, also when assessing the capacity of existing structures, where they are inevitable.

For the experimental campaign, in any case, the mounting of the arch could be performed in the best way to avoid the presence of these imperfections, in order to obtain the less scattered possible results and to be able to compare the different repetitions, making an average on homogeneous results. To this scope, particular attention has to be paid to the selection of the correct span for all the joints to be closed. In addition, a wooden wedge was used to close the joints at the base supports, resulting from a slightly imperfect cut of the angles of the voussoirs.

The theoretically perfect configurations, though, with all joints perfectly closed, a perfect out of plane alignment of the supports, the voussoirs cut with perfectly planar surfaces and angles that form an arch of exactly 180°, are conditions that in practice are rather difficult to obtain. Nevertheless, with a good control on the mounting operations, it is possible to obtain an initial configuration of the structure close to the theoretical, and get homogeneous results from the repetitions of the test.

In the next part of the work, the results of these tests will be compared to the analytical and numerical approaches of analysis of arches, adapted to take into account the presence of a small number of voussoirs. The approaches that will be used are the limit analysis, both in static and kinematic formulation, and the Finite Element method, through a simplified micro-model of the arch. These theoretical results will be compared to the experimental ones to check the applicability of the hypotheses that will be made, and to prove their effectiveness in estimating the load capacity of the studied structure. The experimental results present some variations in the ultimate load, due to the factors already discussed, but they were obtained in homogeneous conditions. For this reason, the average of the results found for each load configuration will be used as the quantitative experimental determination of the load capacity.

Chapter 3.

Structural analysis through Classical methods

3.1 Lower bound analysis (Safe Theorem)

Limit analysis is a powerful tool for the analysis of masonry structures, and in particular of arches, as it provides, with a limited number of input parameters and with some basic hypotheses, a solution of the structural problem and an intuitive insight on the behaviour of the structure. The theory of limit analysis as we intend it now was developed since 1936 by Gvozdev, Drucker, Prager, and Kooharian, among the others, and promoted by the work of Heyman. The method, though, is based on assumptions that were made since the first studies on arches (Hooke, Poleni, Coulomb), in an intuitive way, without the sound theoretical background provided by the theory of limit analysis.

Limit analysis is based on the assumption of a rigid-perfectly plastic material model. In order to mathematically implement this material model, a yield function, named φ, has to be defined as a function of the local stresses or of the generalised stresses at sectional level. The model that is implemented through the yield function assumes that the material remains rigid (not damaged) for $\varphi < 0$, plastic (damaged) for $\varphi = 0$, and inadmissible states correspond to $\varphi > 0$. For this reason, the yield condition can be expressed by the expression $\varphi \geq 0$, defining a limit domain for admissible generalised stresses.

When the yield function equals zero the material becomes plastic and it is necessary to define the flow direction. Superposing the stress space and the flow space, the classical limit analysis theory accepts that the flow direction is normal to the yield surface (Orduña, 2003), being in this case associated flow. This hypothesis, called normality condition, implies that the energy dissipated by the flow is the maximum possible, or that such flow provides the greatest resistance against deformation. A consequence of the normality condition is that the yield surface must be convex. Although the normality condition is at the base of the demonstrations of limit analysis theorems, its application to some materials, like masonry or soils, is not completely acceptable. These materials, indeed, have a dilatancy angle very close to zero, considerably different from the friction angle, that controls the normal direction to the yield surface, if a Mohr Coulomb criterion is applied to the describe the frictional behaviour.

A structure is said to be in a statically admissible state when the internal stresses are in equilibrium with the external forces and the yield conditions are respected in all points. Alternatively, the definition can be extended to generalised stresses at sectional level. In the hypothesis of associated flow rule, this condition corresponds to a safe state. As is a common approach to limit analysis, once defined a non-negative load factor α that multiplies the variable loads on the structure (such that the variable load is

$\alpha \boldsymbol{F_v}$), the safety factor is defined as the largest load multiplier that can be applied to the structure for it to remain safe. The static theorem of limit analysis (also called safe theorem or lower bound theorem), states that the safety factor is the largest of all the statically admissible load factors; the load cannot be increased beyond that limit without violating the equilibrium or the yield condition.

Another possibility that will be presented in the following is the kinematic approach, for which a kinematically admissible mechanism is, in general, unsafe and the load factor associated to it is larger or at least equal to the safety factor. The upper-bound theorem of states, indeed, that the safety factor is the smallest of all the kinematically admissible load factors. As the safety factor has to be the same, weather it is obtained through upper bound or lower bound theorem, then the only way in which a structure in a statically admissible state can be unsafe is by reaching the yield surface in an enough number of sections as to form a kinematically admissible mechanism. The uniqueness theorem establishes that the largest of all the statically admissible load factors equals the smallest of all the kinematically admissible load factors, and is so the safety factor.

These theorems are formulated in the hypothesis of associated flow. If a different flow rule is adopted, as is more realistic in the case of masonry, then the uniqueness of the solution, i.e. the condition that the largest statically admissible load factor has to be equal to the smallest kinematically admissible one, is not assured. There can exist, indeed, statically admissible states, for load factors smaller than the largest statically possible one, under which a kinematically admissible mechanism can form. In this case the problem should be solved in the mixed statical-kinematical formulation (imposing at the same time the conditions for statical and kinematical admissibility), and the smallest of the different possible solutions should be assumed, even if this approach is rather conservative in certain cases. The limit analysis with non-associated flow will not be solved in this work; as in the experimental campaign the failure modes that were measured are only rotational, without crushing in compression of the material, the assumption describes correctly the expected failure (the rocking of rigid blocks respects the normality condition).

3.1.1 Definition of limit domains

To analyse structures like arches it is convenient to define the yield function at sectional scale, considering the generalised stresses at each section, that, for 2D analysis, are the normal force, the shear force and the bending moment. The limit domain should take into account the possibility of rocking, sliding and crushing of the material, where the sliding is generally uncoupled from the rotational problem.

Sliding can be modelled through a Coulomb criterion, where the maximum shear that a section can support is proportional to the normal (compressive) force. The frictional coefficient is equal to the tangent of the friction angle, a parameter that can be easily measured but which is not simple to

estimate in existing structures. One classical hypothesis on the friction coefficient is that it is large enough to prevent sliding of the sections; this hypothesis comes from the observation that sliding failure, in real arches, is rather rare (but it happens in some cases, as also Heyman, who defined this approach, recognised). In this case the definition of a yielding function for shear and normal force is not needed, as any shear force is considered acceptable.

Another approach is to define the yielding criterion through Coulomb's formulation, the most used to describe sliding failure. The relation is linear and uncoupled from the rocking problem. One point that can be discussed is the normality condition: for the flow rule to be associated a dilatancy angle, equal to the friction angle, should be assumed (Figure 41). The dilatancy in these structures, although different from zero (Figure 42) is low, and the hypothesis leads to unrealistic assumptions on the direction of the plastic strain rate.

$$\begin{cases} V + \mu N = V + N \tan \varphi_f \leq 0 \\ -V + \mu N = -V + N \tan \varphi_f \leq 0 \end{cases} \tag{5}$$

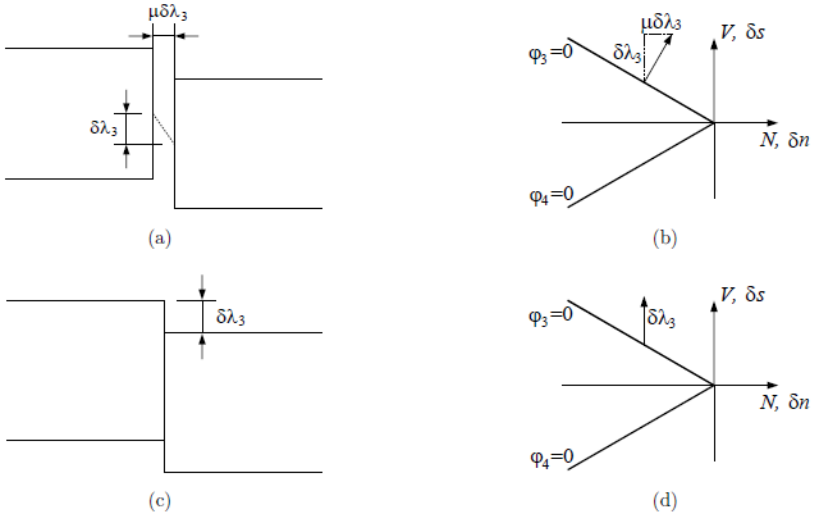

Figure 41. Mohr Coulomb failure criteria: formulations for associated (a,b) and non-associated flow (c,d) (Orduña, 2003)

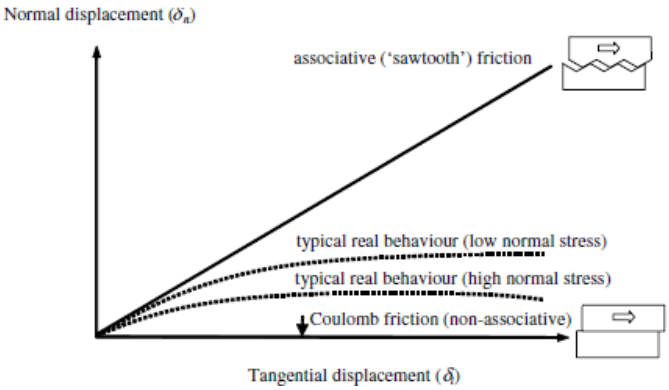

Figure 42. Dilatancy angle in real structures: comparison between associative, non-associative (Coulomb) friction and real behaviour (Gilbert et al., 2006)

The limit domain of normal force and bending moment can be built considering different hypotheses for the material. These hypotheses are based on the observation of the mechanical behaviour of the material (masonry, stone, mortar), but also on the expected level of stresses on the structural element under consideration. The cases that can be considered are:

- Infinite compressive strength, zero tensile strength
- Finite compressive strength, zero tensile strength
- Finite compressive and tensile strength

The first case is the most simple and constitutes the most common assumptions when limit analysis is applied to the study of arches. The real compressive strength is not infinite but, as the stresses are generally low compared to it, the assumption is acceptable for common arches, built in a material which is not particularly weak. In the case of arches with low number of voussoirs, object of this work, the assumption of zero tensile strength for the voussoirs can be too conservative, but the model is certainly applicable to the interfaces. In this case the yield function is simply described by the 2 disequations (Orduña, 2003):

$$\begin{cases} N + \frac{1}{a}M \leq 0 \\ N - \frac{1}{a}M \leq 0 \end{cases}, \qquad \begin{matrix} \frac{\delta\varphi}{\delta N} = 1 \\ \frac{\delta\varphi}{\delta M} = \pm\frac{1}{a} \end{matrix} \tag{6}$$

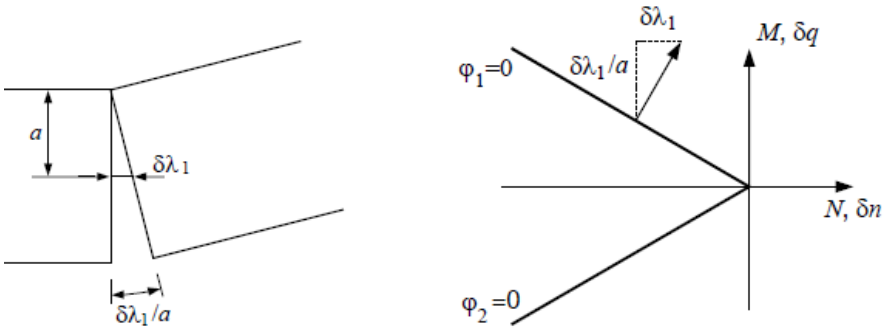

Figure 43. Yield function and flow rule for infinite compressive strength and zero tensile strength (Orduña, 2003)

The case with a finite compressive strength of the material and a zero tensile strength has a simple formulation that, though, converts the yield surface in a convex curve (Figure 44). A common approach is to linearize the function, to avoid the resolution of a nonlinear problem (or a linear programming involving quadratic forms, as in this case). If this curve is approximated by piecewise linear functions the problem of finding a maximum or minimum load multiplier is reduced to a linear programming problem, easier and faster to solve, through more robust methods. The curve could be approximated by a linearization through 6 linear conditions (De Rosa and Galizia, 2007), as in Figure 44, or more if a more detailed model is needed, with a benefit on the safety of the method (through the linearization some states that are theoretically non possible appear to be admissible).

$$\begin{cases} N = tbf_c \\ M = tbf_c \cdot (a - {}^{t}/_{2}) = -\dfrac{N^2}{2bf_c} + aN \end{cases} \quad , \quad \begin{cases} -\dfrac{N^2}{2bf_c} + aN + M \leq 0 \\ -\dfrac{N^2}{2bf_c} + aN - M \leq 0 \end{cases} \tag{7}$$

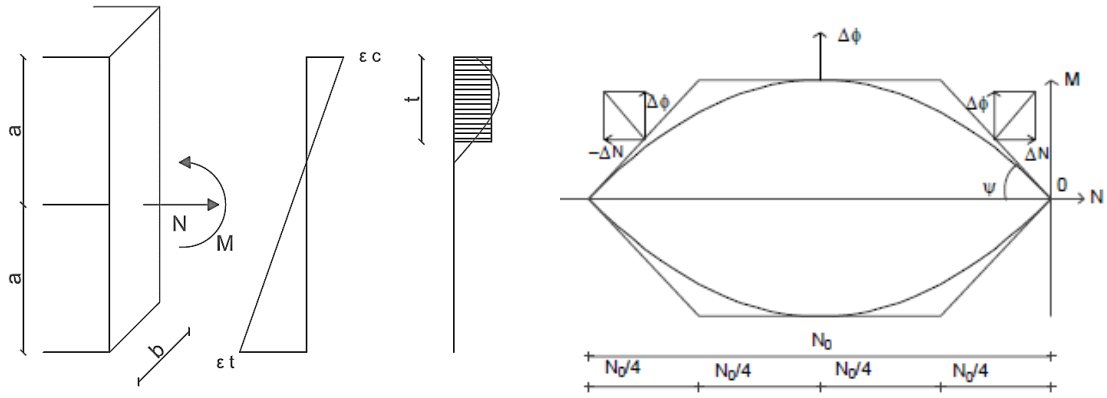

Figure 44. Yield function for finite compressive strength and zero tensile strength, with piecewise linearization of the function (De Rosa and Galizia, 2007)

The third method, suitable only for the voussoirs and not for interfaces, is considering a finite compressive strength and a finite tensile strength, in a reasonable range of 5-10% of the compressive strength. Considering only a linear distribution of stresses in the section, in the hypothesis that the material has some tensile strength described by the parameter T (in the order of 0.05-0.1) and is subjected by a compressive stress controlled by the parameter C, the normal force and the bending moment assume the following formulations:

$$\begin{cases} N = abf_c \cdot (C - T) \\ M = a^2 bf_c \cdot (C + T) = \dfrac{1}{3}aN + \dfrac{2}{3}a^2 bf_c T \end{cases} \tag{8}$$

$$ecc = \frac{M}{N} = \frac{a}{3} + \frac{2}{3}a\frac{T}{C - T} = \frac{a}{3} \cdot \left(1 + \frac{2abf_c}{N}T\right) = \frac{a}{3} \cdot \left(1 + \frac{N_0}{N}T\right)$$

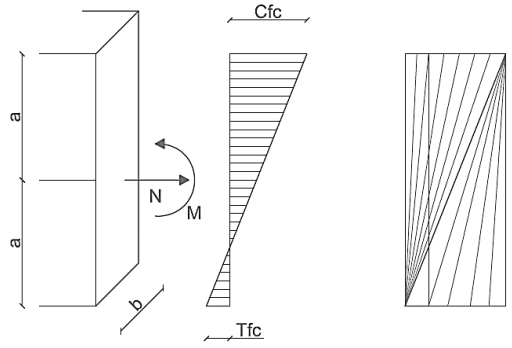

Figure 45. Linear stress distribution for the construction of a limit domain with finite tensile strength and compressive strength

The expressions are found in the hypothesis of linear distribution of stresses because the experimental observations suggest that the stress distribution inside the voussoirs is generally far from causing cracks in the material before the opening of cracks in the existing joints. After reaching the maximum bending moment for each normal force with linear distribution of stresses as described in equations 7, anyway, we can assume that the section starts to develop cracks at the tensile edge and eventually develop the same ultimate condition considered for the case of finite compressive strength and zero tensile strength. The only difference is the appearance, before the beginning of the crack, of some tensile stresses, that have, in any case, little influence on the capacity of the section.

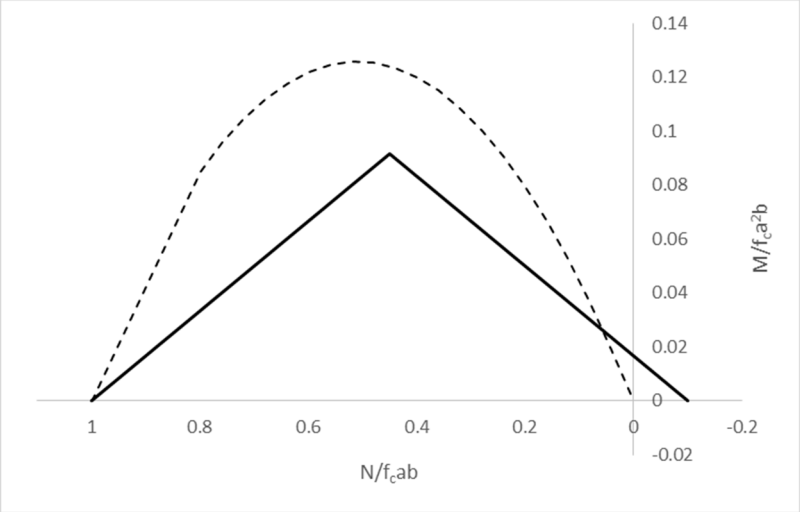

Figure 46. Limit normalised MN domains for linear stress distribution (continuous line) and ultimate condition (dashed line) for a material with finite compressive and tensile strength

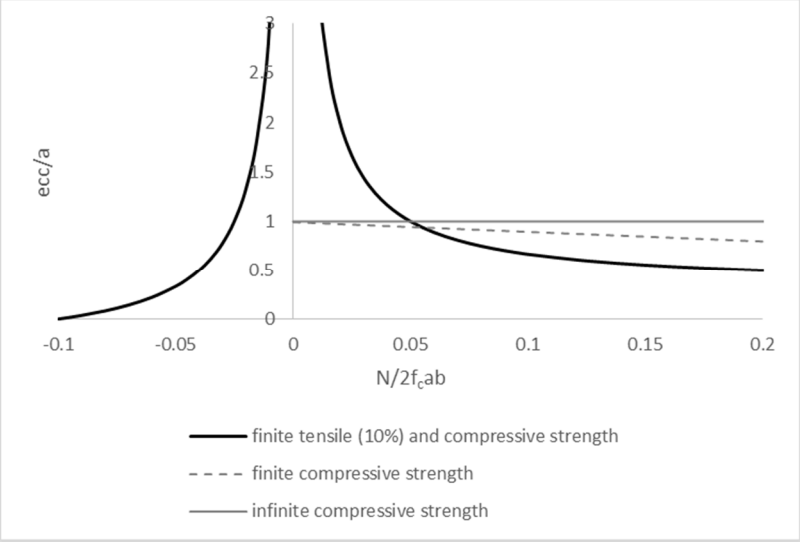

Figure 47. Admissible eccentricities in function of the intensity of the normalised normal force for the different hypotheses on the strength of the material

In Figure 46 the limit domain for bending moment and normal force (normalised) are represented in the hypothesis of finite tensile and compressive strength. The area of interest of the graph is the one for low compressive force, for the already cited reasons. In Figure 47 the admissible eccentricity of the normal force is compared for the hypotheses of infinite compressive strength (consisting in a constant eccentricity equal to half of the section), finite compressive strength (with a decreasing eccentricity for high compressive forces) and finite compressive and tensile strength, with the latter equal to the 10% of the compressive strength. In this case the variability of the admissible eccentricity is more dependent on the normal force; for low compression the possible eccentricity is considerably larger than the geometrical dimensions of the section.

On the base of these considerations on the tensile strength of the material, the possibilities for the analysis of arches with a limited number of voussoirs through the safe theorem of limit analysis could be carried out with following approaches:

- Defining a yield criterion for the voussoirs that includes the presence of a tensile strength of the section, different from the criteria for the interfaces, with no tensile strength;
- Equivalently, defining strength boundaries for the voussoirs different from the geometrical boundaries to take into account the possibility of higher eccentricities;
- Assuming the structure as a complex of rigid bodies (the voussoirs) for which no yielding function is checked, and interfaces at which the plastic strains can develop

The first approach requires the definition of a yielding function proper to model the tensile strength of the voussoirs. If the proposed yielding function were assumed, with a linear distribution of stresses in the section, the normality condition would result rather unrealistic and it would be necessary to define a non-associated flow rule and to perform a non-standard limit analysis, with complications for the non-uniqueness of the solution.

The second option could represent a simple solution, but the theoretical base of the problem is the same as the first approach. In addition, although the approach would be simple through graphical instruments for thrust line analysis, the definition of the (larger) strength boundaries depends on the acting normal force, so, in a rigorous way, an iterative process would be necessary.

The third approach is the simplest but it can provide reasonably good results, as the hypotheses on which it is based are confirmed in the real structures and in the experimental campaign that was carried out. The assumption of the voussoirs as rigid bodies allows to check the yielding function only in the interfaces, where the common hypothesis on the material are completely applicable, concentrating there the possibility of plastic strains. The observation that the cracking and opening of a hinge in between of a single voussoir is unlikely to happen, and the calculation of possible eccentricities of the normal force in a section with tensile strength and moderate compression, justify the assumption of such hypotheses. In this way, the problem is defined in the theoretical context of standard limit analysis and common solution procedures can be applied.

Two approaches might be followed to perform this type of analysis, the first consisting in considering the equilibrium conditions of each single voussoir and the yielding function at the interfaces as conditions in a linear programming procedure to maximize the load factor for variable loads. Another approach for the solution of this problem can be the calculation of a thrust line, integrating its differential formulation, and the optimization of the solution to find a maximum load factor for which the thrust line is inside the boundaries of the arch in each interface (regardless of its position in the middle of a voussoir). Both approaches will be implemented in a MATLAB code and solved.

The complete yielding function should be defined in the 3-dimensional space of the generalised stresses (normal force, shear force and bending moment), even if the 2D representation of the domains describes completely the problem, as the bending moment is uncoupled from the shear force. In Figure 48 such domain is represented in the hypothesis of infinite compressive strength, zero tensile strength and Coulomb friction. This yielding function, for the observations made in the experimental tests, will be considered adequate to model the interfaces.

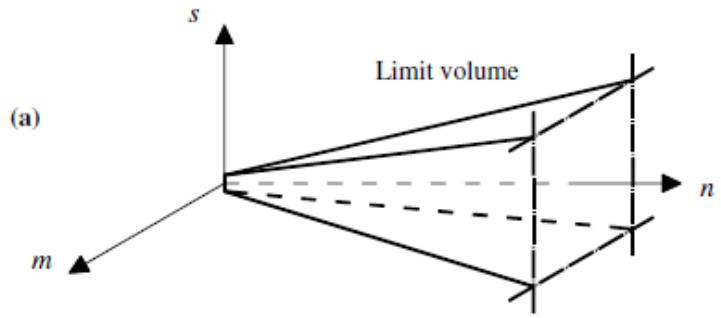

Figure 48. Representation of the yielding function in the 3-dimensional space of the generalised stresses (n,s,m) in the hypothesis of infinite compressive strength, zero tensile strength, Coulomb friction (Gilbert et al., 2006)

Adopting the notation used in Orduña (2003), the definition of this type of limit domain can be written in a compact form as:

$$\boldsymbol{\varphi} = \boldsymbol{N^T Q} \leq \mathbf{0} \tag{9}$$

Where $\boldsymbol{N^T}$ is the matrix containing the coefficients to apply to the generalised stresses $\boldsymbol{Q}$ in the formulation of the yield function. The matrix $\boldsymbol{N^T}$, for infinite compressive strength, is a $4m$ x $3m$, as 4 conditions are defined for each section. The formulation, which will be used in the following, is given in equation 10. If a model with finite compressive stress is applied the matrix has dimensions of $6m$ x $3m$.

$$[\boldsymbol{N^T Q}]_i = \begin{bmatrix} 1 & 0 & 1/a \\ 1 & 0 & -1/a \\ \mu & 1 & 0 \\ \mu & -1 & 0 \end{bmatrix} \cdot \begin{bmatrix} N_i \\ V_i \\ M_i \end{bmatrix} \tag{10}$$

3.1.2 Equilibrium of a finite voussoir

The limit analysis of a structure subjected to constant and variable loads, through the lower bound formulation with associative flow, can be performed finding a maximum load multiplier that verifies both the yielding conditions in every section and equilibrium. The two conditions correspond to finding a statically admissible state, which maximizes the load multiplier; the maximum load multiplier, for the uniqueness theorem, is the safety factor. For the problem to be solved (through a linear programming procedure), once defined a yielding function, as done in paragraph 3.1.1, the equilibrium conditions have to be formulated.

The forces acting on the finite voussoir are represented in Figure 49. In the 2-dimensional case, considering rigid blocks in mutual contact through interfaces, the equilibrium of the single voussoir of finite dimensions leads to the formulation of 3 conditions (two translational conditions and one rotational). The global equilibrium will be defined imposing the equilibrium of each voussoir, writing, for a structure made of *n* blocks in contact through *m=n+1* interfaces, *3n* conditions. The number of variables to determine the stress state (in generalised stresses) is equal to *3m* (3 generalised stresses for each interface). As can be seen, the imposition of only equilibrium conditions is not enough to find a unique solution, as the problem is 3 times statically indeterminate.

The equilibrium of the single voussoir is here formulated considering some convenient assumptions for the nature of the problem that is analysed. Different assumptions can be made without losing any generality, resulting in general only in a more complex formulation. These assumptions are:

- Semi-circular arch of constant thickness
- Radial stereotomy
- Centre of mass of the voussoirs located in the central axis of the arch (acceptable for moderate thickness to radius ratios, as will be discussed in 3.1.4)
- Loads applied to the centre of mass of each voussoir (any load distribution could be expressed in an equivalent form with all loads applied to the nodal points)

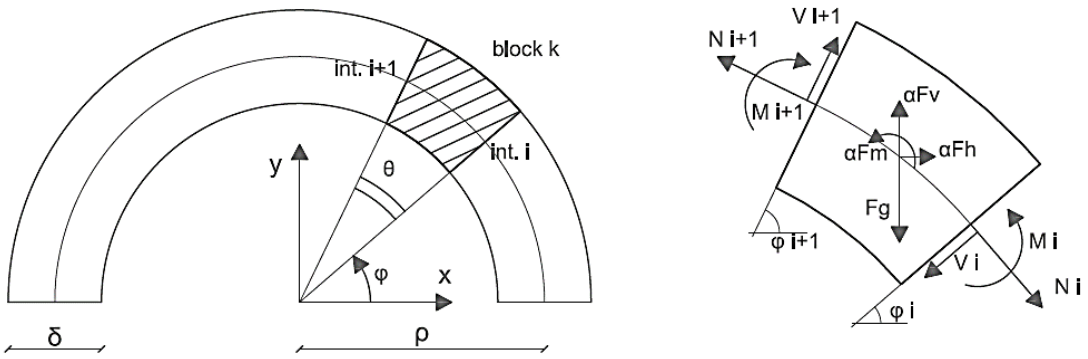

Figure 49. Equilibrium of a finite voussoir

The equilibrium in horizontal and vertical direction for the single voussoir k is formulated in equations

$$\begin{aligned} N_i \sin\varphi_i - V_i \cos\varphi_i - N_{i+1} \sin\varphi_{i+1} + V_{i+1} \cos\varphi_{i+1} + \alpha P_{0i,x} = 0 \\ -N_i \cos\varphi_i - V_i \sin\varphi_i + N_{i+1} \cos\varphi_{i+1} + V_{i+1} \sin\varphi_{i+1} - P_{gi} + \alpha P_{0i,y} = 0 \end{aligned} \tag{11}$$

For the rotational equilibrium around the point of application of the loads (the centre of mass of the voussoir, on its central axis) it is better to define the distances d_i and d_{i+1} and their angle with the interfaces i and i+1. The rotational equilibrium is in this way defined in equation 13.

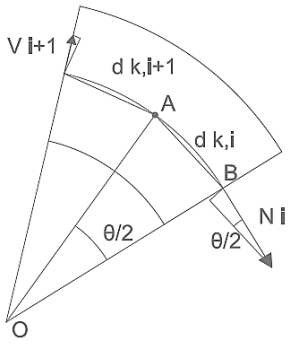

$$\overline{AB} = 2\rho \sin\frac{\theta_k}{4} = 2\rho \sin\frac{\varphi_{i+1} - \varphi_i}{4} = d_{k,i} = d_{k,i+1} \tag{12}$$

$$\begin{aligned} -N_i \sin\frac{\theta_k}{4} \cdot d_{k,i} - V_i \cos\frac{\theta_k}{4} \cdot d_{k,i} + M_i + N_{i+1} \sin\frac{\theta_k}{4} \cdot d_{k,i+1} \\ - V_{n+1} \cos\frac{\theta_k}{4} \cdot d_{k,i+1} - M_{i+1} + \alpha M_{0i} = 0 \end{aligned} \tag{13}$$

Figure 50. Rotational equilibrium of the finite voussoir

The system of equilibrium equations for all the voussoirs can be assembled and written in the compact matricial formulation (Orduña, 2003):

$$\boldsymbol{C^T Q} + \boldsymbol{F_g} + \alpha \boldsymbol{F_0} = \boldsymbol{0} \tag{14}$$

Where $\boldsymbol{Q}$ is the vector of the $3m$ generalised stresses, $\boldsymbol{C^T}$ is the matrix that contains the coefficients of the $3n$ equilibrium conditions (dimensions $3n$ x $3m$), $\boldsymbol{F_g}$ and $\boldsymbol{F_0}$ are the vectors (dimension $3n$) of the constant and variable forces applied to the n blocks. The notation $\boldsymbol{C^T}$ is used in literature because it is possible to demonstrate that the transpose of this matrix is the compatibility matrix. Its formulation for each block k, modifying the general expressions given in Orduña (2003) to take into account radial voussoirs of a semi-circular arch, can be written as:

$$[\boldsymbol{C^T Q}]_{\boldsymbol{k}} = \begin{bmatrix} \sin\varphi_i & -\cos\varphi_i & 0 & -\sin\varphi_{i+1} & \cos\varphi_{i+1} & 0 \\ -\cos\varphi_i & -\sin\varphi_i & 0 & \cos\varphi_{i+1} & \sin\varphi_{i+1} & 0 \\ -d_{k,i}\sin\frac{\theta_k}{4} & -d_{k,i}\cos\frac{\theta_k}{4} & -1 & d_{k,i+1}\sin\frac{\theta_k}{4} & -d_{k,i}\cos\frac{\theta_k}{4} & 1 \end{bmatrix} \cdot \begin{bmatrix} N_i \\ V_i \\ M_i \\ N_{i+1} \\ V_{i+1} \\ M_{i+1} \end{bmatrix} \tag{15}$$

3.1.3 Definition of the mathematical problem and computational solution

The relationships already presented are enough to establish the structure of the mathematical problem of finding a maximum load factor which satisfies both the equilibrium for each block and the yielding condition. As all relationships are linear, or have been linearized, the problem can be solved through linear programming. The structure of the problem, as expressed in Orduña (2003) is:

$$\begin{aligned} &\text{Maximise:} && \alpha \\ &\text{Subject to:} && \boldsymbol{C^T Q + F_g + \alpha F_0 = 0} \\ & && \boldsymbol{\varphi = N^T Q \leq 0} \end{aligned} \tag{16}$$

The structure of the problem can be expressed in more standard format for linear programming problems, as:

$$\begin{aligned} &\text{Maximise:} && [\boldsymbol{0^T} \;\; 1] \cdot \begin{bmatrix} \boldsymbol{Q} \\ \alpha \end{bmatrix} \\ &\text{Subject to:} && [\boldsymbol{C^T} \;\; \boldsymbol{F_0}] \cdot \begin{bmatrix} \boldsymbol{Q} \\ \alpha \end{bmatrix} = \boldsymbol{-F_g} \\ & && [\boldsymbol{N^T} \;\; \boldsymbol{0}] \cdot \begin{bmatrix} \boldsymbol{Q} \\ \alpha \end{bmatrix} \leq \boldsymbol{0} \end{aligned} \tag{17}$$

In this formulation the problem can be solved through a standard linear programming problem of the type in equation18, that can be easily implemented in MATLAB.

$$\begin{aligned} &\text{Maximise:} && \boldsymbol{c^T x} \\ &\text{Subject to:} && \boldsymbol{A_{eq} x = b_{eq}} \\ & && \boldsymbol{A_{dis} x \leq b_{dis}} \end{aligned} \tag{18}$$

The routines used to implement the analysis of the studied arch in MATLAB are provided in annex 1. The geometry is defined and the equilibrium matrix is built with the relations provided in equation 15. The yielding function is implemented through the matrix defined in equation 10. The aspect of the built matrixes, highly diagonal for their construction, is presented in Figure 51.

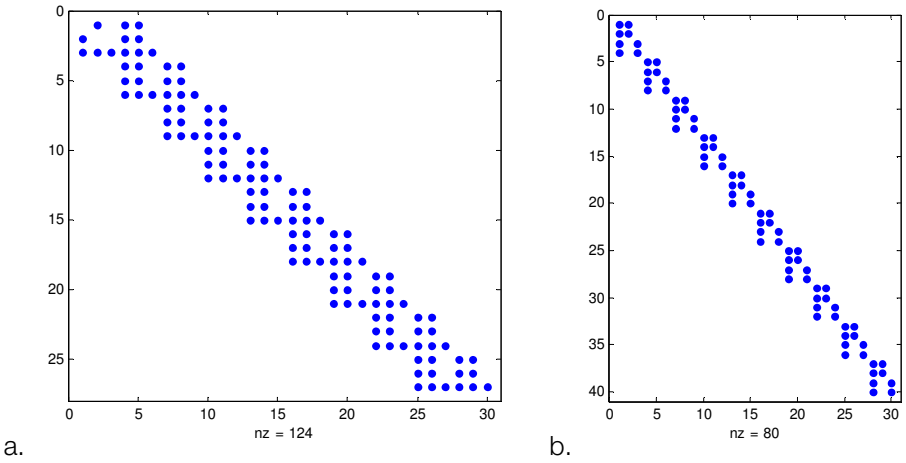

Figure 51. Non-negative elements of the matrices C^t (a), of the equilibrium conditions, and N^t (b) of the yielding function

The mathematical problem is solved through the function “linprog” in MATLAB, that solves exactly this typology of problems, expressed exactly in the formulation of equation 18. The computation of the maximum load is fast (in the order of a second), and robust (it does not diverge or depend on the initial point). The MATLAB code was used to perform the lower bound analysis in the hypotheses of voussoirs as rigid bodies, infinite compressive strength of the interfaces and zero tensile strength, Coulomb friction. The influence of friction will be discussed in the following. To compute the ultimate load with the tested load configurations a frictional coefficient of 0.5 was imposed, and was large enough to prevent sliding failure. As no sliding was measured in the tests, the assumption seems acceptable. Figure, Figure 53 and Figure 54 show the results of the analysis with the 3 tested load configurations. The red line constitutes an approximation of the thrust line: it connects the point of application of the thrust in the interfaces, but has no information about the position of the thrust inside the blocks, nor this information is needed for the assumption that are made here. The blue line connects the points where the yielding function is equal to 0, describing the mechanism that is forming. If the failure is in shear, the line passes through the centre of the section, evidencing the possibility of a sliding plane more than a hinge. As said, all the failures computed here involve only rocking of the blocks, as sliding was prevented setting an adequate coefficient.

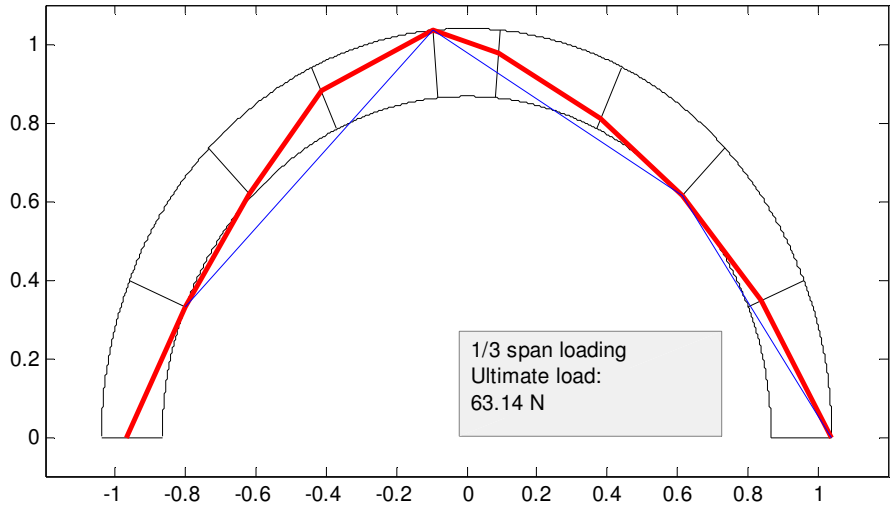

Figure 52. Third span loading, computation of the ultimate load and thrust line through limit analysis, lower bound (rigid blocks)

The analysis gives the ultimate load and the mechanism that is possible at failure. Such mechanisms, determined only by the position of the hinges, as no sliding is calculated nor measured, are the same as the ones obtained in the experimental tests for the same loading conditions. The ultimate loads have some differences that will be discussed in the last chapter. The solution is rather sensible to the friction coefficient that is imposed to the base interfaces: as in the experimental campaign the horizontal displacements at the base were restrained, an artificially higher friction coefficient is applied to those sections.

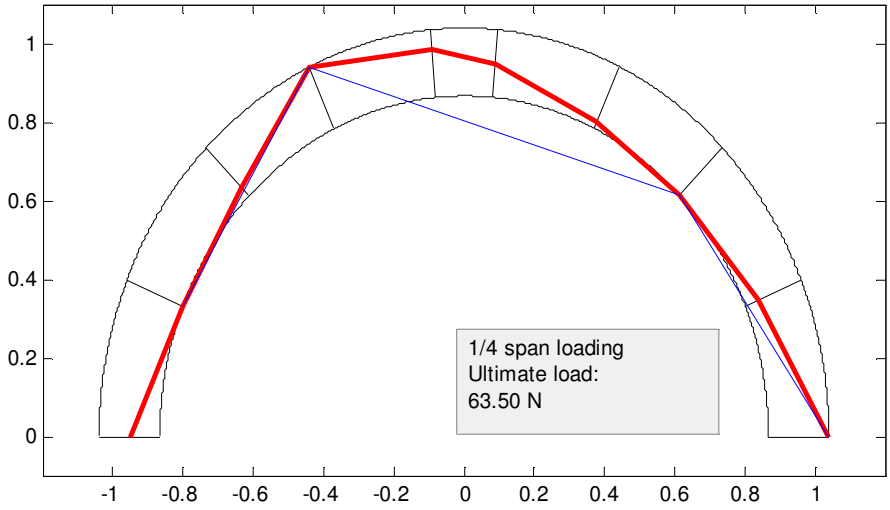

Figure 53. Quarter span loading, computation of ultimate load and thrust line through limit analysis, lower bound (rigid blocks)

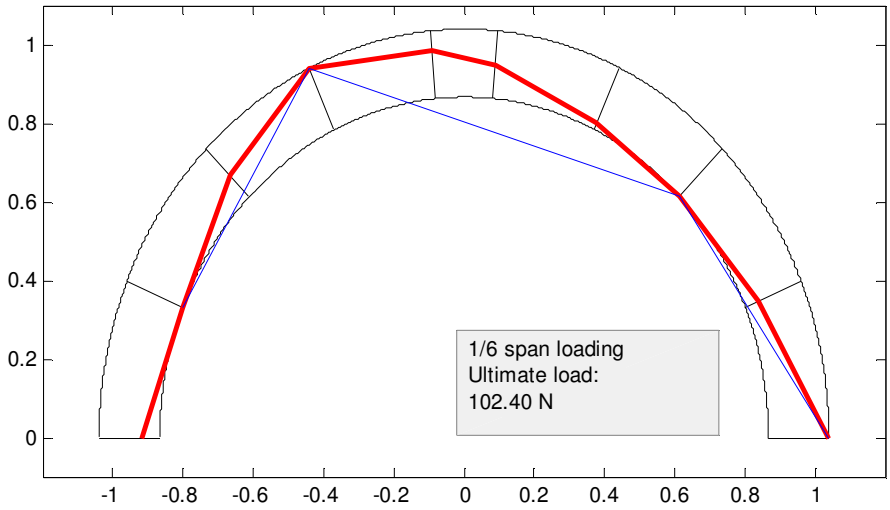

Figure 54. Sixth span loading, computation of ultimate load and thrust line through limit analysis, lower bound (rigid blocks)

The influence of the friction coefficient on the ultimate load is presented in Figure 55. The ultimate load was computed, for the different load configurations, varying the friction coefficient in the range [0.18-0.7], with steps of 0.02. For friction coefficients larger than 0.47 the failure load is constant, for all load configurations, corresponding to the formation of 4 rotational hinges. For smaller friction coefficients, the mechanisms changes and the possibility of formation of a sliding plane is found. The load multiplier, in these cases, decreases considerably. The critical friction coefficient, 0.47, corresponds to a friction angle of 25.1°; normal values for this parameter in existing masonry structures are generally larger. The method, anyway, allows the investigation also of sliding failures, which could be meaningful for different geometries (thicker arches or smaller number of interfaces).

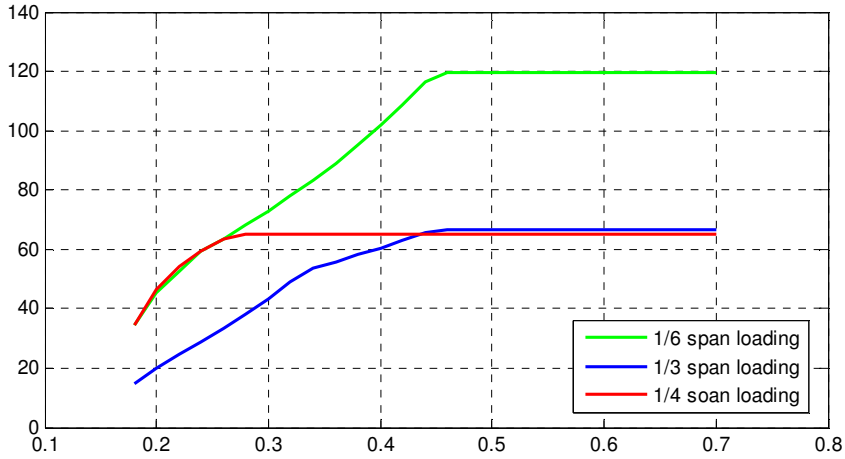

Figure 55. Influence of the friction coefficient on the ultimate load for the formation of different failure modes

The method allows to perform quickly an analysis on the influence of the number of voussoirs on the ultimate capacity, estimated through limit analysis (static approach, in this case). The MATLAB routine was adapted and the ultimate load was calculated, for quarter-span loading, varying the number of voussoirs from 4 to 100 (Figure 56). For a high number of voussoirs, the solution stabilizes around and asymptotical value, corresponding to the solution of a monolithic arch with zero tensile strength. The thrust line is calculated in many sections, and the condition that the thrust has to be located inside the geometrical boundaries of the arch is checked by the yield function in each of the calculated section. The small variability that is visible even for a high number of interfaces is due to the fact that a finite number of sections are calculated, and the position of the hinges in the theoretical case might be slightly different from the possibilities of the arch for the real position of the joints

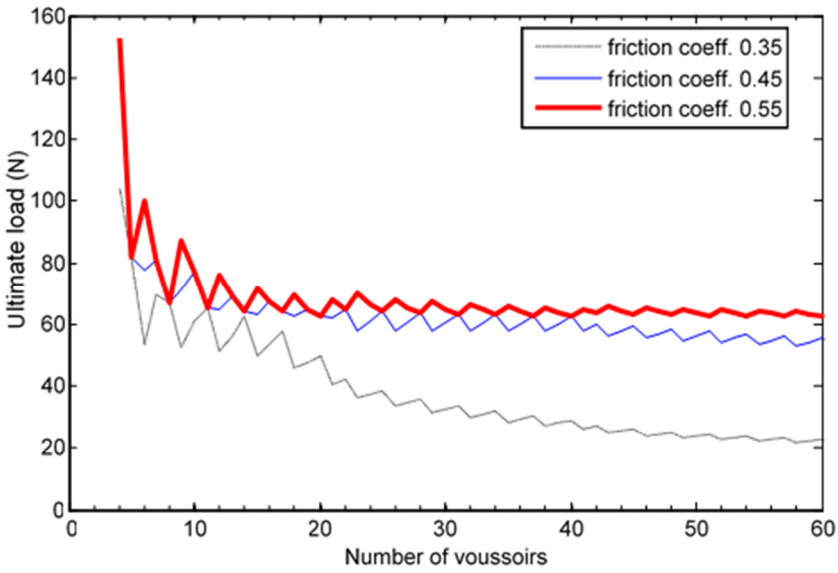

Figure 56. Ultimate load computed for arches with a variable number of voussoirs, for different friction coefficients

The reduced possibilities of formation of hinges for smaller number of voussoirs cause an increase in the calculated capacity of these arches, as shown better in Figure 57. The peaks correspond to those configurations in which the joints are the furthest from the position of the theoretical solution; in those cases, the thrust line, inside the single voussoirs, is allowed to stay out of the geometrical boundaries, and for this reason, the calculated load increases. This effect, depending highly on the position of the joints, is particularly relevant for a very small number of voussoirs.

It is not immediate, though, to give an estimation of this (calculated) effect based only on the number of voussoirs, for the variations induced by the position of the closest joint to the theoretical hinge. For the same number of voussoirs, for example, different results are found for different geometries of the voussoirs. The case that was studied, with different dimensions of the voussoirs, has a calculated ultimate load of 65.7 N for quarter span loading, while if a geometry with equally spaced voussoirs is imposed (as in the case of Figure 57) an ultimate load of 78.9 N is found, with a variation of 20%. It appears that, for this typology of arches, a detailed study taking into account the real position of the joints is needed.

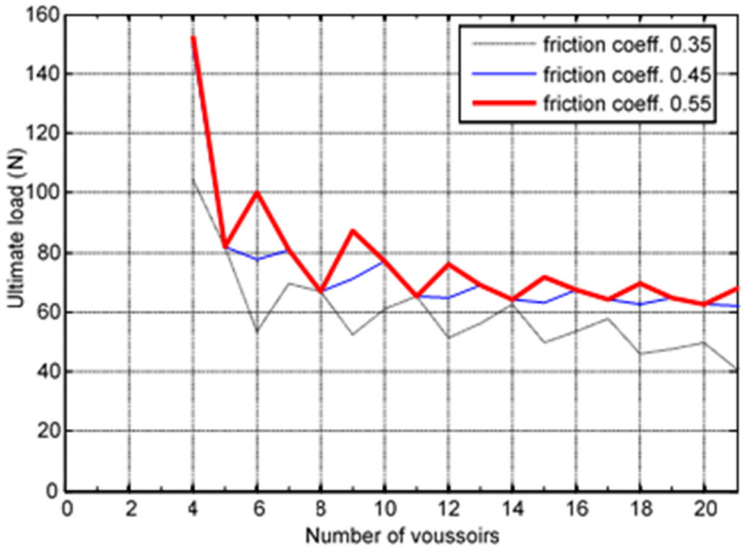

Figure 57. Capacity of arches with low number of voussoirs, limit analysis

It is still possible to estimate an effect of the number of voussoirs on the ultimate load (Figure 58), approximating a lower and upper bound, for the particular nature of the problem, linked not only to the number of interfaces but also to the position of the joints. It must be specified, though, that these relations are found for a specific geometry (semi-circular arch with thickness to span ratio of 1/10) and a standard stereotomy (equally spaced voussoirs) in the hypothesis of rigid blocks and interfaces with infinite compressive strength, zero tensile strength and a friction coefficient of 0.5. Changing some of these parameters, the results would be different. For this reason, a specific study of each case, with its real geometry, stereotomy, and material properties, is in general needed for this typology of arches.

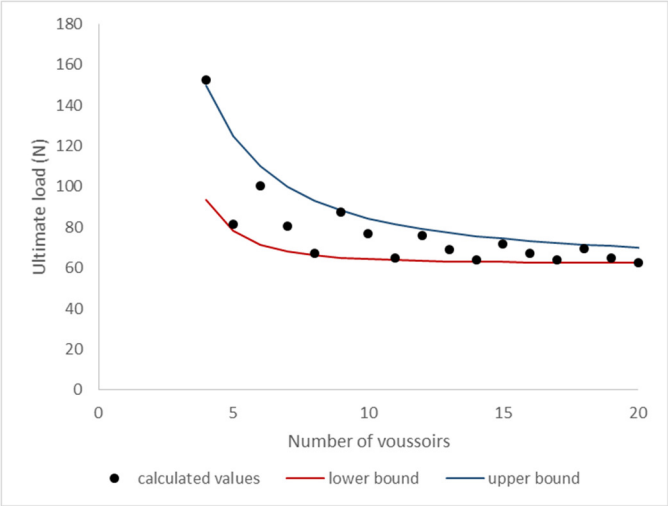

Lower bound curve:

$$P(n) = P_\infty + \left(\frac{3.2}{n}\right)^3 P_\infty \quad (19)$$

Upper bound curve:

$$P(n) = P_\infty + \left(\frac{5}{n}\right)^{3/2} P_\infty \quad (20)$$

Figure 58. Estimation of the effect of the number of voussoir for the studied geometry

The friction coefficient has an important role in determining the capacity of arches, modelled with this scheme of rigid voussoirs and interfaces, especially for arches with very low number of voussoirs. The results correspond to a friction coefficient of 0.5, except for the base interfaces, for which, to reproduce the conditions of the tested arch, a higher coefficient was set to prevent sliding. If an equal friction coefficient were imposed to each section the capacity of arches with very low number of voussoirs (4-7) would be consistently reduced, as the failure would correspond to the sliding of the right support or to the sliding of the voussoir to which the load is applied (or both). The failure mechanisms will be clearer in the kinematic limit analysis, but also with this approach, although without a simple graphical representation, it is possible to identify the type of failure of each section calculating the yield function and checking for which conditions it is equal to 0.

A validation of the method was performed using the software RING to compare the results obtained for the same hypotheses. The obtained values differ of less than 1% and correspond to the same failure mechanisms. An example is given in Figure 59.

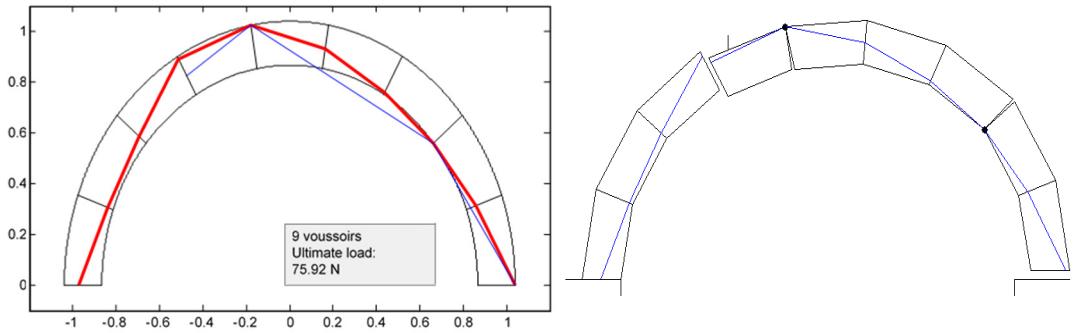

Figure 59. Validation of the procedure though comparison with software RING (failure load obtained by RING of 75.6 N)

Figure 60 shows the results of the analysis of arches of the same typology for geometry and material (corresponding to the testing conditions), with a rising number of voussoirs.

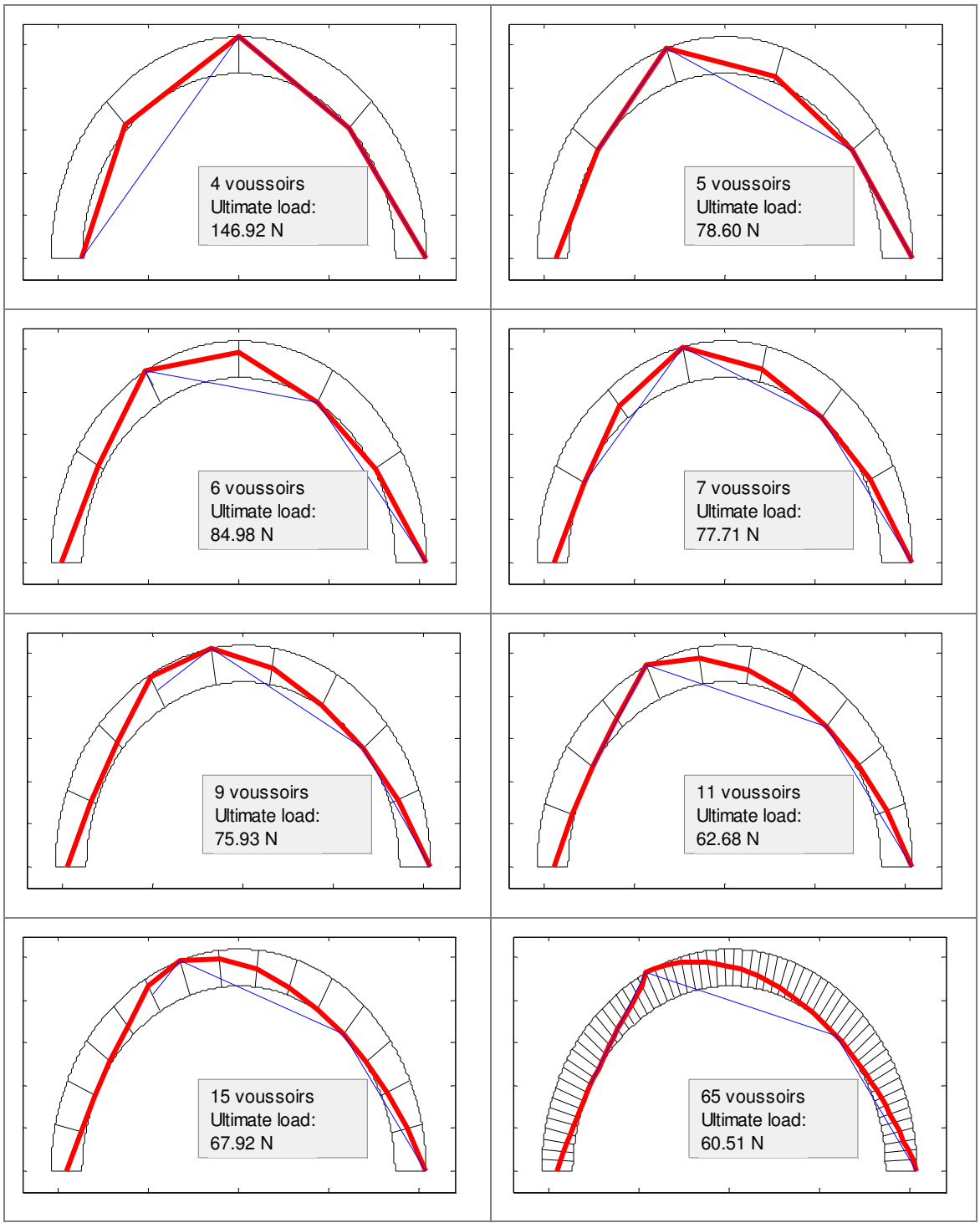

Figure 60. Limit analysis of arches with rising number of voussoirs, quarter span loading, static approach

3.1.4 Differential formulation of the equilibrium of an infinitesimal voussoir

The solution through static approach of limit analysis can be found also identifying a statically admissible configuration with the use of the thrust line: if a thrust line which satisfies some requirements is found, that solution is safe for the safe theorem (the conditions, in classical analysis, correspond to the fact that the thrust line should be inside the geometrical boundaries of the arch). The equations of the yield function that implicitly are checked with this condition are the two equations of the rocking of the section. If an evaluation of the compatibility of the shear is needed, this condition has to be checked *a posteriori* with the angles between the thrust line and the joints, that must be less than the friction angle.

The approach is simple and can be performed by means also of graphic statics. Finding an ultimate load for the structure, though, corresponds to an optimisation of the solution that is found until it is not possible to find another compatible thrust line for a higher load. This process, if performed through graphic statics, can be long and lead to excessively conservative solutions, if the optimisation process is not effective. In this work a different approach was followed, solving numerically both the problem of finding a thrust line and the optimisation of the solution.

The profile of the thrust line of a generic arch can be expressed through a differential formulation, based on the equilibrium condition of an infinitesimal voussoir. The formulation of the mechanical problem, and its the results, depend on the stereotomy of the arch, or, more precisely, on the shape that is assumed for the infinitesimal voussoir. The difference in the results can be easily explained with the fact that a two-dimensional problem is converted into a one-dimensional problem, implicitly assuming a certain path for the flow of forces. If a radial stereotomy is assumed, as it is the most diffused typology in existing arches, and as the cracks and discontinuities in arches appear generally in radial direction, the equilibrium of a radial voussoir has to be evaluated. If, on the other hand, the equilibrium of vertical voussoirs is considered, the assumed path for the forces is different and the solution differs slightly both in the formulation and in the results. This second hypothesis, even if more immediate from the analytical point of view, appears though less realistic.

The first approach, related to a radial stereotomy, found a complete formulation in the work of Milankovitch (1904) “Beitrag zur Theorie der Druckkurven” (presented in Foce, 2007). This study, although developed when the elastic theory was widely used for all kinds of structures, analyses the problem only through equilibrium conditions of a radial infinitesimal voussoir, infinitely rigid and resistant.

The problem is formulated in a completely general and rigorous way. No assumptions are made on the shape of the arch: a radius of curvature, variable in general, is assumed for each voussoir, that is considered perpendicular to the curve of the arch. The thickness of the arch is defined for each section and can be variable. The centre of mass of the infinitesimal voussoir can be expressed and has a finite distance from the centre line of the arch. This distance, as expressed in equation 25, deriving from the

proportions of areas of triangles (equation 24), depends on the thickness of the arch and on its radius, and is negligible only for arches with limited thickness to span ratio or parallel joints.

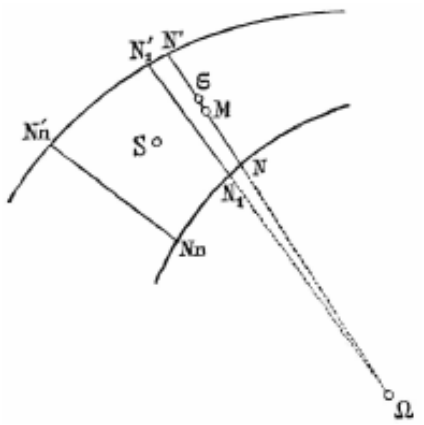

$$\overline{\Omega M} = \rho; \quad \overline{NN'} = \delta \tag{21}$$

$$df_1 = A_{\Omega N'_1 N'}; \quad df_2 = A_{\Omega N_1 N} \tag{22}$$

$$(df_1 - df_2) \cdot \overline{\Omega G} = \frac{2}{3}\left(\rho + {}^{\delta}/_{2}\right)df_1 - \frac{2}{3}\left(\rho - {}^{\delta}/_{2}\right)df_2 \tag{23}$$

$$df_1 : df_2 = (\rho + {}^{\delta}/_{2})^2 : (\rho - {}^{\delta}/_{2})^2 \tag{24}$$

$$\overline{\Omega G} = \rho + \frac{\delta^2}{12\rho} \tag{25}$$

Figure 61. Determination of the centre of mass of the infinitesimal voussoir

The equilibrium of the infinitesimal radial voussoir can be written, in the general case, referring to the symbols and the system of coordinates in Figure 62, as:

$$Vdx - Hdy + M_g + M_{extrados} + M_{intrados} = 0 \tag{26}$$

Where M_g, $M_{extrados}$ and $M_{intrados}$ are, respectively, the moments around the center of application of the the thrust in the section corresponding to $\varphi + d\varphi$, of the self weight, the load applied to the extrados and the one to the intrados. These loads have in general a direction of application defined by the angles ϵ and η. V and H are the vertical and horizontal component of the thrust at the section.

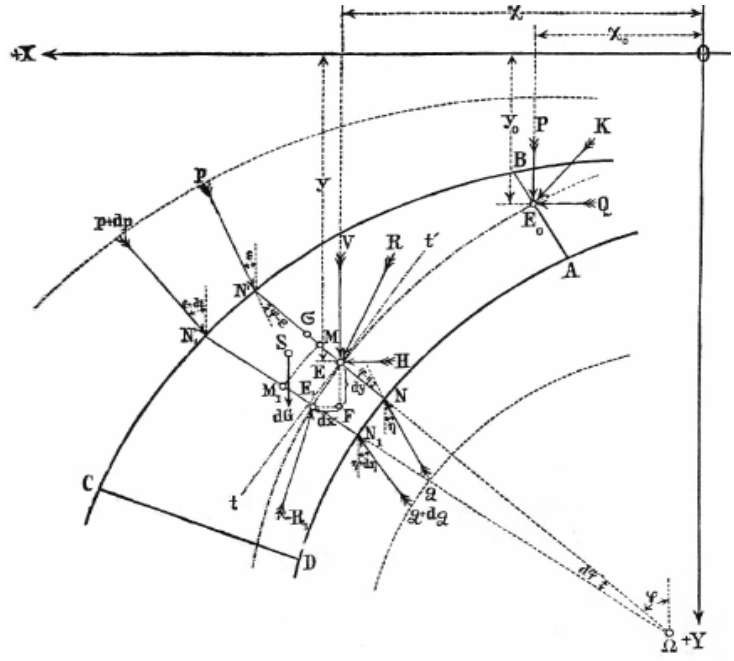

Figure 62. Equilibrium of the infinitesimal voussoir: general condition

The three moments, where ξ is the eccentricity of the thrust with respect to the centre line of the arch, can be expressed as:

$$M_g = -dG(\overline{MG} + \overline{ME})\sin\varphi = -gt\delta\left(\frac{\delta^2}{12\rho} + \xi\right)\sin\varphi\,\rho d\varphi \tag{27}$$

$$M_{extrados} = -(pde)(\overline{N'E})\sin(\varphi - \varepsilon) = -p\left(\frac{\delta}{2} + \xi\right)\sin(\varphi - \varepsilon)de \tag{28}$$

$$M_{intrados} = -(qdi)(\overline{NE})\sin(\varphi - \eta) = -q\left(\frac{\delta}{2} - \xi\right)\sin(\varphi - \eta)di \tag{29}$$

From equation 26, substituting equations 27, 28 and 29, and dividing by Hdx derives the general differential equation of the thrust line derived by Milankovitch:

$$\frac{dy}{dx} = \frac{V}{H} - \frac{1}{H}\left[gt\delta\rho\left(\frac{\delta^2}{12\rho} + \xi\right)\sin\varphi\frac{d\varphi}{dx} + p\left(\frac{\delta}{2} + \xi\right)\sin(\varphi - \varepsilon)\frac{de}{dx} + q\left(\frac{\delta}{2} - \xi\right)\sin(\varphi - \eta)\frac{di}{dx}\right] \tag{30}$$

The value of the vertical and horizontal component of the thrust can be derived from general equilibrium, calling H_0 and V_0 the values of the the horizontal and vertical thrust in the starting point of integration:

$$V(x) = V_0 + gt\int_{x_0}^{x}\delta\rho d\varphi + \int_{x_0}^{x} p\cos\varepsilon\, de - \int_{x_0}^{x} q\cos\eta\, di \tag{31}$$

(

$$H(x) = H_0 - \int_{x_0}^{x} p\sin\varepsilon\, de + \int_{x_0}^{x} q\sin\eta\, di \tag{32}$$

The general equation 30 can be considerably simplified in the case studied in this work of a semi-circular arch of constant thickness, loaded in the central line only vertically. The equation, for this particular case, becomes:

$$\begin{gathered}\frac{dy}{dx} = \frac{V}{H} - \frac{1}{H}\left[gt\delta\rho\left(\frac{\delta^2}{12\rho} + \xi\right)\sin\varphi\frac{d\varphi}{dx} + p(\xi + \frac{\delta}{2})\sin\varphi\frac{de}{dx}\right] \\ V(x) = V_0 + gt\delta\rho(\varphi(x) - \varphi_0) + \int_{x_0}^{x} pde \\ H(x) = H_0\end{gathered} \tag{33}$$

Applying the transformation into polar coordinates, with the system as indicated in Figure 62, the derivatives in equation 33 can be expressed. Equation 36 is simplified because for the semi-circular extrados the radius is constant.

$$\begin{cases} x = r\sin\varphi \\ y = -r\cos\varphi \end{cases}; \qquad \begin{cases} r = \sqrt{x^2 + y^2} \\ \varphi = \arcsin\dfrac{x}{\sqrt{x^2 + y^2}} \end{cases} \tag{34}$$

$$\frac{d\varphi}{dx} = \frac{\dfrac{1}{\sqrt{x^2 + y^2}} - \dfrac{x^2}{(x^2 + y^2)^{3/2}}}{\sqrt{1 - \dfrac{x^2}{x^2 + y^2}}} = \frac{\dfrac{1}{r} - \dfrac{x^2}{r^3}}{\sqrt{1 - \dfrac{x^2}{r^2}}} \tag{35}$$

$$\frac{de}{dx} = \frac{d}{dx}\left[\left(\rho + {}^{\delta}/_{2}\right)d\varphi\right] = R\frac{d}{dx}\arcsin\frac{x}{R} = \frac{R}{\sqrt{R^2 - x^2}} = \frac{R}{|y|} \tag{36}$$

The problem, as formulated in equation 33, can be solved numerically or analytically in simple cases (absence of imposed vertical loads, for example). The formulation varies consistently if other hypotheses on the shape of the voussoir are made, like the assumption of vertical voussoirs. In this case, the moments in equations 27, 28 and 29 disappear, and the differential equation is simplified into:

$$\frac{dy}{dx} = \frac{V}{H} \tag{37}$$

From equations 30 and 37 it appears clearly that the assumption that the thrust is tangent in all points to the thrust line is strictly valid only in the case of vertical joints, while for radial joints an additional term appears and the direction of the thrust line remains, in general, different from the tangent to the thrust line. The problem is discussed also in Heyman (2009), showing that for a radial joints there must be a difference between the direction of the thrust and the direction of the tangent to the thrust line to assure equilibrium (Figure 63). This concept, anyway, is not due only to the work of Milankovitch, as it was already present in some of the first studies on the statics of arches (Moseley, 1848).

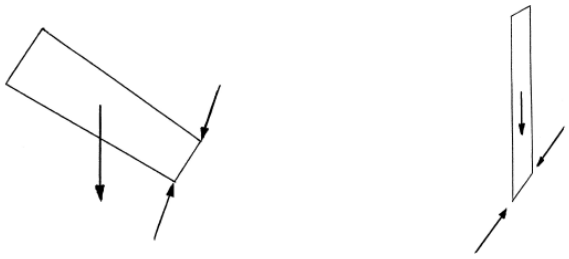

Figure 63. Direction of the thrust for voussoirs of different stereotomy (Heyman, 2009)

Equation 37, valid for vertical stereotomy, corresponds, if integrated, to the equation of catenary only in the case of constant vertical load. It is evident, though, that in the case of vertical joints the self-weight applied to each voussoir, in function of x, is not constant; the catenary curve, so, is not a physically admissible thrust line of an arch subjected to its self-weight (Makris and Alexakis, 2013). The difference between the formulations, generally little for ultimate loads of real arches, can be noticed when the problem of the minimum thickness of an arch subjected only to self-weight is solved (Couplet's problem). One thing to be underlined in this context is that, when an elastic solution of a cable element is used to calculate the thrust line of an arch, procedure that is commonly followed, this implies the assumption of vertical stereotomy. If the solution for radial stereotomy has to be calculated, the analogy with cable elements does not stand anymore and different solution procedures have to be applied.

3.1.5 Calculation of an optimised thrust line solution

The calculation of an admissible thrust line can be based on the differential formulation presented in paragraph 3.1.4. In particular, to analyse the case of the arch studied in this work, equation 33 (relative to the case of a semi-circular arch of constant thickness) can be used. The formulation should be slightly adjusted to take into account the fact that the imposed load is applied to the centre line of the arch and not to the extrados or intrados: this can be done modifying, in the moment of the imposed load, the arm from $(\xi + \delta/2)$ to simply ξ.

Equation 33 is a first-order differential equation, expressed as a Cauchy's problem:

$$\begin{cases} y'(x) = f(x, y(x)) \\ y(x_0) = y_0 \end{cases} \tag{38}$$

Where:

$$f\big(x, y(x)\big) = \frac{V}{H} - \frac{1}{H}\left[gt\delta\rho\left(\frac{\delta^2}{12\rho} + (\rho - r)\right)\sin\varphi\,\frac{\frac{1}{r} - \frac{x^2}{r^3}}{\sqrt{1 - \frac{x^2}{r^2}}} + p(\rho - r)\sin\varphi\,\frac{1}{y}\right] \tag{39}$$

$$r = r(x, y) = \sqrt{x^2 + y^2}$$

$$\varphi = \varphi(x, y) = \arcsin\frac{x}{\sqrt{x^2 + y^2}}$$

$$V(x, y) = V_0 + gt\delta\rho(\varphi(x) - \varphi_0); \quad H = H_0$$

As no distributed load is applied to the tested arch, there is not the need to calculate the integral in equation 33b; the differential equation can be solved separately in the two parts of the domain, and the applied load appears only as an initial condition. The integration of the differential equation depends in general from 4 parameters as initial conditions:

- the two coordinates of the initial point x_0, y_0
- the two values of the horizontal and vertical thrust in (x_0, y_0): H_0, V_0

Once set the initial conditions, the Cauchy's problem can be solved numerically. The calculation of the thrust line, though, does not require only the integration of the differential equation in the domain, but also the optimisation of the parameters to obtain an acceptable solution. This optimised solution was considered the one which has the higher geometrical safety factor, as defined in (Heyman, 1966):

$$GSF = \frac{eccentricity}{half\ thickness} = \frac{\max(\xi)}{\delta/_2} \tag{40}$$

Even if a the calculation of one solution with a geometrical safety factor of more than one (or equal to 1) is sufficient to prove the stability of the arch through the safe theorem of limit analysis, the optimisation process, in this case, was continued until the higher geometrical safety factor is found. This, anyway, does not imply that the solution has to be considered the most accurate prediction of the real state of stress of the arch, but rather the an optimised solution, the furthest possible from the geometrical

boundaries of the arch. The optimisation procedure allows as well to find the ultimate load of an arch, if the applied load is increased until the optimisation process does not find a maximum geometrical safety factor greater than 1.

The procedure that was implemented in MATLAB is fully presented in the annex 3. The routines were developed to compare the results of this experimental tests, so they apply the hypothesis of semi-circular arch of constant thickness with concentrated applied load. The logical process that was followed can be described in the following steps:

1. definition of the geometry of the arch (radius, thickness, number and position of joints)
2. approximation of an initial vector of parameters as a first step for the solution
3. solution of the differential equation in two domains separated by the applied load
4. approximation of the solution through linear interpolation in the points of interest that were not directly numerically calculated (to obtain the solution exactly in the joints)
5. computation of the geometrical safety factor
6. optimisation of 3 parameters to obtain a (global) maximum safety factor, repeating the procedure from step 3.

An initial vector for the parameters of the solution requires a rough determination of the order of magnitude of the horizontal and vertical component of the thrust in the initial point. This point can be assumed, for the first solution, in the middle of the thickness of the first joint. As an admissible thrust line has to pass inside the last joint, the parameters to set are only three, because the y coordinate of the first point can be set always equal to 0.

The solution of the differential equation is fast and rather stable, even if the solution could diverge if unrealistic initial conditions are set. The solver that was used in MATLAB is ode45, which uses Runge-Kutta methods of the fourth and fifth order, but any other numerical method is applicable. The solution of the differential equation could be done in a single step, opportunely defining a function for the integral of the applied load. This method, though, does not assure that the point of application of the load is exactly among the calculated integration steps, and this could result in a slight variation of the calculated loading conditions. For this reason, it is preferable to integrate the differential equation in two steps, separated by the point of application of the load, with adequate initial conditions for the second step. These conditions are the initial point, corresponding to the last point calculated in the first part of the domain, and the vertical component of the thrust, that has to take into account the last calculated vertical component and the applied load. As the solution is calculated in some integration steps it is possible that in some sections of interest, that are in particular the joints, as will be presented in the following, the solution is not calculated. In these sections the solution is approximated through linear interpolation from the closer calculated points.

The solution of the differential equation is used to compute a geometrical safety factor, that can be calculated following different assumptions, that are the real objective of this study. For example, apart

from the classical hypothesis that the thrust line has to be inside the geometrical boundaries of the arch, the geometrical safety factor could be calculated only in the joints, allowing the thrust line to stay out of the boundaries of the arch in the voussoirs. Alternatively, another approach can be considering different boundaries for the voussoirs and for the joints, eventually depending on the applied forces, as the solution is available also in terms of vertical and horizontal component in each point, or checking, together with the eccentricity of the thrust, the admissibility of the frictional component.

Once a geometrical safety factor is calculated, the solution can be repeated for different values of the initial parameters, in an optimisation process to find the maximum geometrical safety factor. To avoid the determination of local minima, depending strongly on the initial point, and find a global minimum of the function, a multi-point optimisation procedure was applied.

This optimisation procedure is in some cases problematic for the nature of the function to minimise, dependent on the integration of a differential equation. Much more efficient and robust procedures were used to solve the linear programming problem in 3.1.3. The solver requires an initial point and a range of variability of the parameters to optimise, to spread the different starting points in the whole possible domain. The definition of this range requires, once again, an estimation of the order of magnitude of the horizontal and vertical component of thrust. If the defined range is too large the optimisation procedure could not come to any result, as the solution of the differential equation could diverge, or the density of the starting points in the domain of real interest could be not enough. The last parameter to set is of easier determination, as the position of the thrust line in the initial section (the first joint) has a well-defined possible domain. The repetition of the procedure until an optimised solution is found requires some seconds of execution time. From a computational point of view, the process adopted in paragraph 3.1.3 is far more efficient.

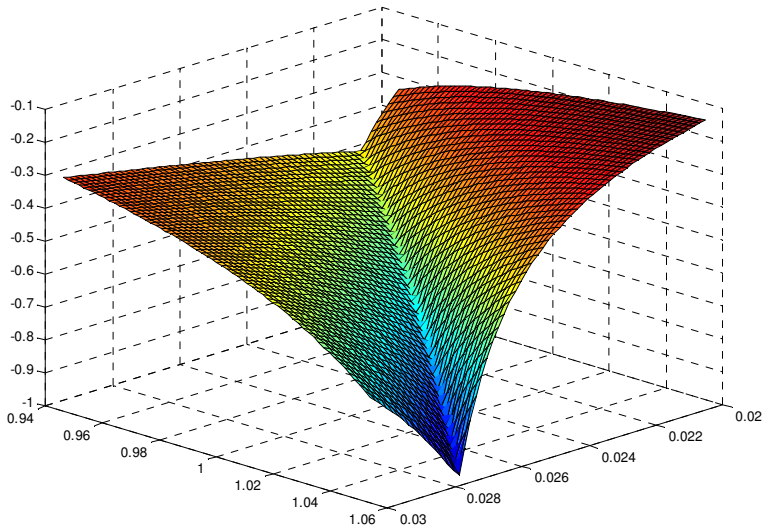

Figure 64. Function to minimise (the geometrical safety factor) when two parameters are needed (horizontal and position of the thrust, for symmetrical loading)

The process was applied to the studied arch loaded at 1/3 of the span. The results are given in Figure 65. The criteria applied to calculate the safety factor are different: in solution a the thrust line if forced to stay inside the geometrical boundaries of the section only in the joints, while no other condition is applied to the blocks. Solution b is the classical solution, in which the thrust is considered admissible only if it is completely inside the geometrical boundaries of the arch.

The first solution is close to the value calculated in 3.1.3 (63 N, while this is 66 N). The positive difference could be due to the fact that here the solution is calculated in a number of points depending on the tolerances that are set, and extrapolated in the points of interest, leading to possible imprecisions and to non-conservative results. The classical solution, on the other hand, gives a low value if compared to the solution calculated in 3.1.3 for a large number of voussoirs (62 N), possibly for a scares efficiency of the optimisation. It is possible to see, indeed, that the thrust line is close but not tangent to the intrados; the solution is presented, anyway, to stress the problems of the automatic optimisation of this type of solution. Analogous results were obtained for the other two configurations (Figure 66, Figure 67); tor quarter span loading, as the position of the hinges found with classic limit analysis almost coincides with the existing joints, the two solutions differ very little.

a.

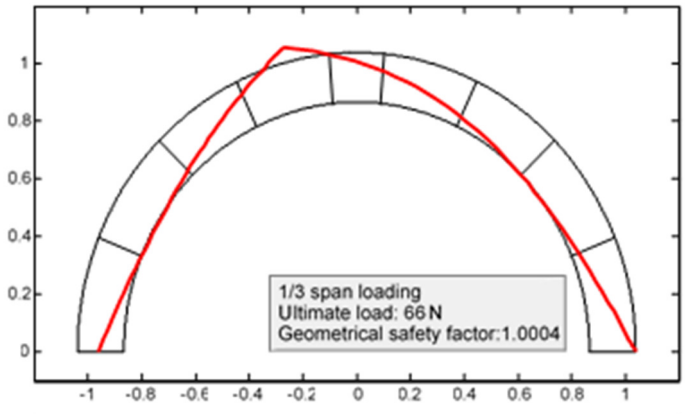

b.

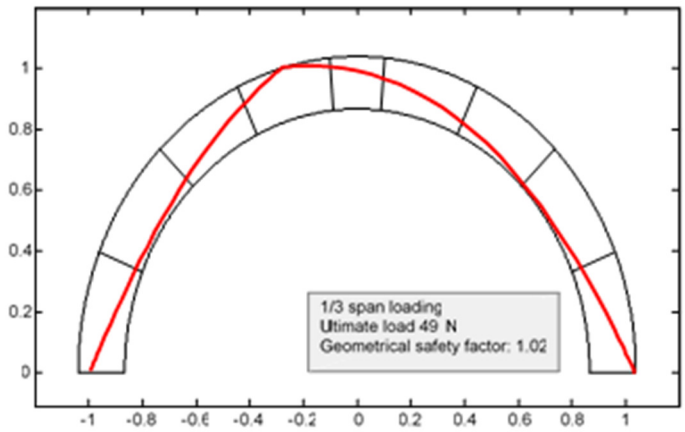

Figure 65. Calculated (optimised) solution for third span loading with direct integration of the differential equation of the thrust line. Solutions for thrust line inside the geometrical boundaries of the arch only in the joints (a) or in the complete arch (b)

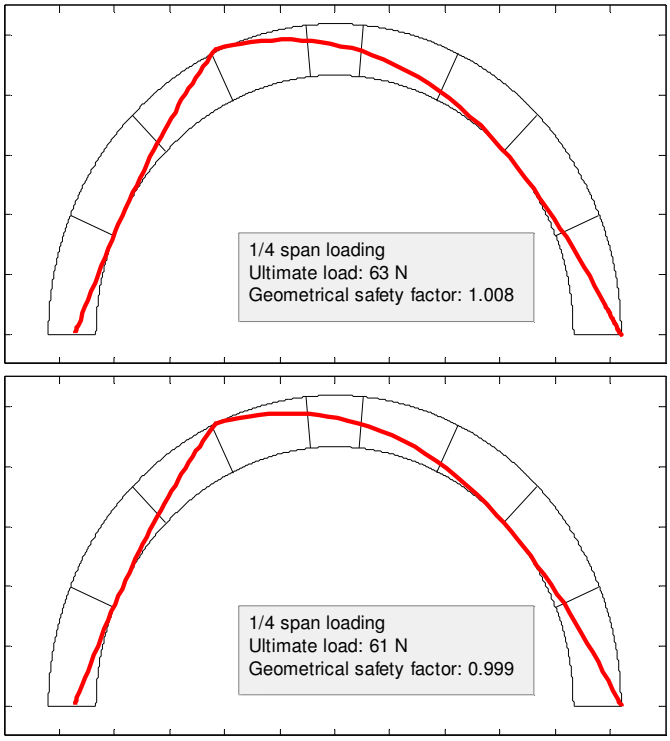

Figure 66. Optimised solution for quarter span loading: Solutions for thrust line inside the geometrical boundaries of the arch only in the joints (a) or in the complete arch (b)

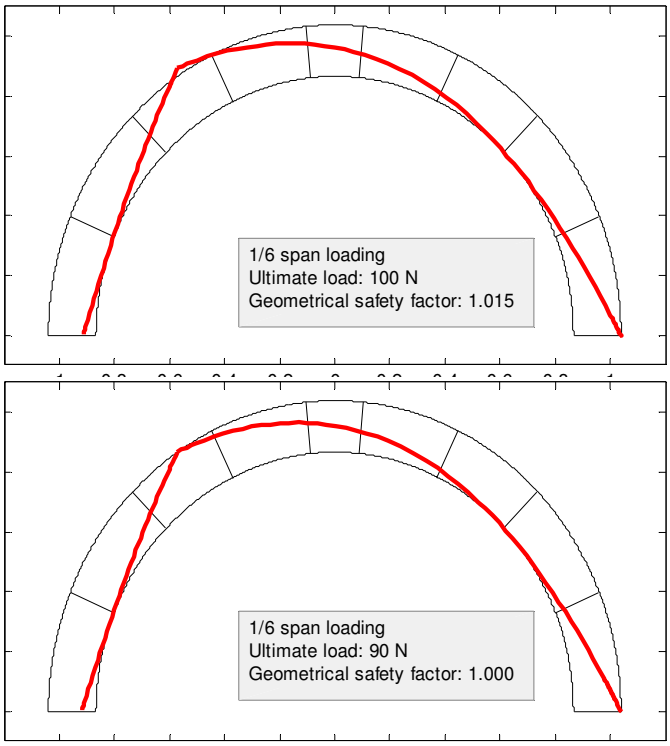

Figure 67 Optimised solution for sixth span loading: Solutions for thrust line inside the geometrical boundaries of the arch only in the joints (a) or in the complete arch (b)

3.2 Upper bound analysis (kinematic approach)

The kinematic approach of limit analysis is based on the kinematic theorem, that states that the safety factor is the smallest of all the possible load multiplier correspondent to kinematically compatible mechanisms. For the uniqueness theorem, this safety factor has to be the same as the static load multiplier, and the kinematic formulation is just the dual problem of the one solved with static approach. For non-associated flow rule, as said, the solution might not be unique and a mixed problem has to be solved, taking into account both the equations of static ad kinematic approach, looking for the smallest load multiplier satisfying both static and kinematic conditions. In this work only associated flow will be treated, for the characteristics of the problem that is analysed, on the basis also of the experimental results. The extension of the problem to non-associated flow, anyway, could be done with the same instruments and a methodology that will be briefly discussed.

A mechanism in a structure of rigid blocks is formed when an enough number of hinges or sliding planes appear, and unbounded displacements can occur. In this configuration, the virtual work principle (or more precisely the virtual power principle), can be used in order to calculate the load factor associated with the particular mechanism. As confirmed also by experimental evidence, at failure the arch behaves as a set of rigid blocks interacting between them, with all the plastic flow at the sections of contact between the rotating blocks.

The problem can be solved also by hand application of the theorem of virtual works to all possible (reasonable) mechanisms that might develop, until the minimum load multiplier is found. The procedure is simple, but the identification of the correct mechanism might be not immediate. In this work, a computational formulation is adopted, consisting in expressing the conditions for a mechanism to be kinematically compatible and performing the solution of a minimisation problem through linear programming to identify the minimum load multiplier (and the relative failure mechanism).

A kinematically compatible mechanism must satisfy the condition that the generalised strains $\delta \boldsymbol{q}$ (as defined in Figure 68), at the interfaces, linked to the plastic strains $\delta \boldsymbol{\lambda}$ at each interface by the flow rule, are compatible with the displacement rates $\delta \boldsymbol{u}$ of the centroids of each rigid block. There exist, as will be presented, analogies between the matrixes defined in 3.1.3 and the compatibility and flow rule matrix defined here to express the relations between plastic strain rates, generalised strains and displacements of the blocks.

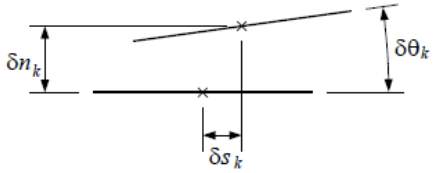

Figure 68. Generalised strains at the interfaces: physical meaning of the components and adopted sign convention

As described in Figure 70 the relation between plastic strain rates $\delta\boldsymbol{\lambda}$ and generalised strains $\delta\boldsymbol{q}$ can be expressed, in the hypothesis of associated flow, by the matrix $\boldsymbol{N_0}$. As can be noticed, because the flow is associated, this matrix is the transpose of the matrix $\boldsymbol{N^T}$ as defined in 3.1.3, describing the yield function.

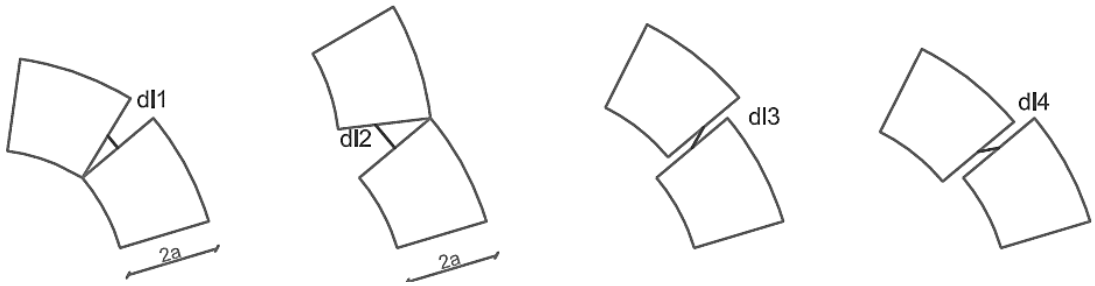

$\delta n = \delta\lambda_1$ $\quad \delta\theta = \frac{1}{a}\delta\lambda_1$ $\qquad$ $\delta n = \delta\lambda_2$ $\quad \delta\theta = -\frac{1}{a}\delta\lambda_2$ $\qquad$ $\delta n = \mu\delta\lambda_3$ $\quad \delta\theta = \delta\lambda_3$ $\qquad$ $\delta n = \mu\delta\lambda_3$ $\quad \delta\theta = -\delta\lambda_3$

Figure 69. Relation between plastic strain rates and generalised stresses (associated flow rule)

$$\delta\boldsymbol{q} = \boldsymbol{N_0}\cdot\delta\boldsymbol{\lambda} = \begin{bmatrix} 1 & 1 & \mu & \mu \\ 0 & 0 & 1 & -1 \\ 1/a & -1/a & 0 & 0 \end{bmatrix}\cdot\begin{bmatrix}\delta\lambda_1 \\ \delta\lambda_2 \\ \delta\lambda_3 \\ \delta\lambda_4\end{bmatrix} \tag{41}$$

Similarly, the relation between generalised strains and displacements of the blocks can be described in matrix form through $\boldsymbol{C}$ which is the opposite of the transpose of matrix $\boldsymbol{C^T}$, as already defined. Its components are defined in Figure 70.

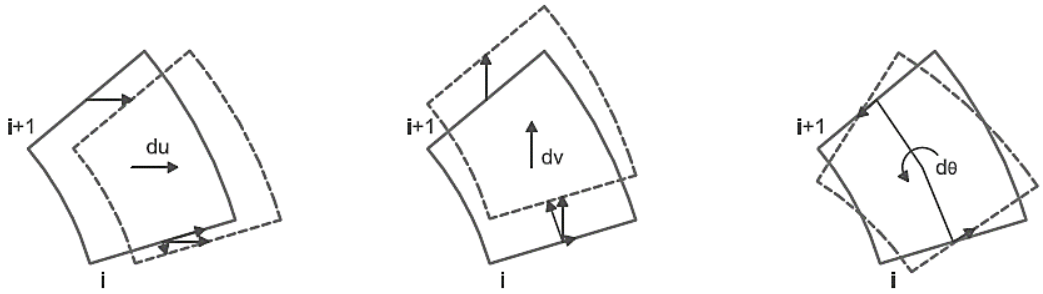

$\delta n_i = -\sin\varphi_i\cdot\delta u_k$
$\delta s_i = \cos\varphi_i\cdot\delta u_k$
$\delta n_{i+1} = \sin\varphi_{i+1}\cdot\delta u_k$
$\delta s_{i+1} = -\cos\varphi_{i+1}\cdot\delta u_k$

$\delta n_i = \cos\varphi_i\cdot\delta v_k$
$\delta s_i = \sin\varphi_i\cdot\delta v_k$
$\delta n_{i+1} = -\cos\varphi_{i+1}\cdot\delta v_k$
$\delta s_{i+1} = -\sin\varphi_{i+1}\cdot\delta v_k$

$\delta n_i = d\sin{}^{\theta}/_{4}\cdot\delta\theta_k$
$\delta s_i = d\cos{}^{\theta}/_{4}\cdot\delta\theta_k$
$\delta\theta_i = \delta\theta_k$
$n_{i+1} = -d\sin{}^{\theta}/_{4}\cdot\delta\theta_k$
$\delta s_{i+1} = d\cos{}^{\theta}/_{4}\cdot\delta\theta_k$
$\delta\theta_{i+1} = -\delta\theta_k$

Figure 70. Relation between displacements of the block k and generalised strains at joint I and i+1

$$\delta \boldsymbol{q} = [\boldsymbol{C}]_{k/ij} \cdot \delta \boldsymbol{u}_k = \begin{bmatrix} -\sin\varphi_i & \cos\varphi_i & d_k \sin\theta_k/4 \\ \cos\varphi_i & \sin\varphi_i & d_k \cos\theta_k/4 \\ 0 & 0 & 1 \\ \sin\varphi_{i+1} & -\cos\varphi_{i+1} & -d_k \sin\theta_k/4 \\ -\cos\varphi_{i+1} & -\sin\varphi_{i+1} & d_k \cos\theta_k/4 \\ 0 & 0 & -1 \end{bmatrix} \cdot \begin{bmatrix} \delta u_k \\ \delta v_k \\ \delta\theta_k \end{bmatrix} \tag{42}$$

Using equations 41 and 42 it is possible to assemble the matrixes $\boldsymbol{C}$ and $\boldsymbol{N_0}$ for the whole structure. In particular, the last equation defines the components of $\boldsymbol{C}$ relative to the generalised strains in the joints I and j due to the displacement of block k. If the structure has m interfaces between the $n = m - 1$ blocks, the matrix $\boldsymbol{N_0}$ has dimensions $[3m, 4m]$ and the matrix $\boldsymbol{C}$ is $[3m, 3n]$. Equating equations 41 and 42 one obtains (Orduña, 2003):

$$\delta \boldsymbol{q} = \boldsymbol{C}\delta \boldsymbol{u} = \boldsymbol{N_0}\delta \boldsymbol{\lambda} \tag{43}$$

Once defined the compatibility matrix $\boldsymbol{C}$ and the flow rule in $\boldsymbol{N_0}$ it is possible to write the principle of virtual work as:

$$\boldsymbol{Q^T}\delta \boldsymbol{q} = (\boldsymbol{F^T}_g + \alpha \boldsymbol{F}_0^T)\delta \boldsymbol{u} \tag{44}$$

The first term refers to the internal work: it is possible to demonstrate that the internal work is equal to 0, at least for associated flow rule. Since the displacement rates are arbitrary at collapse, it is possible to simplify the formulation imposing that $\boldsymbol{F^T}_0 \delta \boldsymbol{u} = 1$ wihout losing generality. In this way the problem can be formulated as:

$$\begin{aligned} &\text{Minimise:} && \alpha = -\boldsymbol{F}_{\boldsymbol{g}}^{\boldsymbol{T}} \delta \boldsymbol{u} \\ &\text{Subject to:} && \boldsymbol{C}\delta \boldsymbol{u} = \boldsymbol{N_0}\delta \boldsymbol{\lambda} \\ & && \boldsymbol{F^T}_0 \delta \boldsymbol{u} = 1 \\ & && \delta \boldsymbol{\lambda} \geq \boldsymbol{0} \end{aligned} \tag{45}$$

An equivalent formulation, expressed with the structure typical of linear programming problems, is given in

$$\begin{aligned} &\text{Minimise:} && \begin{bmatrix} -\boldsymbol{F}_{\boldsymbol{g}}^{\boldsymbol{T}} & \boldsymbol{0} \end{bmatrix} \cdot \begin{bmatrix} \delta \boldsymbol{u} \\ \delta \boldsymbol{\lambda} \end{bmatrix} \\ &\text{Subject to:} && \begin{bmatrix} -\boldsymbol{C} & \boldsymbol{N_0} \end{bmatrix} \cdot \begin{bmatrix} \delta \boldsymbol{u} \\ \delta \boldsymbol{\lambda} \end{bmatrix} = \boldsymbol{0} \\ & && \begin{bmatrix} \boldsymbol{F^T}_0 & \boldsymbol{0} \end{bmatrix} \cdot \begin{bmatrix} \delta \boldsymbol{u} \\ \delta \boldsymbol{\lambda} \end{bmatrix} = 1 \\ & && \delta \boldsymbol{\lambda} \geq \boldsymbol{0} \end{aligned} \tag{46}$$

3.2.1 Computational solution with kinematic approach

The problem of the kinematic analysis, as structured in equation 46, was implemented in a MATLAB routine, similarly to what was done for the static approach. The code, presented in annex 2, writes the compatibility and flow rule matrixes, and solves the minimisation problem through linear programming. The solution is stable and fast and the procedure of optimisation is effective enough for the two solutions of static and kinematic approach to coincide. The implemented code works in the hypotheses of associated flow, infinite compressive strength and zero tensile strength of the interfaces, rigid blocks, Coulomb friction, semi-circular arch of constant thickness, generic dimensions of radial voussoirs.

The solution is given in terms of displacements of the centroid of each blocks and plastic strain rates at the interfaces: to ease the interpretation of the results, the routine draws a deformed configuration, based on the first part of the solution (the displacements of the blocks). Results for the loading cases applied in the experimental campaign are given in Figure 71, Figure 72 and Figure 73.

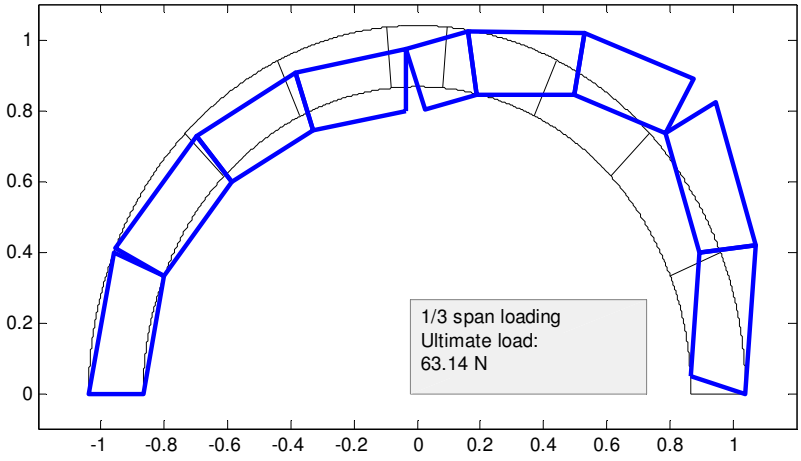

Figure 71. Third span loading, kinematic analysis

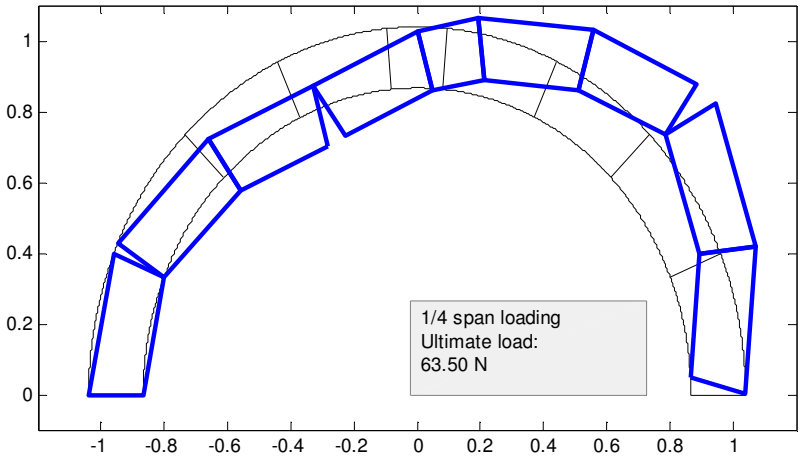

Figure 72. Quarter span loading: kinematic analysis

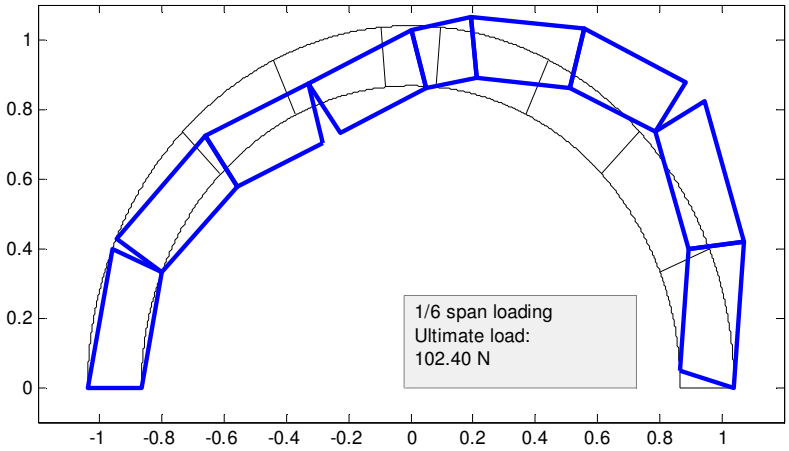

Figure 73. Sixth span loading, kinematic analysis

The ultimate loads found for these load configurations, corresponding to the load configurations of the test, are exactly the same as the one computed through static approach. The same results would have been obtained if, through hand calculations, the principle of virtual works were applied to the same mechanisms, that are corresponding to the ones obtained experimentally. The selection of the right mechanism, though, might be not immediate for a generic existing arch to assess, if there is no evidence of formation of hinges or sliding planes. Anyway, through an iterative process, if the voussoirs are not too many, it is possible to proceed to the calculation of each of the weakest mechanisms and, by comparison within them, to the ultimate load.

Through the implemented procedure, this is not necessary, as the process is carried out by the solver. The confirm on the efficiency of the procedure of minimization of the load multiplier comes from the equality of static and kinematic load multipliers. In Figure 74 are represented the mechanisms computed for arches with a growing number of voussoirs, from the, rather academic, case of 4 voussoirs to an arch with a large number of voussoirs, which can be considered the reference solution of limit analysis for generic arches.

The failure involves also sliding, for some cases, as already presented in 3.1.3. The friction coefficient that was imposed (0.5) was indeed chosen in the lower range of its expectable variability to evidence possible sliding failures. The voussoirs in the deformed configuration are represented with straight lines, but in the computation they are always assumed with their actual shape. The only imprecision is related to the position of their centre of mass, that, as already presented, is located at a finite distance from the centre of the section. This distance, though, is very little for normal proportions of arches.

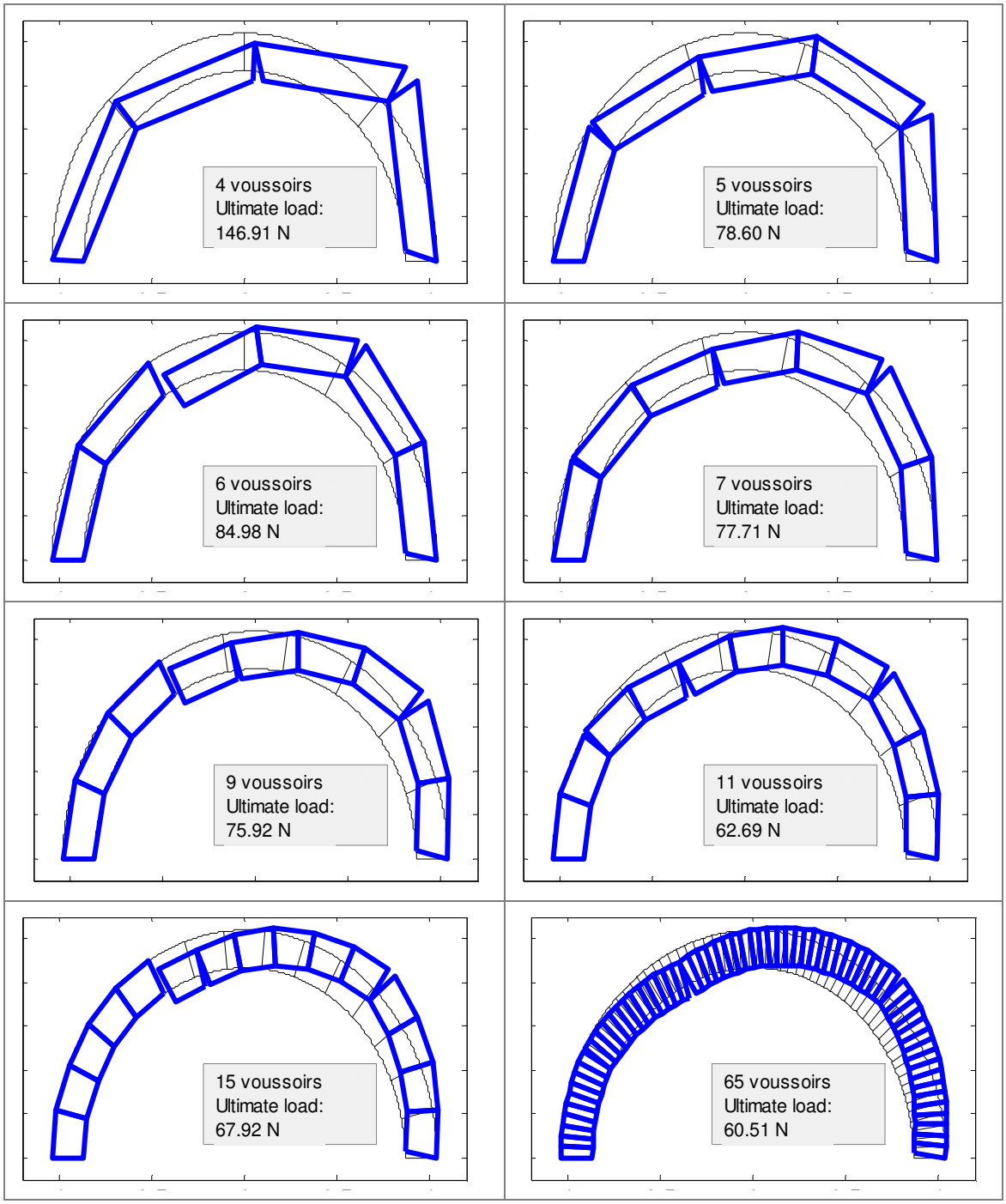

Figure 74. Failure mechanisms of arches with a growing number of equally spaced voussoirs (friction coefficient 0.5, quarter span loading, prevented sliding of the base interfaces)

Chapter 4.

Structural analysis through Finite Element Method

Another approach for the structural assessment of existing structures, including of course arches of any typology, as the Finite Element Method. This method allows the study of any geometry and does not impose particular constraints in the hypotheses to make on the mechanical behaviour of the material or of the structure. Non-linear material models, cracking or damage models, micro-models with the properties of all materials and interfaces between them, geometrically non-linear analyses, are all possibilities allowed by the method.

The increased complexity of these types of models, though, introduces the problem of the determination of a number of parameters on which the models are based, whose determination might constitute a problem especially for existing buildings. The calibration of the parameters of numerical models is a complex task, in particular for existing buildings: in these structures, indeed, in most cases there is little knowledge about the values of some parameters, that determine relevantly the results of a FEM analysis. For this reason, the application of simplified models is in general preferred, if the simplifications introduced allow an adequate description of the structural problem.

The flexibility of the method, and the possibility of implement a wide range of structural and material models, anyway, are at the base of the diffusion of the FEM in many fields of engineering, including the structural analysis of existing buildings. In this work the FEM is used as a reference solution to compare to the results of limit analysis and to experimental data, to check the applicability of limit analysis procedures, the main interest of this work, to the typology of arches with limited number of voussoirs. Without describing in detail the basis of the method, here will be presented its application to the structural analysis of the arch, as it was modelled for the experimental campaign.

A FE model of the studied arch was built and solved through the software DIANA. The geometry of the numerical model corresponds to the one of the experimental timber arch: as was done through limit analysis, the numerical results are aimed to reproducing the testing conditions to compare later the results, and check the applicability of the different analysis techniques. The model was studied in 2D, as out of plane effects were avoided in the testing and are not of interest. The model reproduces the shape of the tested arch, the locations of the joints, and the position and shape of the voussoirs (assuming a straight geometry of the voussoirs to reproduce more accurately the testing conditions).

The modelling approach consisted in a simplified micro-model, where the voussoirs are modelled through linear elastic blocks and the joints through interface elements. The hypothesis of linear elasticity for the voussoirs is coherent with the general purpose of a simplified micro-model, where the non-linearity is concentrated in the interfaces and the blocks are generally assumed with a simpler (linear)

behaviour. There could be, anyway, the possibility to implement different material models, such as non-linear material models, also for the voussoirs. The assumption of linear elasticity is related to the type of material (timber) and to the observation of the failure mechanisms of the tested arch. The fact that, as expected, the arch collapses for the formation of a mechanism around rotational hinges located at the joints, without crushing of the material or any type of damage or non-linear behaviour of the voussoirs, confirmed the applicability of this hypothesis. For the usual stress levels present in arches, it is might be possible to apply these assumptions, although with a more problematic approach, also to stone voussoirs.

The plane model was analysed in plane stress for the limited thickness of the arch, assuming the absence of any constraint to the out of plane deformation of the elements. The element type that was chosen is a standard 8-node element for plane stress analysis, named CQ16M in Diana, with shape functions defined as second order polynomials. The deriving strain field, for the strain ε_{xx}, varies linearly in x direction and quadratically in y direction (the opposite is valid for ε_{yy}). The shear strain varies quadratically in both directions. The integration scheme that is applied by default computes 2x2 Gauss points and was not changed. A simple linear elastic material model was implemented for the voussoir, requiring only the definition of a Young's modulus and Poisson's ratio (the used parameters are summarised in Table 7).

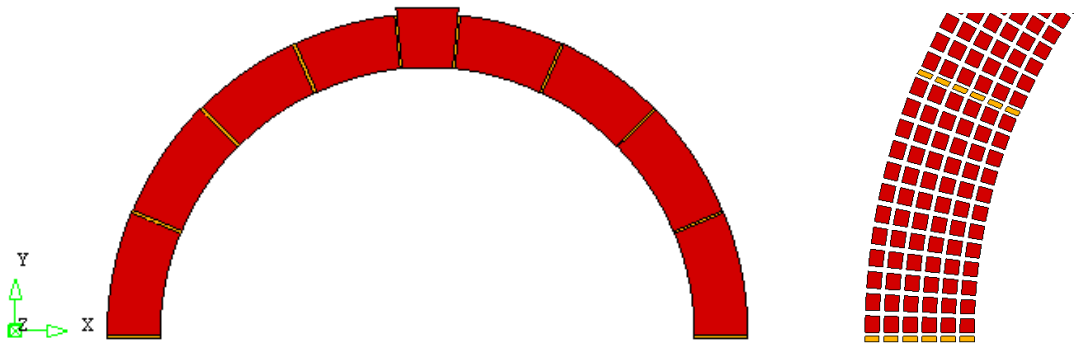

Figure 75. Left: geometry of the model; right: detail of the modelling of the joints through interface elements

The joints were modelled through interface elements (Figure 75), implementing a material model based on the Coulomb friction criterion. The element that was used is an interface element, named in Diana CL12I, suitable to connect 8-node plane elements, as it connects three nodes at one side with three corresponding nodes at the other side. The element considers normal and tangential displacements according to the convention shown in Figure 76 for curved geometries (in this case the configuration is simpler, the joints are linear and the tangential direction is clearly defined).

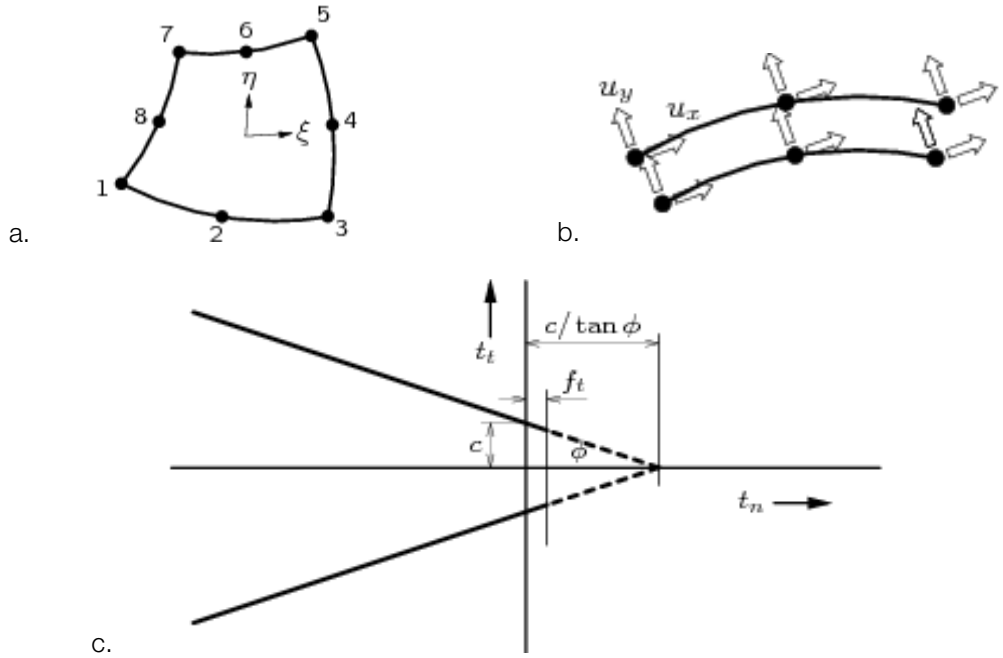

Figure 76. a. Plane stress element CQ12M; b. interface elements CL12I, definition of the tangential and normal direction, defined by the orientation of the first two nodes; c. general definition of a Mohr Coulomb criterion in Diana

Table 7. Parameters used to define the materials

Voussoirs		Interfaces	
Density	385 kg/m^3	Density	385 kg/m^3
Young's modulus	10 GPa	Young's modulus	10 GPa
Poisson's ratio	0.20	Poisson's ratio	0.20
		Normal stiffness	10 GPa
		Tangential stiffness	10 GPa
		Cohesion	0 MPa
		Friction angle	atan(0.5)=27°
		Dilatancy angle	0

The weight of the blocks that were used was measured, obtaining in this way the density of the material. The stiffness of 10 GPa is assumed for structural timber from EN338; the influence of the parameter will be discussed trough a brief sensitivity analysis. The Mohr Coulomb material model is applied to the interfaces, replicating the assumptions made for the limit analysis and confirmed by the experimental tests. The tensile strength was assumed equal to 0, no cohesion was applied (as the joints are dry the cohesion is zero or very low), and a friction coefficient of 0.5 was applied. This friction coefficient was assumed, in the lower range, among those that prevented sliding of the voussoirs, as will be discussed in the following. The justification of this relies on the experimental results, that did not show any sliding. The implementation of the Coulomb criterion requires also the definition of a dilatancy angle, that was assumed equal to 0, corresponding to a non-associated flow rule.

The mesh that was used has 678 elements and 2203 nodes. The constraints that were applied are the vertical displacements at the base and the horizontal displacements of the two external nodes of the supports, to replicate the action of the constraining steel plates that were used in the experimental tests to avoid sliding at the base. The applied loads were the self-weight of the material and a concentrated load applied in the same position as the experimental (three load cases with the load applied at 1/6, 1/4 and 1/3 of the span).

The solution of the model is non-linear in geometry and material. The dead load is applied in 4 steps, while the concentrated load is applied in about 40 steps of variable size, applying line search to be able to follow also the softening part of the curve. The non-linearity in the geometry is needed as the deformations at failure are relevant, and the failure itself is related to the development of a mechanism. The solution requires around 1-2 minutes of execution.

4.1 Sensitivity analysis

The sensitivity of the model to variations of the main parameters that are set are analysed here for the case of loading at 1/3 of the span. The effect of the calibration of the Young's modulus, the geometrical non-linearity, and the friction coefficient are presented.

The elastic modulus controls the behaviour of the structure for little deformations, while for bigger deformations its influence is very little (Figure 77) because the behaviour is controlled by the development of a mechanism. The increasing deformations before the structure reaches its maximum load capacity have the effect of lowering this maximum load. The studied range for the elastic modulus is from 1 GPa to 20 GPa, considering a value of around 10 GPa a realistic estimation. The ultimate load varies from 63.6 N to 50.6 N, with a decrease of about the 20% (Figure 78).

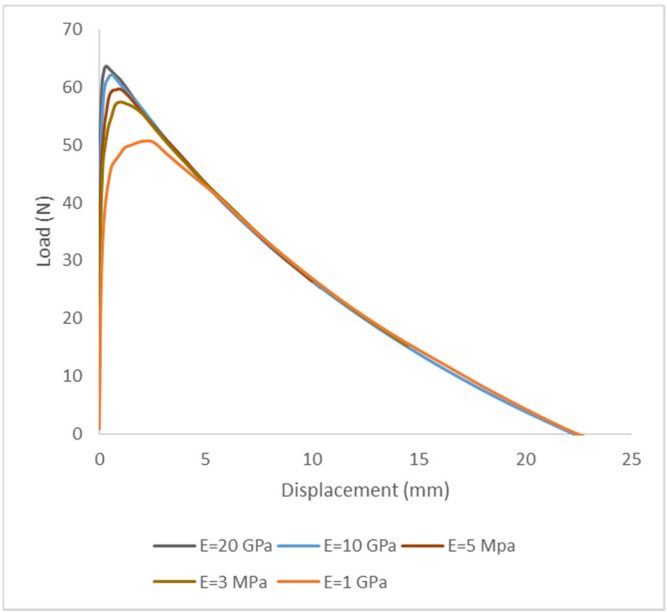

Figure 77. Sensitivity analysis: effect of the variations of the Young's modulus in the displacements and ultimate load

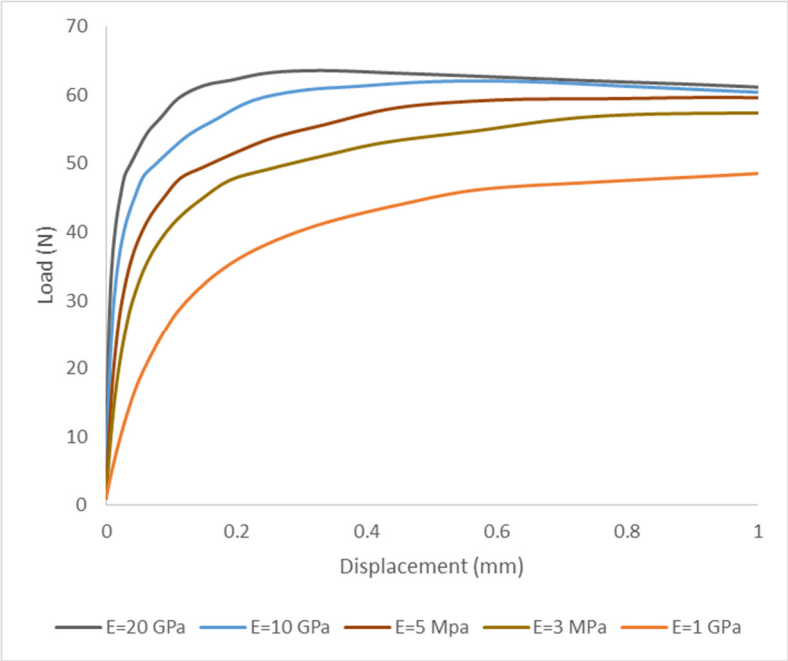

Figure 78. Sensitivity analysis: effect of the variations of the Young's modulus in the ultimate load capacity (small displacements)

As will be seen from the comparison with experimental results, the deformations of the experimental test are large, similar to those obtained imposing a low elastic modulus of 1 GPa, while the ultimate capacity is more similar to the one obtained with a larger elastic modulus. In the following the results will be presented for an elastic modulus of 10 GPa, because this value corresponds to the choice that would have been made in absence of experimental results.

Another factor that influences relevantly the estimation of the maximum load capacity of the structure is making the assumption of little displacements or, on the other hand, to analyse the structure in big displacements with a geometrically non-linear analysis. With the first approach, a higher load is estimated and there is no analysis of the softening part, that is due to the development of a mechanism, with the effect of the large displacements in the decrease of the load capacity. The results of this type of analysis, for the assumption that are made, are close to the results of limit analysis, as the deformations of the structure are not taken into account for the calculation of the failure mechanism.

The approach with geometrical non-linearity appears more adequate to describe the structural behaviour of arches at collapse conditions, as it captures correctly the development of the mechanism, that is the object of interest as the ultimate capacity is related to it. For smaller Young's modulus, the differences between the two analysis approaches are more important, as expected (Figure 79).

As already mentioned in the context of limit analysis, a parameters that controls in a relevant way the behaviour of the structure both in terms of displacements and in terms of ultimate load, is the friction, as presented in Figure 81 and Figure 80.

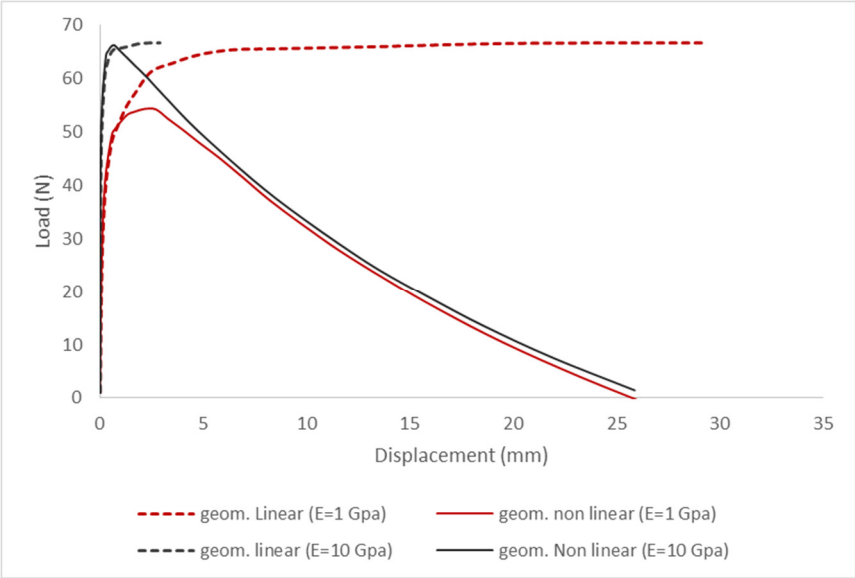

Figure 79 Geometrically linear and non-linear analyses, comparison

The studied range of variability of the friction coefficient goes from 0.30 to 0.50, the friction coefficient that will be assumed for the rest of the analyses. The choice is related to the type of mechanisms that develop (and change) depending on the friction coefficient that is imposed, as shown in Figure 81, to discuss its influence. The values of the friction coefficient for which a sliding mechanism is found, anyway, are rather low, and not very common in real cases (and the hypothesis of absence of sliding, at least for standard arches, is generally acceptable). The after pick behaviour changes with the type of mechanism, from purely sliding to mixed sliding/rotational mechanism, to purely rotational. Values higher of 0.50 for the friction coefficient are not presented as they correspond all to the same curve, as if the mechanism is rotational the friction coefficient does not have any influence.

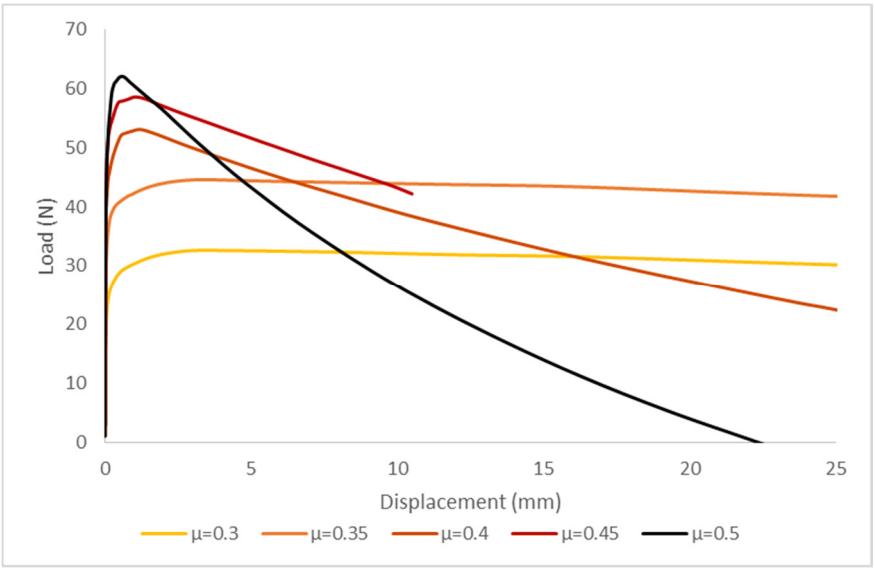

Figure 80. Sensitivity analysis; effect of the friction coefficient, 0.3-0.5 range

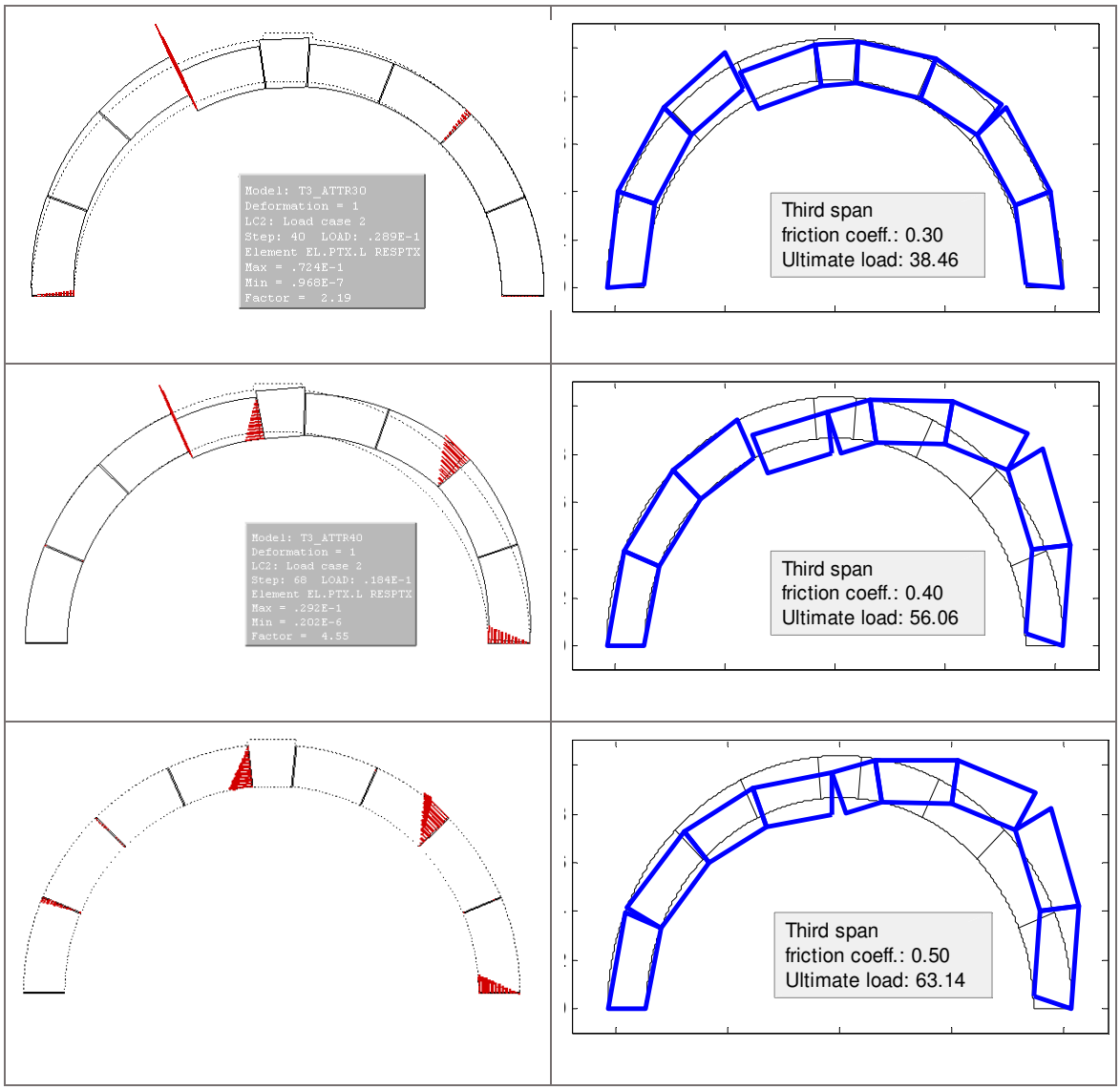

Figure 81 Failure mechanisms for different friction coefficients, comparison between FEM and limit analysis results

4.2 Results

4.2.1 Third span loading

The results that will be presented in more detail are the ones relative to the third span loading, for a Young's modulus of 10 GPa. The choice is related only to the fact that the results of the other cases are qualitatively similar and they do not add any other relevant observation. The main results anyway, will be presented for comparison as well. The geometrically non-linear analysis allows to follow the collapse mechanism until failure (until the load multiplier has a positive value). The displacements of the model, at failure, are presented in Figure 82. The mechanism that is modelled is the same that was found experimentally and predicted through limit analysis.

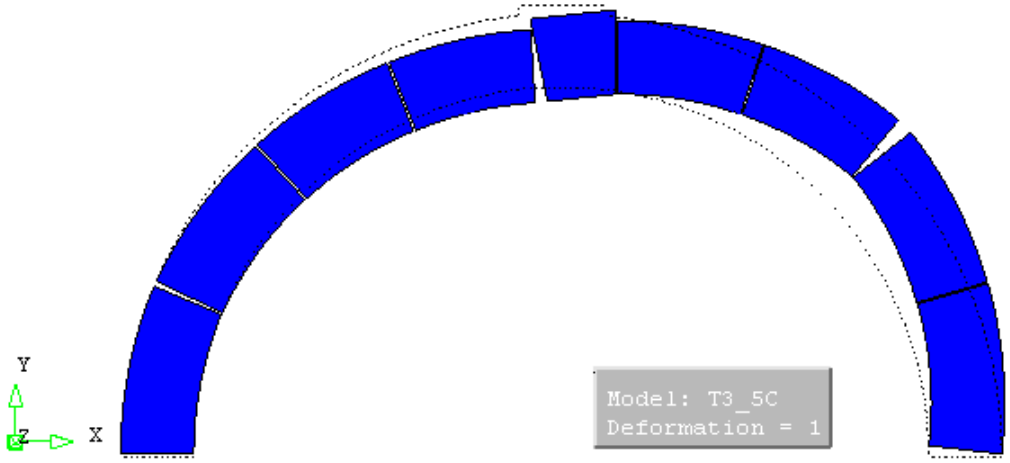

Figure 82. Displacements of the structure at failure (the deformation of the structure is not amplified)

The deformations are concentrated in the interfaces, as the material of the voussoirs is linear elastic and the joints are allowed to open with the application of a Mohr-Coulomb material model. The resulting principal stresses are presented in Figure 83 and Figure 84. The compressive principal stresses evidence the formation, within the voussoirs, of a compressed zone that approximates the profile of the thrust line, giving an idea of the resistance mechanism of the arch. The hinges are evidenced by the concentration of compressive stresses. The order of magnitude of the compressive stresses is rather low, far from being able to produce crushing of the material.

The tensile principal stresses concentrate in the hinges, where they are related to the shear that is concentrated in a small area. Other tensile principal stresses of major interest are the ones appearing in the lower part of voussoir 4 and the upper part of voussoir 2 and 8, related probably to the fact that the thrust, as could be seen also from the compressive principal stresses, in those sections is out of the boundaries of the arch. The eccentricity of the thrust, in this case, could cause the highest principal

stresses. As the material is liner elastic, though, the presence of tensile stresses does not necessarily reveal that the eccentricity of the thrust is bigger than the half of the section, but, rigorously, only that t the thrust is out of the middle third of the section.

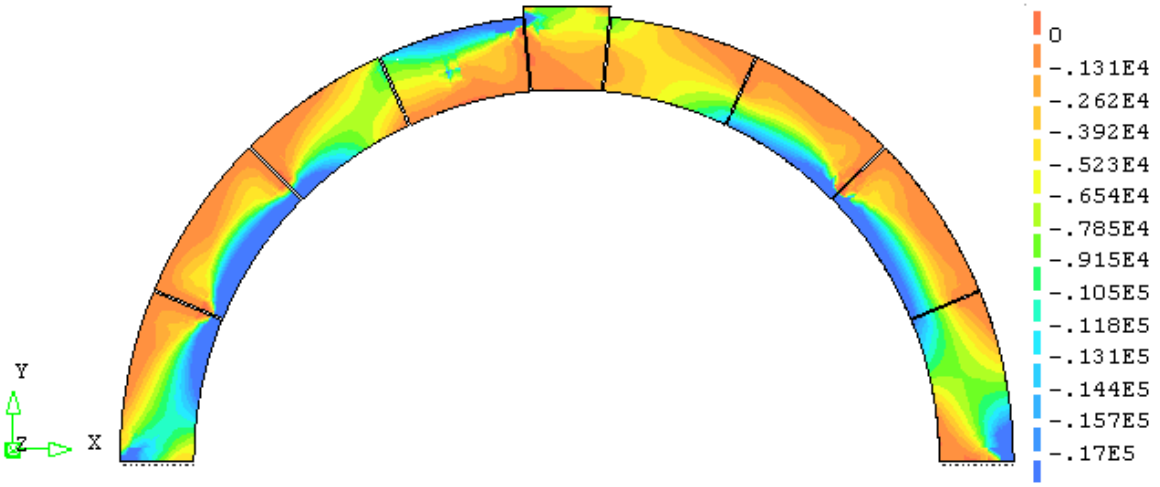

Figure 83 Third span loading, minimum principal stresses at failure

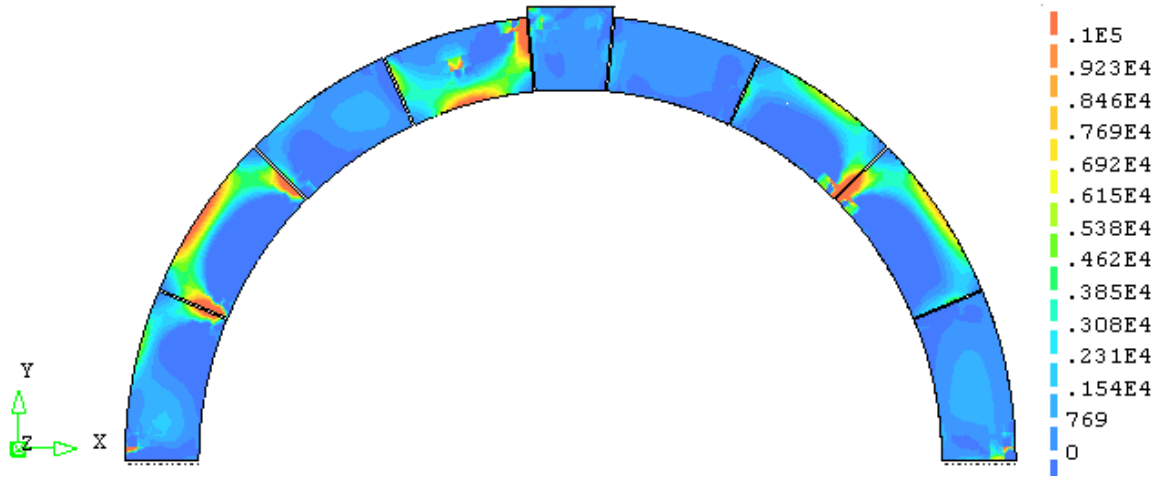

Figure 84. Third span loading, maximum compressive stresses at failure

The evolution of the mechanism of collapse and the internal distribution of compressive principal stresses is shown in Figure 85. The arch passes from a configuration with a symmetrical loading (only the self-weight) and a thrust line that approximates the condition for the minimum horizontal thrust, to an asymmetrical loading. The thrust line chances, and compressive stresses start to concentrate close to the hinges. The first to form are at joint 5 and 8. Once the load increases, the hinge at the base section forms and, last the hinge at section 2. This mechanism is found in a restraint is imposed to the lateral displacement of the base section; if the displacement is free, the failure appears for sliding of the right support, with a failure load of 58 N, close to the failure load of 62 N found for this configuration.

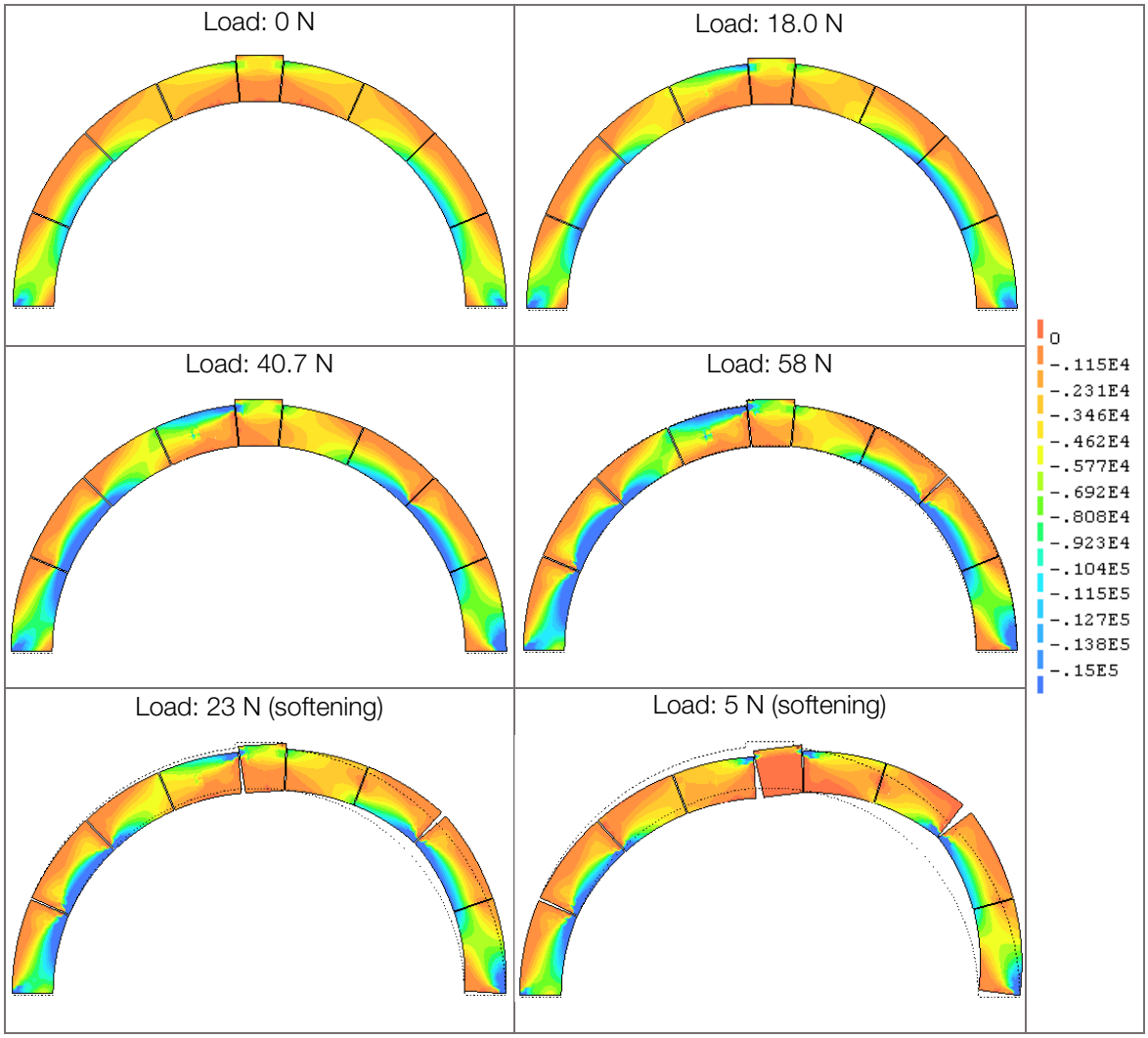

Figure 85. Evolution of the principal compressive stresses with an increasing applied load

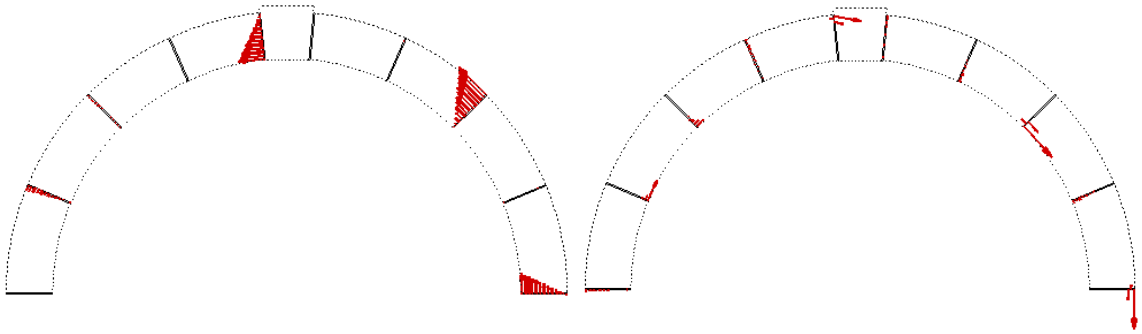

Figure 86. Opening of the joints at pick load (left) and distribution of forces at the interfaces

The strains at the joints are an instrument to check the failure mode of the arch and the order of opening of the hinges. In this case, the appearance order is the one already described, and it is possible to see that no sliding occurs, but only strains normal to the interfaces are present (being the flow rule non-associated, the frictional strains would be only in tangential direction).

The complete load displacement curve for this loading condition is provided in Figure 87. The maximum load estimated by the numerical analysis, assuming E=10 GPa, is 62.0 N.

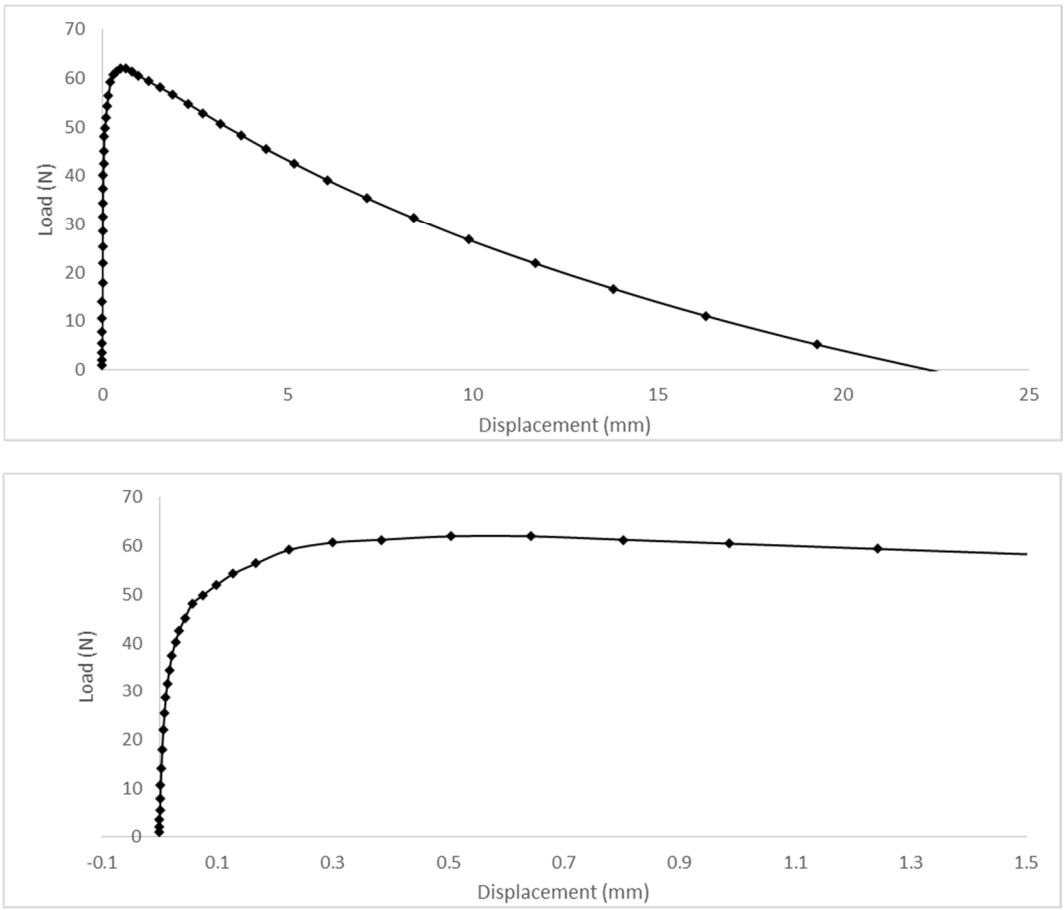

Figure 87 Third span loading: load displacement curve

4.2.2 Quarter span loading

The results of the numerical model with the load at ¼ of the span are listed below. The principal compressive stresses at failure describe also in this case the profile of the thrust line and the position of the hinges (Figure 88). The opening of the joints is presented in Figure 89, and corresponds to the mechanism found experimentally.

The load displacement curve of this load configuration is presented in Figure 90; the ultimate load and the structural behaviour of the arch depend, also in this case, from the properties of the material. The variation of the Young's modulus (in a wide range from 10 GPa to 1 GPa) produces a variation on the ultimate load of the 14%, from 61 N to 52 N. Also the displacement capacity after the peak changes, even if this is not a characteristic of the same interest as the ultimate load.

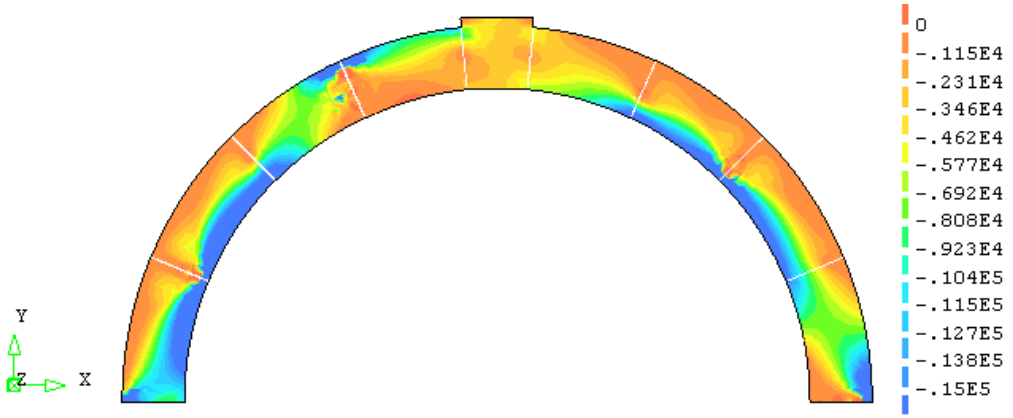

Figure 88 Quarter span loading, compressive principal stresses at pick load

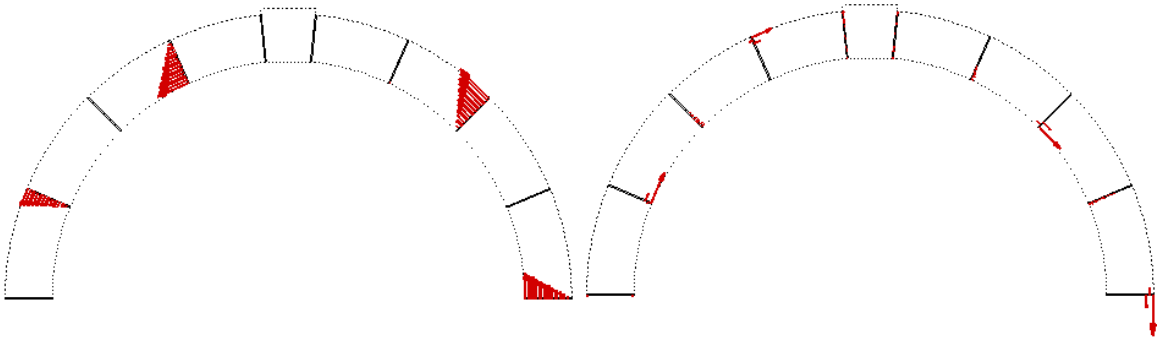

Figure 89 Quarter span loading, opening of the joints at failure (left) at distribution of interface forces at pick load (right)

In these examples it is clearly seen that the elastic properties of the materials, in a FE model, have a primary role, not only for deformations but also for the determination of load carrying capacity, and at the same time they constitute an unknown variable in most cases, of difficult determination. One of the limit of numerical FE models, indeed, is that the calibration of the parameter can lead to a better fit with some experimental results, when available, but could in the same way force the model to give the results that the user considers more realistic or expected.

As will be discussed in the following, the assumption of an elastic modulus of 10 GPa corresponds to the results that better approximate the experimental values in terms of ultimate loads. The displacements, though, are closer to the ones obtained for a numerical model with a Young's modulus of 1 GPa. The difference is probably due the fact the initial imperfections of the arch caused the opening of some joints, at the first load steps or anyway for moderate loads, increasing relevantly the displacements of the structure. If this is the case, the assumption of a low Young's modulus could be a very simplified way of computing these initial imperfections, without modelling them in detail. Since in real arches these imperfections, that as seen play a relevant role in determining the ultimate capacity, are generally unknown or roughly investigated, this could be a (conservative) approach to them into consideration.

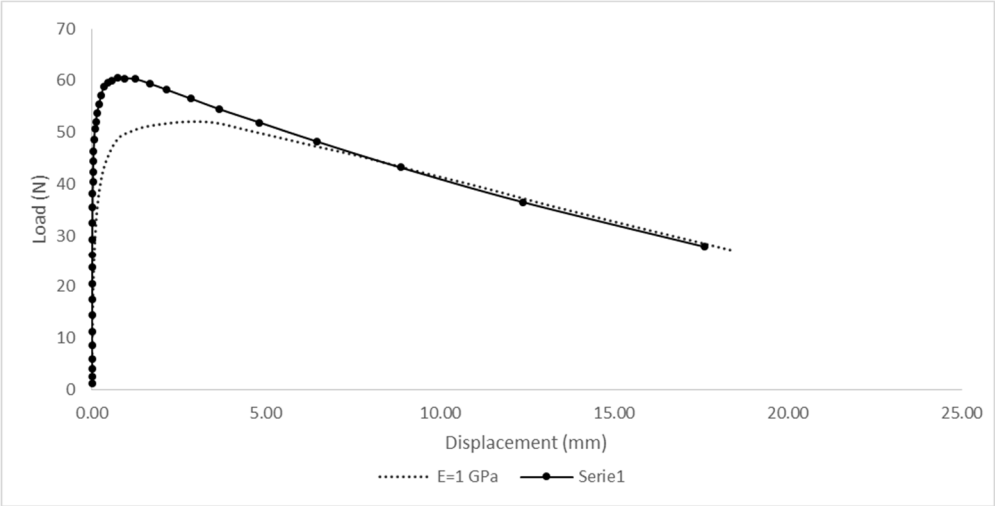

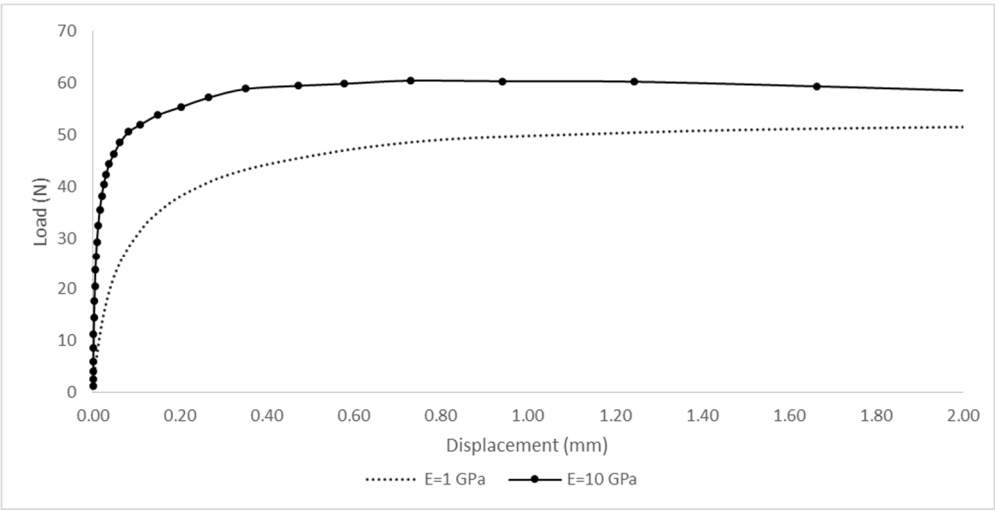

Figure 90 Quarter span loading, load displacement curve

4.2.3 Sixth span loading

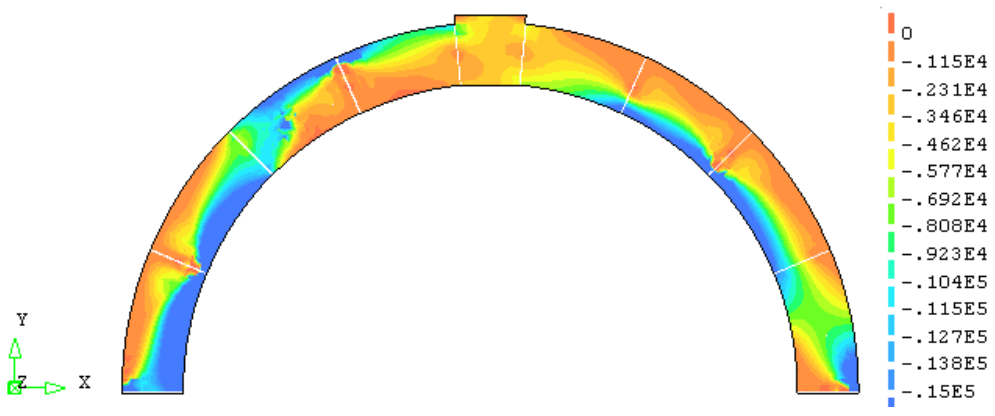

Figure 91 Sixth span loading, compressive principal stresses at failure

The results of the numerical model on the loading at 1/6 of the span are listed in Figure 91 and Figure 92. The load displacement curve has the characteristics of the other, with a certain dependence in both the displacement capacity and in the ultimate load from the selected elastic modulus. The opening of the joints and the collapse mechanism are correspondent to the experimental evidence and to the results of limit analysis.

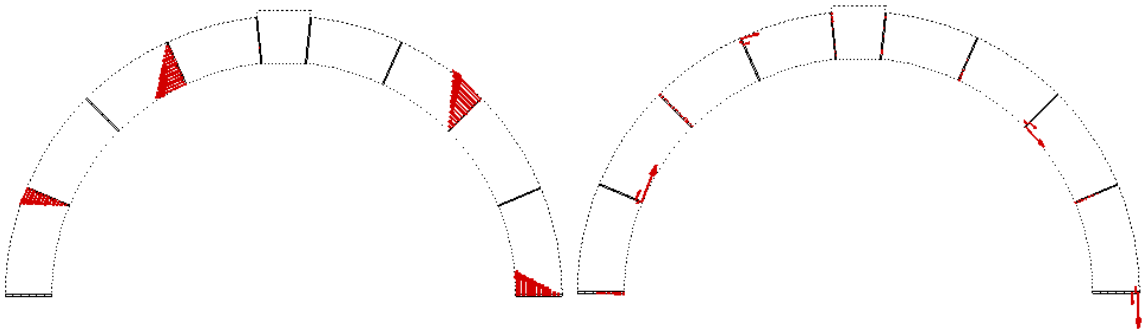

Figure 92 Sixth span loading, opening of the joints at failure (left) and distribution of interface forces at peak load

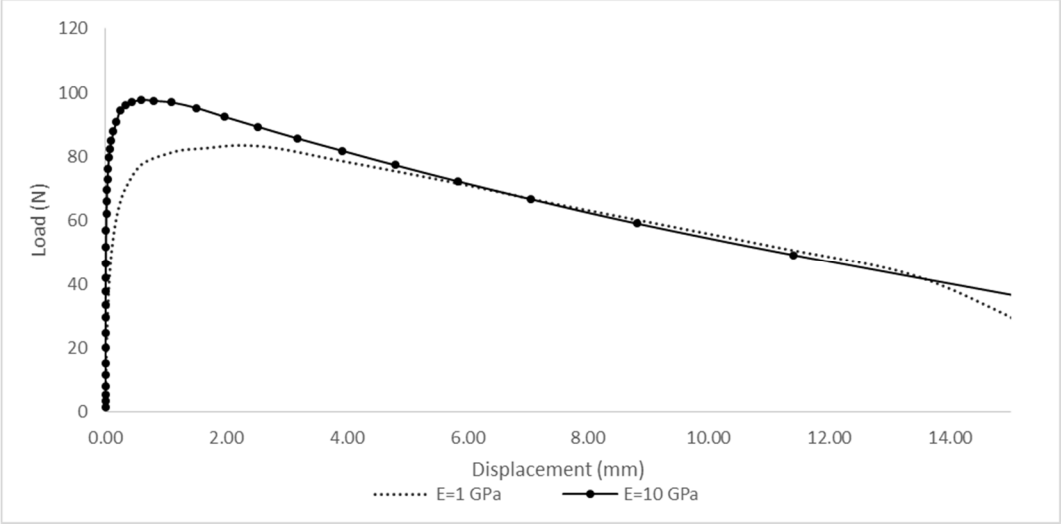

Figure 93 Sixth span loading, load displacement curve

Chapter 5.

Comparison of experimental, analytical and numerical results

The main scope of this work is the evaluation of the applicability of different analysis approaches to the structural evaluation of existing arches made of few voussoirs. This evaluation is based on the comparison of the numerical and analytical results, discussed in chapters 3 and 4, with the experimental results, presented in chapter 2. The focus of the work was the applicability of limit analysis, as a classical and standard method for the analysis of arches, to this typology of arches with a limited number of voussoirs. For this reason, in the comparison of the results, particular attention will be paid to the applicability of limit analysis in its different approaches, to the validation of the hypotheses on which it is based, and eventually to the evaluation of the safety level of the obtained results.

In Table 8 is presented a brief comparison between the experimental, analytical and numerical results obtained, in this work, in the structural analysis of the arch assumed as a case study. The geometry of the arch was derived from the Palladian *serliana* windows of the Palazzo della Ragione in Vicenza (Italy), but the scope of the work was not the evaluation of the safety of that particular arch, but rather the assumption of a typical geometry, representative of the typology of arches with a low number of voussoirs. For this reason, all the computations that were made, and that are summarised in Table 8, are referred to the model of the arch, realised in timber in half scale and tested in the laboratory.

As was mentioned also in the chapters regarding the analytical and numerical computations, some hypotheses that were made are justified from the objective of reproducing in the models the testing conditions. For example, the assumption of a greater friction coefficient of the base section, or the constraints put to the numerical model in the same sections, are meant to reproduce the constraint provided by the steel plates used to prevent the sliding of the base voussoirs.

The experimental results present a variability, linked to the possibility of an imperfect mounting of the arch, as discussed in chapter 2. The control of the mounting operations, of the correct dimension of the span, of the planarity of the structure, can improve in a significant way the homogeneity of the results, reducing a scattering that, otherwise, could mask completely the object of evaluation of the experimental campaign, i.e. the ultimate load of the arch. The initial conditions, indeed, might influence the results much more than the number of voussoirs or the exact position of the joints and the loads. The reduction in the ultimate capacity of an arch whose span was varied of ±5 mm, for example, was in the order of 25% if compared to the best configuration of the arch (that cannot be perfect, but has limited imperfections). This effect might be reduced in arches with mortar joints, that could accommodate local defects much better that dry-joints arches.

Table 8. Comparison between experimental, analytical and numerical results

	Loading 1/3 of the span	Loading ¼ of the span	Loading 1/6 of the span
Experimental results			
Average ultimate load (N)	60.0	60.5	97.3
Standard dev. Ultimate load (N)	3.48	1.74	2.47
COV Ultimate load	5.8%	2.9%	2.5%
Max Ultimate load (N)	63.7	62.8	99.9
Min Ultimate load (N)	55.8	58.8	95.0
Limit Analysis, 9 voussoirs			
Static Approach, Ult. Load (N)	63.1	63.5	102.4
Thrust line analysis, Ult. Load (N)	66.0	63.0	100.0
Kinematic Approach, Ult. Load (N)	63.1	63.5	102.4
Limit analysis, classical hypotheses			
Static Approach, Ult. Load (N)	46.4	60.9	92.3
SA, finite friction angle, Ult. Load (N)	47.6	59.9	87.0
Thrust line analysis, Ult. Load (N)	49.0	61	90.0
Kinematic Approach, Ult. Load (N)	47.6	59.9	87.0
SA, finite friction angle, Ult. Load (N)	46.4	60.9	92.3
FEM numerical model			
Ultimate load, E=10Gpa (N)	62.0	60.5	97.8
Ultimate load, E=1Gpa (N)	50.6	52.0	83.5
Ult. Load, E=10Gpa, geom. Linear analysis (N)	66.6	-	-

The coefficients of variation of the experimental data are in the order of 2.5-5%, with a controlled mounting. Different variations were found for displacements, which depend more directly on the presence of initial imperfections. The evaluation of the displacement capacity, though, is not the main scope of this work, that concentrates more on the evaluation of the load carrying capacity, which can be compared to all analytical results (limit analysis does not provide quantitative information of the displacements, but only the type of mechanism that theoretically develops). The parameter that will be compared to the analytical results will be the average ultimate load for each load configuration, assumed as the most representative as the different repetitions of the test are considered homogeneous. When necessary, the maximum and minimum loads that were measured in the repetitions of the same test will be taken into account.

The results of limit analysis are divided, counting in one group the ones obtained considering the real number of voussoirs and their geometry, and in the other group the results of the standard approach of limit analysis in the study of the stability of arches, that does not consider the stereotomy of the voussoirs. This latter approach is based on the assumption that the thrust line must be inside the

geometrical boundaries of the arch to assure safety, or equivalently, that the limit condition is reached when there is the possibility for a generic mechanism to develop, not necessarily considering the joints in their real position. The calculation of these results of the standard approach of limit analysis, that is largely accepted for generic arches, was obtained through the use of the same computational tools developed in chapter 3, with the use of a large number of theoretical voussoirs (101 in this case). The solution, in this way, approximates the behaviour of an arch with a hypothetically infinite number of voussoirs, in which hinges can open at any position.

As shown in Figure 94, two solutions are calculated for the standard approach of limit analysis, one considering the possibility of sliding, with the same friction coefficient of 0.5 imposed in the other analyses, and the other obtained in absence of sliding (through the imposition of a large friction coefficient). The second approach corresponds to the most common hypothesis that are generally made in the limit analysis of arches, corresponding to Heyman's hypotheses. The solution was computed both in the kinematic approach (presented in Figure 94) and in the static approach, obtaining the same failure loads.

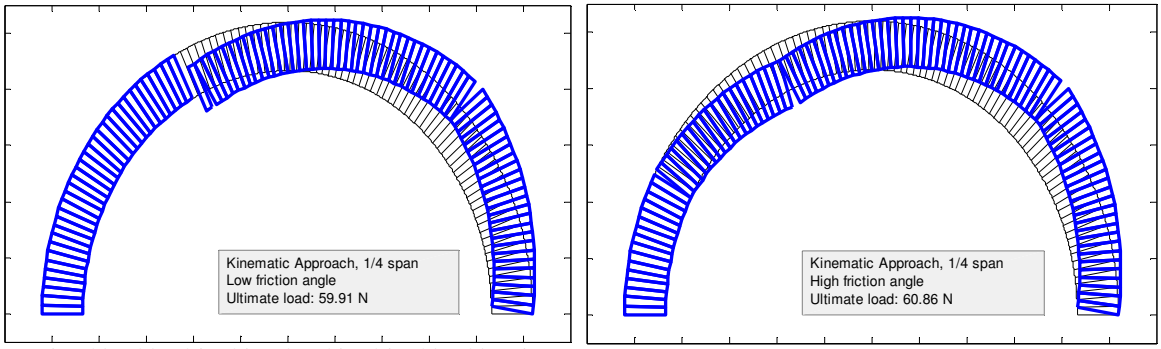

Figure 94. Classic approach to limit analysis (quarter span loading): left: possibility of (associated) sliding; right: absence of sliding, coherently with Heyman's hypotheses

The results of static and kinematic approach, for and arch of the studied geometry, modelled with rigid blocks, are obtained with the methodology presented in chapter 3. The "thrust line analysis" corresponds to the method of solving the differential equation of the thrust line and optimising the solution, through the three parameters on which it depends, until a failure load is identified. For the reasons explained in 3.1.5, the solution of this problem, in particular the optimisation procedure, and the density of the calculated points of the thrust line, can affect the accuracy of the results. The reference limit analysis result, so, will be assumed to be the one obtained through static or kinematic approach (as they coincide) in the hypothesis of rigid blocks in contact by interfaces.

The numerical results compared in Table 8 correspond to the results of the analyses in non-linear material and geometry, for different values of the elastic modulus; an example is given of a solution with the hypothesis of small displacements (no geometrical nonlinearity) The selected values are considered

limit values, where the first (10 GPa) meets both the expectations on the Young's modulus of timber, at least as an order of magnitude, and the ultimate loads with a better accuracy, and the second is calibrated to reproduce deformations close to the ones observed in the experimental campaign. The comparison between numerical and experimental results, in terms of load displacement curve, are presented in Figure 95, Figure 96 and Figure 97 for the three load configurations.

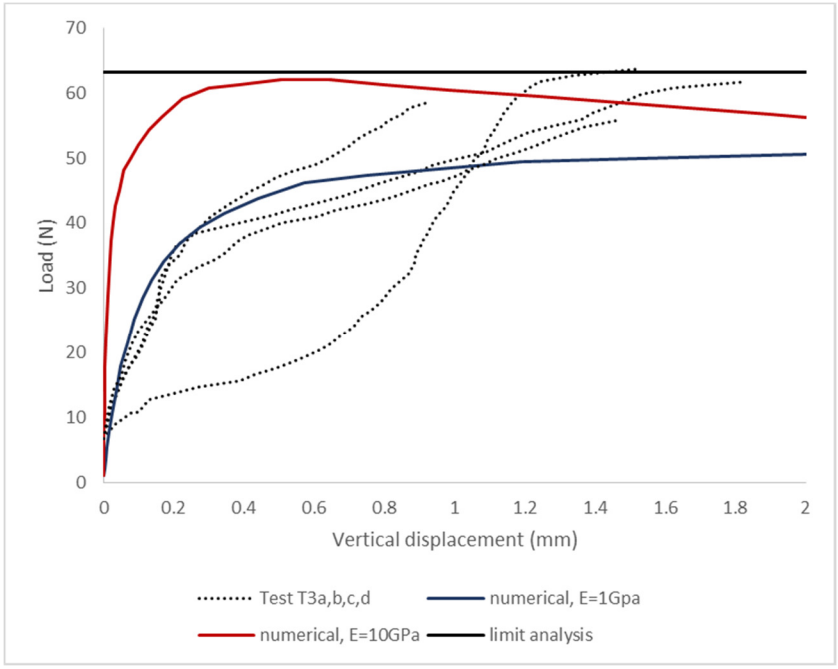

Figure 95 Third span loading, comparison between experimental and FEM numerical results

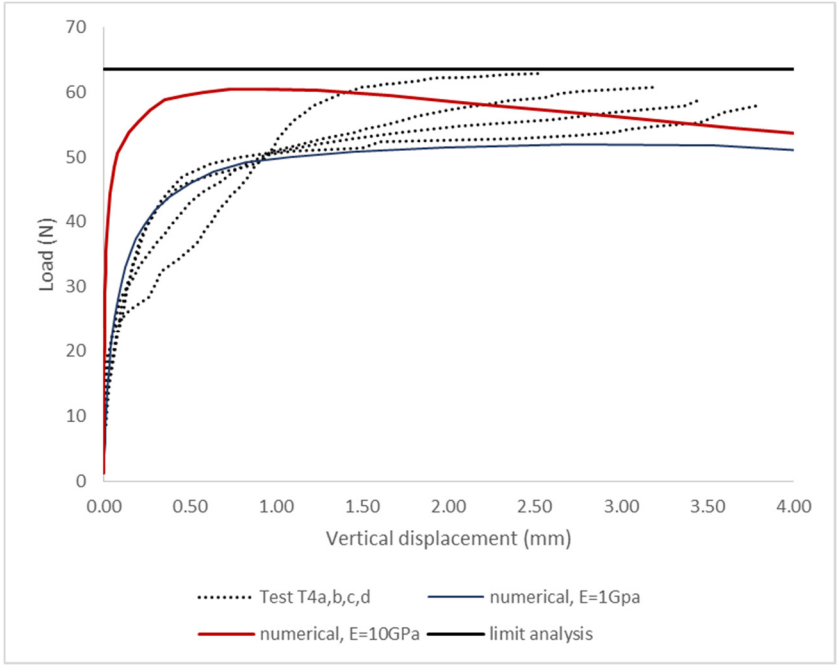

Figure 96. Quarter span loading, comparison between experimental and FEM numerical results

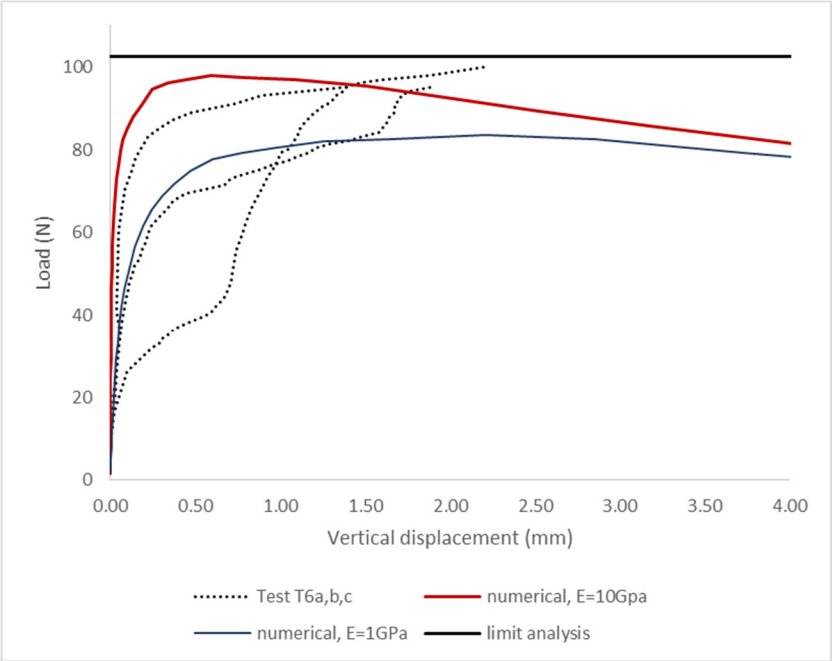

Figure 97. Sixth span loading, comparison between experimental and FEM numerical results

As can be seen the figures, the assumption of a Young's modulus of 10 GPa gives a better estimation of the ultimate loads, while the reduction of the elastic modulus provides a better agreement with the deformations measured in the tests, losing, though, part of the accuracy in the determination of the ultimate load (remaining anyway in the safe side). The two solutions proposed for the numerical model appear to be limit solutions, and the best calibration of the parameter is probably a value in between the two. If the purpose of the numerical model is to check the accuracy of a generic model in predicting the ultimate capacity of an arch, when no calibration data are available, the reference solution would correspond to the one obtained with a Young's modulus of 10 GPa, as it is a characteristic value generally applied to structural timber (EN 338), when no other determinations are available.

On the contrary, if calibration data are available, a corrected value would be applicable. It has to be underlined that, for existing structures, there is usually little knowledge of these elastic parameters. In this case, finally, the reduction of the Young's modulus to obtain displacements closer to the experimental ones, might be a simplified way of modelling the reduction in stiffness due to the presence of initial imperfections or opening of joints. It is not much realistic, as a matter of fact, that the timber that was used had such a low elastic modulus. Once again, it is evident that the calibration of parameters of numerical models could help reproducing the desired structural behaviour, but at the same time could reduce the generality of the analysis when the determination of some uncertain parameters affects deeply the final results.

The limit analysis approach is inserted in the graphs as a limit line, since the approach of limit analysis, as it was performed in this work, is based on the assumption of small displacements. Also the kinematic

approach does not follow the displacements of the structure, nor does it give information on the development of the failure mechanism. It provides an evaluation of the weakest mechanism under which the structure can fail, based on the expression of the infinitesimal virtual displacements that the structure could present.

The limit analysis considered here is the one performed in the hypothesis of an exact number and shape of voussoirs. The usual limit analysis, performed without regard to the number of voussoirs and position of the joints, gives generally too conservative results for this typology of arches. The limit analysis applied to a structure of rigid blocks and interfaces in the real position gave results that slightly overestimate the ultimate load, as can be seen in Figure 98, Figure 99 and Figure 100, as expected. In these graphs, to ease the reading, the experimental results are expressed only by the range in which the maximum and minimum ultimate load were found, and by the average of these values (dotted line).

The numerical results of the FEM model, depending on the choice of the Young's modulus, gave values that overestimated or underestimated the measured ultimate load, in a range of ±10-15%. Limit analysis performed on rigid blocks and numerical modelling, especially with a high Young's modulus, give similar results, as expectable as the models are based on the same assumptions. The main differences in the two approaches are the possibility to implement in the FEM model geometrical non-linearity and the deformability of the blocks, features that it is not possible to consider in the limit analysis and whose effect is considered, for standard arches, of minor importance..

In the comparison between results of FEM models and limit analysis it has to underlined that the solutions are rather sensible to the precise position of the joints. Slight variations of this positions, geometrical imperfections in the models, the modelling of straight or curved voussoirs, result in differences in the ultimate load in the range of 5%.

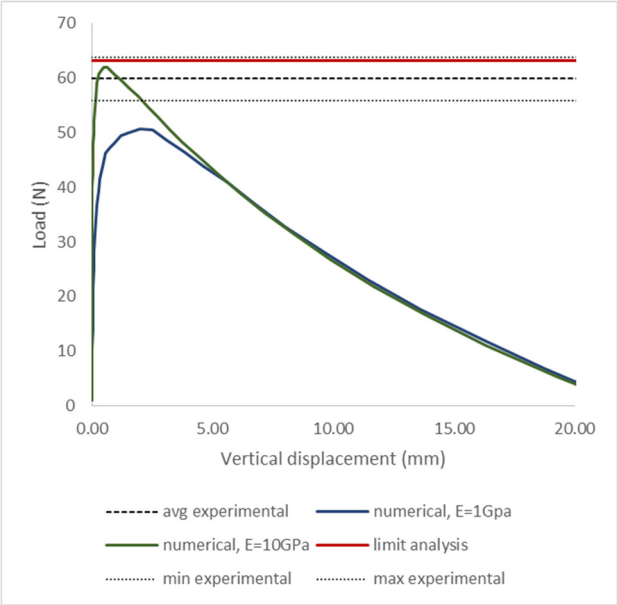

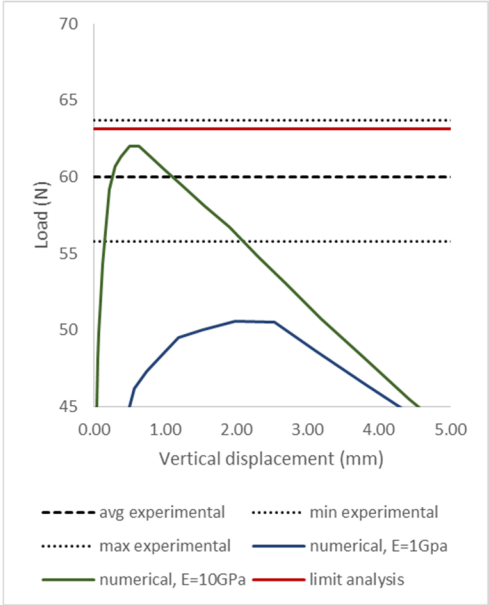

Figure 98 Third span loading, comparison of ultimate loads predicted by the different methods and the experimental values

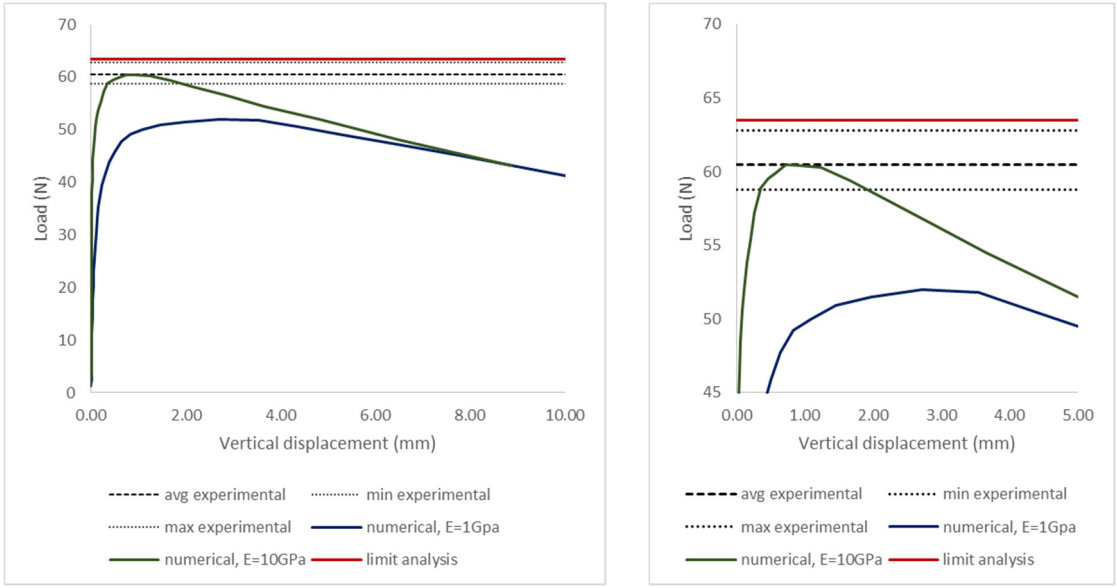

Figure 99 Quarter span loading, comparison of ultimate loads predicted by the different methods and the experimental values

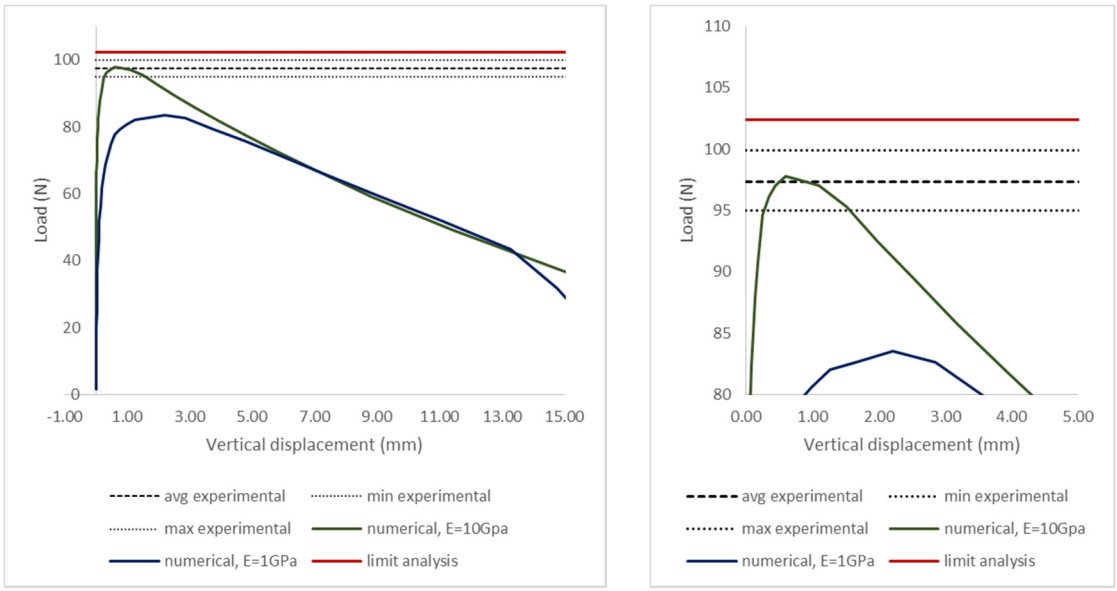

Figure 100 Sixth span loading, comparison of ultimate loads predicted by the different methods and the experimental values

In Table 9 the differences between the results of analytical and numerical approaches are compared in percentage terms, to provide an evaluation of the applicability of the different analysis techniques and on their safety. The difference between the average experimental ultimate capacity and the minimum and maximum values found experimentally for the same load configurations is given to provide an order of magnitude of the dispersion of the experimental results and of the uncertainties related to the geometrical configurations of the arch, to which the accuracy of the analytical methods have to be compared.

Table 9. Percentage differences between the analytical and numerical results and the experimental data

	Loading at 1/3 of the span	**Loading at 1/4 of the span**	**Loading at 1/6 of the span**
Experimental results			
Average ultimate load (N)	60.0	60.5	97.3
Max Ultimate load	3.48	1.74	2.47
Min Ultimate load	5.8%	2.9%	2.5%
	6%	4%	3%
Limit Analysis, 9 voussoirs	-7%	-3%	-2%
Static Approach, Ult. Load			
Thrust line analysis, Ult. Load			
Kinematic Approach, Ult. Load	5%	5%	5%
	10%	4%	3%
Limit analysis, classical hypotheses	5%	5%	5%
Static Approach, Ult. Load			
SA, finite friction angle, Ult. Load			
Thrust line analysis, Ult. Load	-23%	1%	-5%
Kinematic Approach, Ult. Load	-21%	-1%	-11%
SA, finite friction angle, Ult. Load	-18%	1%	-8%
	-21%	-1%	-11%
FEM numerical model	-23%	1%	-5%
Ultimate load, E=10GPa			
Ultimate load, E=1GPa			
Ult. load, E=10GPa, geom. linear analysis	3%	0%	0%

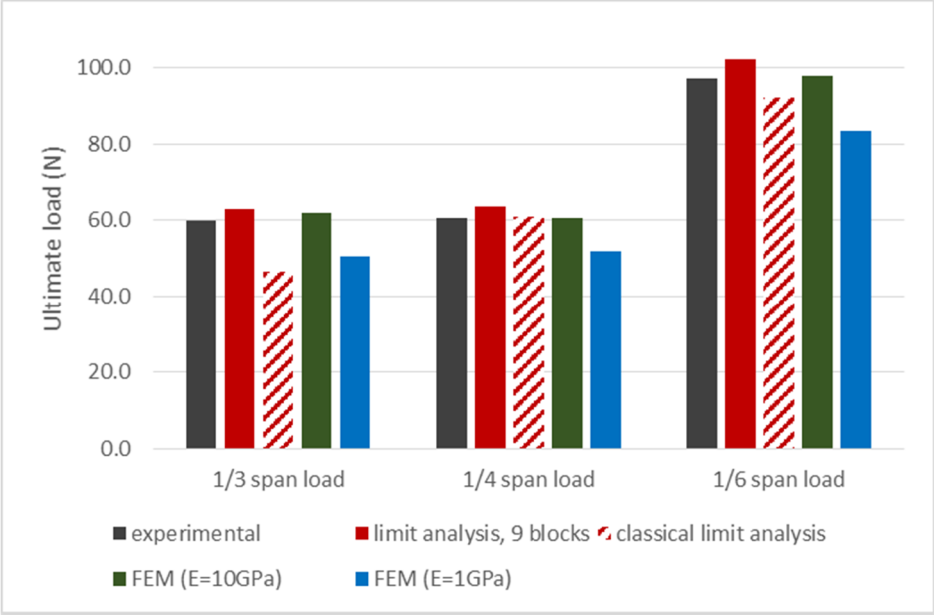

Figure 101. Comparison between the experimental results (grey bars) and limit analysis (red bars) and FEM results (blue and green)

The dispersion of the ultimate loads found experimentally is in the order of 5%, but, as said, this is the result of a rather controlled process of mounting. Little variations of the span of the arch, or the initial opening of some joints, produce variations in the ultimate load of much higher magnitude. This problem is faced also, and particularly, when existing arches are studied. For these arches, as a matter of facts, a deep knowledge of the state of each interface and of the actual geometry itself could be difficult to achieve, despite the great influence that it has on the structural assessment, as discussed in different papers (Drosopoulos et al., 2006, de Arteaga and Morer, 2012).

An acceptable range of variability of the analytical results has to be compared to the nature of the problem to model and the uncertainties involved. As shown in Figure 102, the methods of analysis that were performed gave differences, compared to the experimental results, in a quite limited range, in comparison to the effect of the uncertainties that are generally faced and to the safety factors that have, for this reason to be applied.

The application of limit analysis in its simplest and most used formulation, according to Heyman's hypotheses, gave results that can be considered too conservative, apart from the case of loading in correspondence of the quarter of the span. If, indeed, the present joints that open at failure are close to the ones that would form in a homogeneous material with zero tensile strength, where joints can open in any location, the two failure mechanisms are very close a so are the relative ultimate loads. There are, on the other hand, configurations for which the general approach of limit analysis underestimates the measured ultimate load of up to 20%.

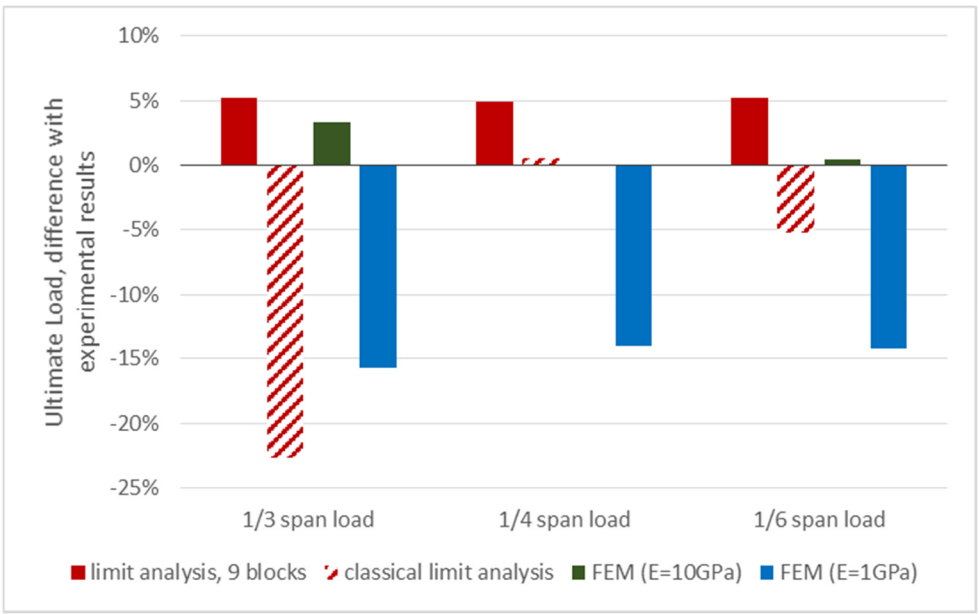

Figure 102. Comparison of the results: percentage difference of the analytical and numerical approaches compared to the average experimental ultimate load

The limit analysis performed with a proper number of rigid blocks and contact interfaces, of the right geometry, gives values for the ultimate capacity that are closer to the experimental. The analysis, as expected, overestimates slightly the failure load. This characteristics, linked to the formulation of the problem that does not take into account the displacements of the structure before the development of a mechanism, can be accepted if the generality of the method, and the intuitiveness and interpretability of the results are considered. The overestimation of the ultimate load is in the order of 5-8%.

Given the fact that the method is expected to give a slight overestimation, and that the hypotheses on which it is based are confirmed by the experimental observations, its application seems effective and gives reasonably good results, with a correct modelling of the structure and of its failure. The overestimation might be compensated by the application of a correctly calibrated safety factor. Other approaches of limit analysis, like the definition of a conventional increase of thickness, do not describe the nature of the problem with the same accuracy, even if their implementation can be simpler, and were not considered in this work.

The numerical models, as already discussed, are able to reproduce the structural behaviour with a certain accuracy, once the parameters on which the results depend are correctly calibrated. If there is no possibility of any calibration, as is a frequent case, the estimations provided by the FE method might be conservative or non-conservative, depending on the choice of the parameters. The range of variability of the results, anyway, can be considered acceptable and is of the same order of magnitude of the results of a “correct” limit analysis through rigid blocks.

To conclude the analysis of the results, a comparison between the failure mechanisms estimated by the different methods and the failure that was observed in the experimental campaign is shown in Figure 103, Figure 104 and Figure 105 for the different load configurations. In all the cases the failure mechanisms predicted by the models are the same as the ones measured in the experimental campaign. This should justify the hypotheses that were made on the behaviour of joints and interfaces, in particular regarding the absence of sliding. The fact that, despite being based on the evaluation of the same type of failure, the models can give slightly different results, confirms that those differences that were found are related to the implicit assumptions of the method (the absence of non-linearity in geometry for limit analysis, for example) or by slight differences in the definition of the geometry, to which the problem is rather sensible. The hypotheses made on the failure modes, on the contrary, are fully confirmed and replicated by the models in the correct way.

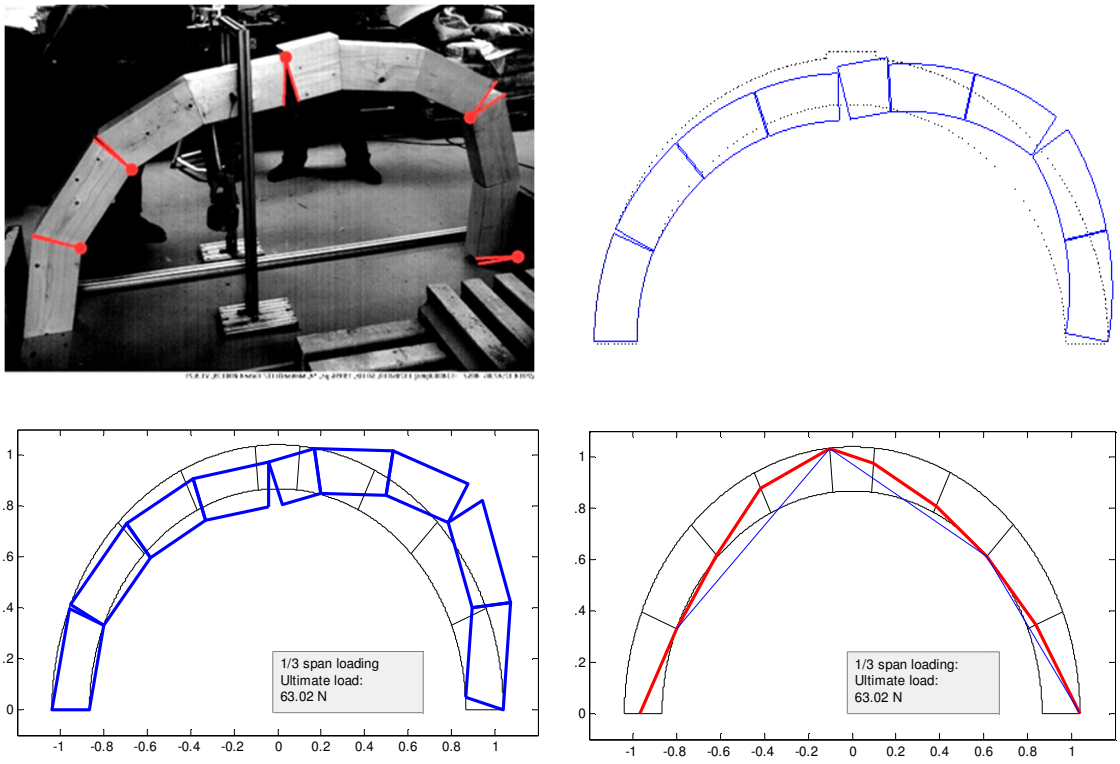

Figure 103. Failure mechanisms: experimental, FEM and limit analysis results for third span loading

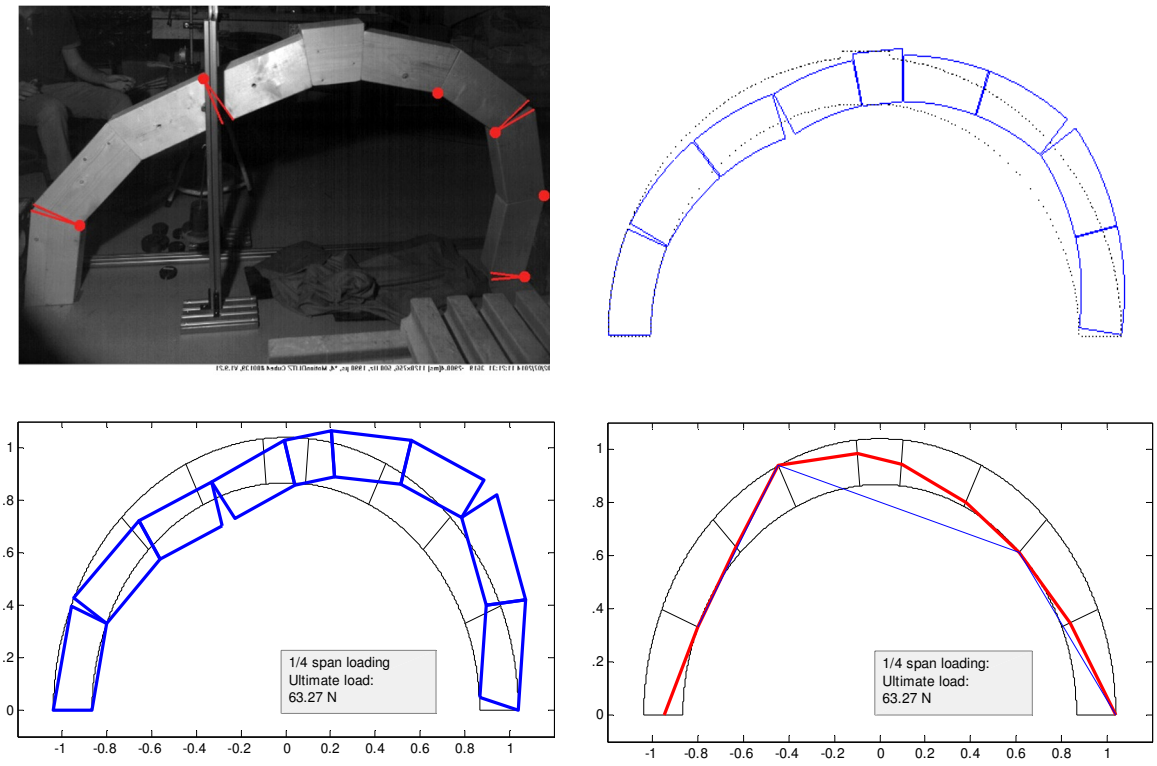

Figure 104 Failure mechanisms: experimental, FEM and limit analysis results for quarter span loading

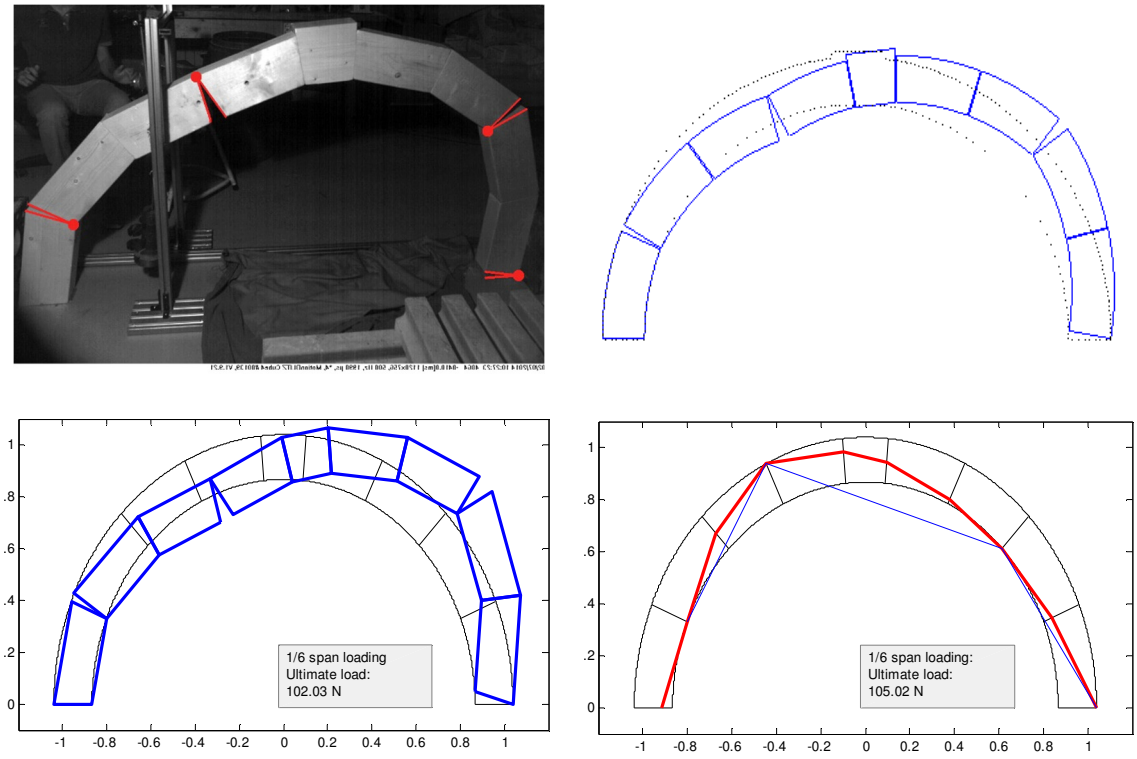

Figure 105 Failure mechanisms: experimental, FEM and limit analysis results for sixth span loading

Conclusions

The study of the structural behaviour of arches with a limited number of voussoirs was the main scope of this work, with particular interest in the evaluation of the applicability of the classical methods of analysis on this particular typology. The main methods for the analysis of arches, and specifically of this typology, are the FEA method, widely used for all types of structures, and the limit analysis. Although the use of limit analysis is widespread and confirmed by different experimental results, its extension to the analysis of arches with a low number of voussoirs can result problematic and requires some modifications in order to be confidently applied.

The method that was followed to investigate the applicability of limit analysis to the particular typology consisted in the realisation of some experimental tests on a model arch, and to the comparison of experimental results with analytical and numerical predictions of the ultimate capacity of the arch, obtained with different methods of analysis. The main objective, indeed, in the structural assessment of these structures, is the determination of the maximum load carrying capacity.

A study on the typological characteristics of arches with a low number of voussoirs was performed in order to define a proper case study to analyse, possibly representative, for its geometry and proportions, of the entire typology. The selected case study, the Palladian arch of the *serliana* windows of *Palazzo della Ragione* in Vicenza (Italy), was then reproduced in a model to test in the laboratory. The model was realised in half-scale, in full timber, to have the possibility to test the arch in multiple load configurations, avoiding the cracking of the model after failure. The applied loads were concentrated asymmetrical loads, increased until failure of the structure, measuring also the displacement of one characteristic point.

The data from the experimental campaign were then compared to the results of different techniques of structural analyses of arches, to evaluate their accuracy and applicability. Limit analysis was performed with two approaches. The first consisted in the implementation, through both the static and kinematic approach, of limit analysis to an arch seen as a structure of rigid blocks (the voussoirs) in reciprocal contact through interfaces, where all the plastic strains take place. The standard hypotheses of limit analyses were applied to the interfaces, being these assumptions largely applicable to the joints (especially if, as in this case, they are dry joints). The possibility of application of different material models (yield functions) were considered. A Matlab code was developed to perform the analysis of the studied arch, in its real configuration, following the static and kinematic approach, solving the linear programming problem of finding the maximum (or minimum) load multiplier.

The second approach consisted in the research of an optimal thrust line which maximises the applied load until a maximum load factor is defined. The conditions to apply to the thrust line to search were modified from the classical ones, in order to adapt this thrust line analysis to the case of arches with

few voussoirs. A Matlab code was developed also in this case, to perform the numerical integration of the differential equation of the thrust line (applied in its general formulation for radial stereotomy), and to optimise the parameters until a maximum applicable load is found.

The FEA was applied through the definition in Diana of a FE simplified micro-model, where the voussoirs are modelled as elastic bodies and all the non linearities are concentrated in the joints.

The experimental, numerical and analytical results were then compared in order to validate the applicability of the different methods of analysis. Once considered an acceptable range of variation of the analytical results from the experimental, coherent to the dispersion of experimental data and uncertainties of the problem, the comparison of the different results confirmed that:

- The limit analysis, implemented through its classical formulations (Heyman's hypotheses) tends to underestimate considerably the ultimate capacity of arches with limited number of voussoirs, especially if the hinges corresponding to the weakest mechanism are relevantly far from the existing joints; this condition depends highly on the geometrical disposition of the voussoirs and on the position of the load;
- The limit analysis performed considering the voussoirs as rigid bodies and locating the non-linearity in the joints is rather simple to implement in a code and apply to the case of arches with a limited number of voussoirs; the hypotheses made on the failure mechanisms, and on the compressive strength of the material, are fully confirmed by the experimental observations, efficiently reproduced by the analysis, in terms of failure mechanism
- The quantification of the failure load through upper bound and lower bound limit analysis of rigid blocks coincides, as the linear programming procedure efficient and stable; the obtained values tend to overestimate of about the 5-8% the experimental results;
- The implementation of limit analysis through thrust line analysis introduces some complications in the procedure of numerical optimisation of the solution, which is less efficient; the hypothesis that the thrust line can stay out of the boundaries of the arch between the joints seems to be confirmed by both the similarity of limit analysis of rigid blocks and by the experimental results;
- The application of a FE simplified micro-model is a good way of analysing the problem, keeping a moderate level of complexity for the model, although a certain dependence of the solution on the definition of the elastic parameters was found; the definition of the collapse mechanisms is efficient.

On this base, the applicability of limit analysis to the typology of arches with a limited number of voussoirs seems adequate to model correctly the failure mechanism and to provide a fairly good estimation of the failure load. The implementation of limit analysis, though, to obtain results in a better agreement with the experimental tests and not too conservative, should take into account the real geometry and disposition of voussoirs and joints.

With regards to the effect of the number of voussoirs on the ultimate capacity of an arch, it was found, through the application of limit analysis, that the arches with a lower number of voussoirs, as expected, have an increasing capacity. The correct definition of the geometry, though, has a primary role, as solutions are rather sensible to the real position of joints, even if the same number of voussoirs is composing the arch. The nature of the difference between the structural behaviour of standard masonry arches and these arches with few voussoirs, indeed, more than the number of joints is their distance from the weakest position, in which a hinge tends to open.

A problematic issue to solve is the determination of the structural behaviour of arches with initial imperfections, open joints, not planar contact surfaces, incomplete contact at the surface of the joints resulting in a lower thickness. The effect of these imperfections in the tested arch was relevant. If an existing structure which exhibits some of these initial imperfections, case which is very common, has to be assessed, proper analysis methods or at least a simplified estimation of the reduction of their load carrying capacity, would be required.

5.1 Scope for future development

The future development of the present work might be the definition of adequate methods of computing the load capacity of arches with initial imperfections, in particular for the simpler case, the opening of some joints before the application of a load, as this is a common configuration also for existing arches. Another relevant issue seems the dependence of the capacity of existing arches to slight movements of the abutments.

The methods that were applied in this work can be refined, with the implementation of a specific yielding function that could consider also the cracking of the voussoirs, taking into account a tensile strength that can be assumed for a stone voussoir. In this way, fictitious interfaces might be considered inside the voussoirs, defining more sections of possible cracking, improving the quality of the solution and generalising the solution from the hypothesis of rigid blocks.

One last development is the refinement of the procedure for the thrust line analysis, in particular for the problem of finding an optimised solution calibrating the parameters on which the solution depends. Being the problem non-linear and depending on a maximum value of a numerical integration of a differential equation, the solution is not immediate.

References

Aita, Danila (2003) “Between Geornetry and Rnechanics : A Re-Exarnination of the Principies of Stereotorny Frorn a Statical Point of View.” January (2003): n. pag.

Andreu, A, L Gil, and P Roca (2007) “Computational Analysis of Masonry Structures with a Funicular Model.” April (2007): 473–480.

Bernat-Maso, Ernest, Lluís Gil, and Jordi Marcé-nogué (2012) “The Structural Performance of Arches Made of Few Vossoirs with Dry-Joints.” 44.6 (2012): n. pag.

Bicanic, N., C. Stirling, and C. J. Pearce (2003) “Discontinuous Modelling of Masonry Bridges.” *Computational Mechanics* 31.1-2 (2003): 60–68.

Block, Philippe, and John Ochsendorf (2007) “Thrust Network Analysis : A New Methodology For Three-Dimensional Equilibrium.” (2007): 1–8.

Boothby, Thomas E. (2001) “Analysis of Masonry Arches and Vaults.” *Progress in Structural Engineering and Materials* 3.3 (2001): 246–256.

Buffarini, G, P Clemente, and G De Felice (2006) “Limit Behaviour of Partially Reinforced Masonry Arch Bridges.” (2006): n. pag.

Cavicchi, Andrea, and Luigi Gambarotta (2006) “Two-Dimensional Finite Element Upper Bound Limit Analysis of Masonry Bridges.” 84 (2006): 2316–2328.

Chen, Y., a.F. Ashour, and S.W. Garrity (2007) “Modified Four-Hinge Mechanism Analysis for Masonry Arches Strengthened with near-Surface Reinforcement.” *Engineering Structures* 29.8 (2007): 1864–1871.

Choo, B. S., M. G. Coutie, and N. G. Gong (1991) “Finite-Element Analysis of Masonry Arch Bridges Using Tapered Elements.” *ICE Proceedings* 91.4 (1991): n. pag.

Crisfield, M.A, and A.J Packham (1987) *A Mechanism Program for Computing the Strength of Masonry Arch Bridges*. Crowthorne (UK): Transport and Road Research Lab. (TRRL). Crowthorne (UK): Transport and Road Research Lab. (TRRL).

Cundall, Peter, and Roger D. Hart (1992) “Numerical Modelling of Discontinua.” *Engineering Computations* 9.2 (1992): 101–113.

De Arteaga, I., and P. Morer (2012) “The Effect of Geometry on the Structural Capacity of Masonry Arch Bridges.” *Construction and Building Materials* 34 (2012): 97–106.

De Lorenzis, Laura, Mathhew De Jong, and John Ochsendorf (2007) “Failure of Masonry Arches under Impulse Base Motion.” *Earthquake Engineering and Structural Dynamics* 36.14 (2007): 2119–2136.

De Luca, Antonello, Aldo Giordano, and Elena Mele (2004) “A Simplified Procedure for Assessing the Seismic Capacity of Masonry Arches.” *Engineering Structures* 26 (2004): 1915–1929.

De Rosa, E., and F. Galizia (2007) “Evaluation of Safety of Pointed Masonry Arches through the Static Theorem of Limit Analysis.” *ARCH 07 - 5th International Conference on Arch Bridges*. N. p.

Del Piero, G. (1998) “Limit Analysis and No Tension Materials.” *International Journal of Plasticity* 14 (1998): 259–271.

Delbecq, J. (1982) “Stability Analysis of Masonry Arches by Guild Design Method.” *J Mec Theor Appl* 1 (1982): 91.

Dimitri, R, L De Lorenzis, and G Zavarise (2011) “Numerical Study on the Dynamic Behavior of Masonry Columns and Arches on Buttresses with the Discrete Element Method.” *Engineering Structures* 33.12 (2011): 3172–3188.

Drosopoulos, G.a., G.E. Stavroulakis, and C.V. Massalas (2006) “Limit Analysis of a Single Span Masonry Bridge with Unilateral Frictional Contact Interfaces.” *Engineering Structures* 28.13 (2006): 1864–1873.

Drucker, D.C. (1953) “Limit Analysis of Two and Three Dimensional Soil Mechanics Problems.” *Journal of the Mechanics and Physics of Solids* 1 (1953): n. pag.

Foce, Federico (2007) “Milankovitch’s ‘Theorie Der Druckkurven’: Good Mechanics for Masonry Architecture.” *Nexus Network Journal* 9.2 (2007): 185–210.

Gilbert, M (2007) “Limit Analysis Applied to Masonry Arch Bridges : State-of-the-Art and Recent Developments.” (2007): n. pag.

Gilbert, M., C. Casapulla, and H.M. Ahmed (2006) “Limit Analysis of Masonry Block Structures with Non-Associative Frictional Joints Using Linear Programming.” *Computers & Structures* 84.13-14 (2006): 873–887.

Heyman, Jacques (2009) “La Coupe Des Pierres.” May (2009): n. pag.

--- (1966) “The Stone Skeleton.” *International Journal of Solids and Structures* 2 (1966): 249–279.

Hogg, V., and B. S. Choo (2000) “A Study of Scale Effects in Masonry Arch Bridges : Is Testing of Large-Scale Structures Still Necessary?” *Structural Engineer* 78 (2000): 24–29.

Huerta, Santiago (2004) *Arcos, Bóvedas Y Cúpolas*. Ed. Instituto Juan de Herrera. Madrid: N. p. Madrid: N. p.

--- (2001) “Mechanics of Masonry Vaults : The Equilibrium Approach.” (2001): 47–70.

--- (2002) “Thomas Young ’ S Theory of the Arch . His Analysis of Telford ' S Design for an Iron Arch of 600 Feet over the Thames in London.” (2002): n. pag.

Kooharian, Anthony (1952) “Limit Analysis of Voussoir (Segmental) and Concrete Arches.” *ACI Journal Proceedings* 49.12 (1952): n. pag.

Lourenço, P B, and A Orduña (2005) “Three-Dimensional Limit Analysis of Rigid Blocks Assemblages . Part II : Load-Path Following Solution Procedure and Validation.” 42 (2005): 5161–5180.

Lourenço, Paulo B, Gabriele Milani, and Antonio Tralli (2006) “Homogenisation Approaches for Structural Analysis of Masonry Buildings.” (2006): n. pag.

Lucchesi, Massimiliano et al. (1997) “On the Collapse of Masonry Arches.” (1997): 327–346.

Makris, Nicos, and Haris Alexakis (2013) “The Effect of Stereotomy on the Shape of the Thrust-Line and the Minimum Thickness of Semicircular Masonry Arches.” *Archive of Applied Mechanics* 83.10 (2013): 1511–1533.

Molins, C., and P. Roca (1998) “Capacity of Masonry Arches and Spatial Frames.” *Journal of Structural Engineering* 124.6 (1998): 653–663.

Munjiza, A. (2004) *The Combined Finite-Discrete Element Method*. John Wiley and Sons. John Wiley and Sons.

Oliveira, Daniel V., Paulo B. Lourenço, and Cláudia Lemos (2010) “Geometric Issues and Ultimate Load Capacity of Masonry Arch Bridges from the Northwest Iberian Peninsula.” *Engineering Structures* 32.12 (2010): 3955–3965.

Orduña, Agustín (2003) “Seismic Assessment of Ancient Masonry Structures by Rigid Blocks Limit Analysis.” University of Minho, 2003.

Owen, D R J, D Peric, and N Petrinic (1998) “Finite/discrete Element Models for Assessment and Repair of Masonry Structures.” *Arch Bridges – History, Analysis, Assessment, Maintenance and Repair, Proceedings of the Second International Arch Bridge Conference*. N. p. 173–180.

Palladio, Andrea (1570) *I Quatto Libri Dell’architettura*. Venice: N. p. Venice: N. p.

Pelà, Luca, Alessandra Aprile, and Andrea Benedetti (2009) “Seismic Assessment of Masonry Arch Bridges.” *Engineering Structures* 31.8 (2009): 1777–1788.

Pèrez-Aparicio, J. L., R. Bravo, and P. Ortiz (2013) “Refined Element Discontinuous Numerical Analysis of Dry-Contact Masonry Arches.” *Engineering Structures* 48 (2013): 578–587.

Pippard, A.J.S., and JF. Baker (1936) “The Voussoir Arch.” *The Analysis of Engineering Structures*. N. p. 568–595.

Prager, W. (1955) “The Theory of Plasticity: A Survey of Recent Achievements.” *Proceedings of the Institution of Mechanical Engineers*. N. p. 41–57.

Rizzi, Egidio, Fabio Rusconi, and Giuseppe Cocchetti (2014) “Analytical and Numerical DDA Analysis on the Collapse Mode of Circular Masonry Arches.” *Engineering Structures* 60 (2014): 241–257.

Roca, P. et al. (2007) “Limit Analysis of Reinforced Masonry Vaults.” *Engineering Structures* 29.3 (2007): 431–439.

Roca, Pere et al. (2010) “Structural Analysis of Masonry Historical Constructions . Classical and Advanced Approaches.” (2010): 299–325.

Royles, R., and A. W. Hendry (1991) “Model Tests on Masonry Arches.” *ICE Proceedings* 91.2 (1991): 299–321.

Ruskin, John (1851) *The Stones of Venice*. Ed. 1960 J. G. Links. London: N. p. London: N. p.

Sakarovitch, Joel (2003) “Stereotomy , a Multifaceted Technique.” January (2003): n. pag.

Sánchez-Beitia, S. (2013) “Analysis of the Collapse Mechanisms in Uncracked Arches: The Role of Friction Forces and Stereotomy in Masonry.” *Engineering Failure Analysis* 35 (2013): 326–333.

Shi, Gen-Hua, and R. E. Goodman (1992) “Discontinuous Deformation Analysis: A New Numerical Model for the Statics and Dynamics of Deformable Block Structures.” *Engineering Computations* 9.2 (1992): 157–168.

Thavalingam, A et al. (2001) “Computational Framework for Discontinuous Modelling of Masonry Arch Bridges.” 79 (2001): 1821–1830.

Toth, Axel Roland, Zoltán Orbán, and Katalin Bagi (2009) “Discrete Element Analysis of a Stone Masonry Arch.” *Mechanics Research Communications* 36.4 (2009): 469–480.

Annexes

Annex 1:

MATLAB code for lower bound limit analysis: rigid bodies assumption

```
clear all
%definition of the geometrical properties: r (radius of the axis),
%sp (thickness of the arch), fi (angles of the joints, radians), t
%analysed width (0.1 m in this case)
r= 0.9532;
sp=0.1811*r;
fi = [0;0.3927;0.7854;1.1275;1.4696;1.6720;2.0141;2.3562;2.7489;3.1416];
m=length(fi);
n=m-1;
t=0.1;
%vector teta of the angular extension of each voussoir
for i=1:1:n
    teta(i,1)=fi(i+1,1)-fi(i,1);
end
%vector d of the distances of the nodes from the centre of the
interfaces
for i=1:1:n
    d(i,1)=2*r*sin(teta(i)/4);
end
%equilibrium matrix CT
CT=zeros(3*n,3*m);
for i=0:1:n-1                       %(i+1) is the index of each voussoir
   CT(3*i+1,3*i+1)=sin(fi(i+1));  %horizontal equilibrium
   CT(3*i+1,3*i+4)=-sin(fi(i+2));
   CT(3*i+1,3*i+2)=-cos(fi(i+1));
   CT(3*i+1,3*i+5)=cos(fi(i+2));
   CT(3*i+2,3*i+1)=-cos(fi(i+1)); %vertical equilibrium
   CT(3*i+2,3*i+4)=cos(fi(i+2));
   CT(3*i+2,3*i+2)=-sin(fi(i+1));
   CT(3*i+2,3*i+5)=sin(fi(i+2));
   CT(3*i+3,3*i+1)=-d(i+1)*sin(teta(i+1)/4); %rotational equilibrium
   CT(3*i+3,3*i+2)=-d(i+1)*cos(teta(i+1)/4);
   CT(3*i+3,3*i+3)=-1;
   CT(3*i+3,3*i+4)=d(i+1)*sin(teta(i+1)/4);
   CT(3*i+3,3*i+5)=-d(i+1)*cos(teta(i+1)/4);
   CT(3*i+3,3*i+6)=1;
end
%vector Pg of the dead (vertical) loads. 385 kg/m3 of density
for i=0:1:n-1
    Pg(3*i+1,1)=0;
    Pg(3*i+2,1)=-((r+sp/2)^2-(r-sp/2)^2)*teta(i+1,1)/2*t*385*9.81;
    Pg(3*i+3,1)=0;
end
Pg(3*4+2,1)=-((r+sp/2+0.03)^2-(r-sp/2)^2)*teta(4+1,1)/2*t*385*9.81;
%vector P0 of the applied loads
P0=zeros(3*n,1);
P0(2+(6-1)*3,1)=-1;
P0(3+(6-1)*3,1)=1*0.03;
```

```
%matrix NT of the coefficients of the yield function. mu=0.5 (friction
%angle of about 27°. Infinite compressive strength. Lateral restraints
at
%the base with an artificial friction coefficient.
NT=zeros(4*m,3*m);
for i=1:1:m
    NT(4*(i-1)+1,3*(i-1)+1)=1;
    NT(4*(i-1)+2,3*(i-1)+1)=1;
    NT(4*(i-1)+1,3*(i-1)+3)=1/(sp/2);
    NT(4*(i-1)+2,3*(i-1)+3)=-1/(sp/2);
    NT(4*(i-1)+3,3*(i-1)+1)=0.5;
    NT(4*(i-1)+4,3*(i-1)+1)=0.5;
    NT(4*(i-1)+3,3*(i-1)+2)=1;
    NT(4*(i-1)+4,3*(i-1)+2)=-1;
end
 NT(4*(1-1)+3,3*(1-1)+1)=1;
 NT(4*(1-1)+4,3*(1-1)+1)=1;
 NT(4*(m-1)+3,3*(m-1)+1)=1;
 NT(4*(m-1)+4,3*(m-1)+1)=1;
%definition of the linear programming problem. c multiplies the
variables
% [Q alfa] to minimize only -alfa. Aeq and beq impose the equilibrium.
% Adis and bdis impose the yield function to be non positive. Q0 is the
% initial vector for the procedure
Q0=zeros(3*m+1,1);
c=zeros(3*m,1);
c(3*m+1,1)=-1;
Aeq=[CT P0];
beq=-Pg;
Adis=[NT zeros(4*m,1)];
bdis=zeros(4*m,1);
Q=linprog(c,Adis,bdis,Aeq,beq,[],[],Q0);
%drawing of the arch
hold off
arco(r-sp/2,r+sp/2,fi,m);
%definition of 3 vectors of generalised stresses for easier use of the
%results from the vector Q: N-normal force, V-shear, m-bending moment
%ecc-eccentricity of the thrust, alfa-load multiplier
for i=1:1:m
    N(i,1)=Q(3*(i-1)+1)
    V(i,1)=Q(3*(i-1)+2)
    M(i,1)=Q(3*(i-1)+3)
    ecc(i,1)=M(i)/N(i)
end
alfa=Q(3*m+1)
%coordinates of the points of application of the thrust and drawing of a
%piecewise 'thrust line'
ro=r+ecc;
for i=1:1:m
    x(i)=ro(i)*cos(fi(i));
    y(i)=ro(i)*sin(fi(i));
end
plot(x,y,'r','LineWidth',2.5)
yield=Adis*Q;
fail=find(yield>=-0.00001)/4;
for i=1:1:length(fail)
    if (fail(i)-fix(fail(i))==0.5)
        fail(i)=fix(fail(i)+1);
```

```
        xf(i)=(r+sp/2)*cos(fi(fail(i)));
        yf(i)=(r+sp/2)*sin(fi(fail(i)));
    else
        if (fail(i)-fix(fail(i))==0.25)
        fail(i)=fix(fail(i))+1;
        xf(i)=(r-sp/2)*cos(fi(fail(i)));
        yf(i)=(r-sp/2)*sin(fi(fail(i)));
        else
            fail(i)=fix(fail(i))+1;
            xf(i)=(r)*cos(fi(fail(i)));
            yf(i)=(r)*sin(fi(fail(i)));
        end
    end
end
plot(xf,yf,'b')
axis([-1.2 1.2 -0.1 1.1])
```

Annex 2:

MATLAB code for upper bound limit analysis, kinematic formulation

```
clear all
%definition of the geometrical properties: r (radius of the axis),
%sp (thickness of the arch), fi (angles of the joints, radians), t
%analysed width (0.1 m in this case)
r= 0.9532;
sp=0.1811*r;
fi = [0;0.3927;0.7854;1.1275;1.4696;1.6720;2.0141;2.3562;2.7489;3.1416];
m=length(fi);
n=m-1;
t=0.1;
%vector teta of the angular extension of each voussoir
for i=1:1:n
    teta(i,1)=fi(i+1,1)-fi(i,1);
end
% vector d of the distances of the nodes from the centre of the
interfaces
for i=1:1:n
    d(i,1)=2*r*sin(teta(i)/4);
end
% equilibrium matrix CT (the compatibility matrix is the opposite of
% its transpose)
CT=zeros(3*n,3*m);
for i=0:1:n-1                       %(i+1) is the index of each voussoir
   CT(3*i+1,3*i+1)=sin(fi(i+1));  %horizontal equilibrium
   CT(3*i+1,3*i+4)=-sin(fi(i+2));
   CT(3*i+1,3*i+2)=-cos(fi(i+1));
   CT(3*i+1,3*i+5)=cos(fi(i+2));
   CT(3*i+2,3*i+1)=-cos(fi(i+1)); %vertical equilibrium
   CT(3*i+2,3*i+4)=cos(fi(i+2));
   CT(3*i+2,3*i+2)=-sin(fi(i+1));
   CT(3*i+2,3*i+5)=sin(fi(i+2));
   CT(3*i+3,3*i+1)=-d(i+1)*sin(teta(i+1)/4); %rotational equilibrium
   CT(3*i+3,3*i+2)=-d(i+1)*cos(teta(i+1)/4);
   CT(3*i+3,3*i+3)=-1;
   CT(3*i+3,3*i+4)=d(i+1)*sin(teta(i+1)/4);
   CT(3*i+3,3*i+5)=-d(i+1)*cos(teta(i+1)/4);
   CT(3*i+3,3*i+6)=1;
end
%vector Pg of the dead (vertical) loads. 385 kg/m3 of density
for i=0:1:n-1
    Pg(3*i+1,1)=0;
    Pg(3*i+2,1)=-((r+sp/2)^2-(r-sp/2)^2)*teta(i+1,1)/2*t*385*9.81;
    Pg(3*i+3,1)=0;
end
Pg(3*4+2,1)=-((r+sp/2+0.03)^2-(r-sp/2)^2)*teta(4+1,1)/2*t*385*9.81;
%vector P0 of the applied loads
P0=zeros(3*n,1);
P0(2+(7-1)*3,1)=-1;
P0(3+(7-1)*3,1)=-1*0.1113;
%matrix NT of the coefficients of the yield function. mu=0.5 (friction
%angle of about 27°. Infinite compressive strength. Associated flow.
NT=zeros(4*m,3*m);
```

```
for i=1:1:m
    NT(4*(i-1)+1,3*(i-1)+1)=1;
    NT(4*(i-1)+2,3*(i-1)+1)=1;
    NT(4*(i-1)+1,3*(i-1)+3)=1/(sp/2);
    NT(4*(i-1)+2,3*(i-1)+3)=-1/(sp/2);
    NT(4*(i-1)+3,3*(i-1)+1)=0.3;
    NT(4*(i-1)+4,3*(i-1)+1)=0.3;
    NT(4*(i-1)+3,3*(i-1)+2)=1;
    NT(4*(i-1)+4,3*(i-1)+2)=-1;
end
 NT(4*(1-1)+3,3*(1-1)+1)=1;
 NT(4*(1-1)+4,3*(1-1)+1)=1;
 NT(4*(m-1)+3,3*(m-1)+1)=1;
 NT(4*(m-1)+4,3*(m-1)+1)=1;
% definition of the linear programming problem. c multiplies the
variables
% [du dlambda] applying in this formulation the theorem of virtual
works.
% C impose the compatibility of displacements, N the flow rule.
C=transpose(CT);
N=transpose(NT);
Ftemp=[transpose(P0) zeros(1,4*m)];
Aeqk=[C N];
Aeqk=[Aeqk;Ftemp];
beqk=zeros(3*m+1,1);
beqk(3*m+1,1)=1;
delta0=zeros(3*n+4*m,1);
c=[transpose(-Pg) zeros(1,4*m)];
c=transpose(c);
Adisk=zeros(4*m,3*n+4*m);
for i=1:1:4*m
    Adisk(i,i+3*n)=-1;
end
bdisk=zeros(4*m,1);
delta=linprog(c,Adisk,bdisk,Aeqk,beqk,[],[],delta0);
%drawing of the arch
hold off
arco(r-sp/2,r+sp/2,fi,m);
%definition of 3 vectors of displacements of the blocks for easier use
%of the results:
for i=1:1:n
    deltax(i)=(delta((i-1)*3+1));
    deltay(i)=(delta((i-1)*3+2));
    deltat(i)=(delta((i-1)*3+3));
end
maxx=max(abs(deltax));
maxy=max(abs(deltay));
maxt=max(abs(deltat*0.2));
maxdispl=max([maxx,maxy,maxt]);
fatt=0.1/maxdispl;
deltax=deltax*fatt;
deltay=deltay*fatt;
deltat=deltat*fatt;
for i=1:1:9
    xg=[r*cos(fi(i)+teta(i)/2);r*sin(fi(i)+teta(i)/2)];
    dn1=[(r-sp/2)*cos(fi(i));(r-sp/2)*sin(fi(i))]-xg;
    dn2=[(r+sp/2)*cos(fi(i));(r+sp/2)*sin(fi(i))]-xg;
    dn3=[(r+sp/2)*cos(fi(i+1));(r+sp/2)*sin(fi(i+1))]-xg;
```

```
    dn4=[(r-sp/2)*cos(fi(i+1));(r-sp/2)*sin(fi(i+1))]-xg;
    xblocco(1)=deltax(i)-dn1(2)*deltat(i)+(r-sp/2)*cos(fi(i));
    yblocco(1)=deltay(i)+dn1(1)*deltat(i)+(r-sp/2)*sin(fi(i));
    xblocco(2)=deltax(i)-dn2(2)*deltat(i)+(r+sp/2)*cos(fi(i));
    yblocco(2)=deltay(i)+dn2(1)*deltat(i)+(r+sp/2)*sin(fi(i));
    xblocco(3)=deltax(i)-dn3(2)*deltat(i)+(r+sp/2)*cos(fi(i+1));
    yblocco(3)=deltay(i)+dn3(1)*deltat(i)+(r+sp/2)*sin(fi(i+1));
    xblocco(4)=deltax(i)-dn4(2)*deltat(i)+(r-sp/2)*cos(fi(i+1));
    yblocco(4)=deltay(i)+dn4(1)*deltat(i)+(r-sp/2)*sin(fi(i+1));
    xblocco(5)=xblocco(1);
    yblocco(5)=yblocco(1);
    hold on
    plot(xblocco,yblocco,'b','LineWidth',2);
end
```

Annex 3:

MATLAB code for thrust line analysis and optimisation

```
function z = f(x,y,flag,hor,vert,thick,radius)
%UNTITLED3 Differential equation of the thrust line
%   The formulation depends on the horizontal and vertical component of
the
%   thrust in the initial point and on the geometry of the arch
(thickness
%   and radius)
H=-hor;
r=sqrt(x^2+y^2);
phi=asin(x/r);
V=vert+((radius+thick/2)^2-(radius-thick/2)^2)*phi/2*0.1*3.85-p(x);
csi=radius-r;
mom=-4*0.1*radius*thick*(((thick^2)/(12*radius))+csi)*x/r*((1/r-
((x^2)/(r^3)))/(sqrt(1-(x^2)/(r^2))));
z = V/H-mom/H;
end


function load = p( x )
%Definition of the applied loads (through the integral of the applied
loads
%from x=x0 to x)
if x>=-0.2725,
    load=-0.065;
else
    load=0;
end
end


function fgs = fattgeom2(par)
%integration of the differential equation of the thrust line, in two
parts
%separed by the point of application of the load. The geometrical safety
%factor is calculated only in the joints. The solution in the joints is
%calculated through linear interpolation from the closest calculated
points
%parameters are passed through a initial vector for the optimization
spess=par(1);
raggio=par(2);
x0=par(3);
h=par(4);
v=par(5);
%integration of the first part of the thrust line
options=odeset('AbsTol',1e-12,'RelTol',1e-7)
[x1,y1]=ode45('f',[-x0 -0.2725],0.001,options,h,v,spess,raggio);
d1=size(y1);
for i=1:1:d1(1)
    phi(i)=asin(x1(i)/sqrt(x1(i)^2+y1(i).^2));
    if y1(i)>=0,
        r(i)=sqrt(x1(i)^2+y1(i)^2);
    else
```

```
        r(i)=raggio;
    end
end
hold on
plot(x1,y1);
%integration of the second half of the thrust line. If the solution is
%negative (if the integration domain is too long and the solution is
%calculated after the thrust has passed the last joint) the solution is
%corrected
[x2,y2]=ode45('f',[-0.2725
1.2*(raggio+spess/2)],y1(d1(1)),options,h,v,spess,raggio);
d2=size(y2);
for i=1:1:d2(1)
    if y2(i)>=0,
        r(d1(1)+i)=sqrt(x2(i)^2+y2(i)^2);
        phi(d1(1)+i)=asin(x2(i)/sqrt(x2(i)^2+y2(i).^2));
    else
        if y2(i-1)>0,
            x2(i)=x2(i-1)-(x2(i)-x2(i-1))/(y2(i)-y2(i-1))*y2(i-1);
            y2(i)=0;
            r(d1(1)+i)=sqrt(x2(i)^2+y2(i)^2);
            phi(d1(1)+i)=pi/2;
        else
            r(d1(1)+i)=raggio;
            y2(i)=0;
            x2(i)=raggio+spess/2;
            phi(d1(1)+i)=asin(x2(i)/sqrt(x2(i)^2+y2(i).^2));
        end
    end
end
hold on
plot(x2,y2);
%linear interpolation to obtain the position of the thrust line in the
%joints. The vector of joints angle is introduced here (gr)
phi=transpose(phi);
r=transpose(r);
gr = [-1.5708;-1.1781;-0.7854;-0.4433;-
0.1012;0.1012;0.4433;0.7854;1.1781;pi/2];
dtot=numel(r);
rj(1)=r(1);
for i=2:1:9
    k=max(find(phi<=gr(i)));
    if k==dtot,
        rj(i)=r(k);
    else
        rj(i)=r(k)+(r(k+1)-r(k))/(phi(k+1)-phi(k))*(gr(i)-phi(k));
    end
end
k=min(find(phi>=gr(10)));
if numel(k)==0,
    k=dtot;
end
rj(10)=r(k);
%computation of the geometrical safety factor
ecc=transpose(rj-raggio);
mass=-max(abs(ecc));
fgs=spess/2/mass;
end
```

```
%script for the optimization procedure
%introduction of the geometry (radius, thickness, joints)
r1= 0.9532;
s1=0.1811*r1;
r=[r1-s1/2;r1+s1/2]
gr = [0 0.3927 0.7854 1.1275 1.4696 1.6720 2.0141 2.3562 2.7489 3.1416];
%definition of the optimisation problem
%global search is used to avoid local minima. The boudaries for the
%variables to optimise are defined in problem (upper and lower bound).
The
%procedure minimizes the opposite of the gemetrical safety factor
opts = optimoptions('fmincon','Algorithm','interior-point');
problem = createOptimProblem('fmincon','objective',...
 'fattgeom2','x0',xin,'lb',[r(2)-r(1);(r(2)+r(1))/2;r(1);0.001;-0.3],...
 'ub',[r(2)-r(1);(r(2)+r(1))/2;r(2);0.3;0],'options',opts);
gs = GlobalSearch;
xott = run(gs,problem)
%drawing of the arch and the solution
hold off
arco(r(1),r(2),gr,10)
fattgeom2(xott)
```